NOVA SCHOOL OF SCIENCE & TECHNOLOGY

DEPARTAMENT OF LIFE SCIENCES

INÊS DE JESUS NUNES SOARES DIAS GONÇALVES

BSc in Biochemistry

GENERATION AND CHARACTERIZATION OF TRANSGENIC ZEBRAFISH LINES FOR THE STUDY OF VERTEBRATE BRAIN STRUCTURE AND FUNCTION

MASTER'S IN MOLECULAR GENETICS AND BIOMEDICINE

NOVA University Lisbon

September 2022

DEPARTAMENT OF
LIFE SCIENCES

GENERATION AND CHARACTERIZATION OF TRANSGENIC ZEBRAFISH LINES FOR THE STUDY OF VERTEBRATE BRAIN STRUCTURE AND FUNCTION

INÊS DE JESUS NUNES SOARES DIAS GONÇALVES

BSc in Biochemistry

Adviser: Ana Catarina Caetano Certal Afonso
PhD, Head of Fish Platform, Champalimaud Foundation
Invited Assistant Professor, NOVA School of Science and Technology, NOVA University Lisbon

Co-adviser: Pedro Manuel Brôa Costa
Auxiliary Professor, NOVA School of Science and Technology, NOVA University Lisbon
Associate Laboratory i4HB - Institute for Health and Bioeconomy
UCIBIO - Applied Molecular Biosciences Unit

Examination Committee:

Chair: Margarida Casal Ribeiro Castro Caldas Braga
Auxiliary Professor, NOVA School of Science and Technology, NOVA University Lisbon

Rapporteur: Ana Cristina Ribeiro Borges
Aquatic Species Vivarium Coordinator, Instituto Gulbenkian de Ciência

Adviser: Ana Catarina Caetano Certal Afonso
PhD, Head of Fish Platform, Champalimaud Foundation
Invited Assistant Professor, NOVA School of Science and Technology, NOVA University Lisbon

MASTER'S IN MOLECULAR GENETICS AND BIOMEDICINE

NOVA University Lisbon
September 2022

Generation and Characterization of Transgenic Zebrafish Lines for the Study of Vertebrate Brain Structure and Function

This document was created with Microsoft Word text processor and the NOVAthesis Word template.

ACKNOWLEDGMENTS

Doing my master thesis at Champalimaud Foundation was an incredible journey. Not only did I learn a lot from each person I contacted with, but I also had the chance to grow personally and make such good friends, people that I will never forget. Accomplishing this project was definitely challenging at first, but now that it came to an end, I am very proud of what I was able to achieve. Therefore, I would like to thank every person who contributed for this final result.

First, I would like to thank Ana Catarina Certal for the opportunity and trust to carry out this project, and to Joana Monteiro for the time, encouragement, and assistance throughout all of it. Also to my co-adviser, professor Pedro Costa, for all the tips and help in writing this final report.

Additionally, a major thanks to Ruth Diez del Corral for always making me feel welcomed at her bench, for all the advices, patience and specially the time spent working on my images. It was a pleasure collaborating with you Ruth.

An appreciation to the Champalimaud Foundation ABBE Platform for the microscopy infrastructure and specially to Davide Accardi, who taught me how to properly use the confocal microscope, a key element of my project.

A special appreciation to you, Inês Oliveira, for all your guidance, your incredible patience, for the time, and the amazing mentorship you gave me. I once told you that you are the type of person who cares about the small details and that is amazing for anyone who is learning. You always made sure I understood how and why things are done and I can truly say that it was a pleasure learning from you.

To all the Fish Platform staff, Mariana Sampaio, Inês Oliveira, Maria João Pereira, Ricardo Pires, Esperança Ribeiro, Olivia Knight, Pedro Seco and Dionísio Sousa, thank you guys for all the help you gave me. You were all so nice and made me feel part of the team very quickly. Thank you for all you taught me.

At a more personal level, a special thanks to my parents for all the support and encouragement. I will never be able to thank you guys enough for everything you do for me.

ABSTRACT

Understanding the functioning and organization of the brain is crucial to decipher how sensory stimuli are translated into behaviour. Over the last decades, zebrafish has become a model of excellence to address this challenge, with its simple and well described nervous system. The development of new transgenic tools and sophisticated imaging techniques, allied to the embryos' optical clarity and external development, made it possible to generate genetically-modified animals that revolutionized the study of neuron morphology and interaction.

The current work initiated the establishment of a new zebrafish transgenic line, to be used in future studies of neuronal polarization, process characterized by axons extension during the formation of a functional neuronal network. The kif5c^{560} protein, expressed at axon terminals, was previously identified as the earliest marker of axonogenesis, thus revealing an enormous potential to study the neuronal polarization process. One-cell stage zebrafish embryos were microinjected with 10xUAS:Kif5c^{560}-EYFP DNA, in the presence of tol2 mRNA, with a successful generation of fluorescently-labelled larvae. Five lines were selected to be raised as F-1 lines and germ line transmission was confirmed on the next generation (F0).

In parallel, the neuronal expression of other five previously-established lines was studied through confocal microscopy. Although gene expression had already been described, to the best of our knowledge none of the exact lines studied had been registered in the most commonly used zebrafish brain atlases, with great importance for the scientific community as they aggregate information from hundreds of lines into a common reference space. Therefore, the present work was not only essential in confirming the reported expression pattern, increasing the degree of confidence in it, but was also an important step towards the integration of these lines into an international atlas. Neurological disease-associated genes are conserved in zebrafish, so the availability of this information may contribute to future studies on neurological disorders and the identification of molecular drug targets.

Keywords: zebrafish, Kif5c^{560} protein, confocal microscopy, brain atlases

RESUMO

Compreender o funcionamento e a organização do cérebro é crucial para decifrar como os estímulos sensoriais são convertidos em comportamento. Nas últimas décadas, o peixe-zebra tornou-se um modelo de excelência para enfrentar este desafio, pelo seu sistema nervoso simples e bem descrito. O desenvolvimento de novas ferramentas transgénicas e técnicas de imagem sofisticadas, aliadas à clareza ótica e desenvolvimento externo do embrião, possibilitaram a criação de animais geneticamente modificados que revolucionaram o estudo da morfologia e interação dos neurónios.

O presente trabalho iniciou o estabelecimento de uma nova linha transgénica de peixe-zebra, a ser utilizada em estudos futuros de polarização neuronal, processo caracterizado pela extensão axonal durante a formação de uma rede neuronal funcional. A proteína Kif5c^{560}, expressa no terminal dos axónios, foi previamente identificada como o marcador mais precoce do processo de axonogénese, revelando assim um enorme potencial para estudar o processo de polarização neuronal. Embriões de peixe-zebra no estadio de uma célula foram injetados com o plasmídeo 10xUAS:Kif5c^{560}-EYFP e mRNA de tol2, com a geração bem sucedida de larvas com fluorescência. Cinco linhas foram selecionadas para serem criadas como linhas F-1 e a transmissão do transgene foi confirmada na geração seguinte (F0).

Paralelamente, a expressão neuronal de outras cinco linhas previamente estabelecidas foi estudada por microscopia confocal. Embora a expressão destes genes tenha já sido descrita, até onde sabemos nenhuma das exatas linhas estudadas foi registada nos atlas cerebrais de peixe-zebra comumente utilizados, com uma grande importância para a comunidade científica por agregarem informação acerca de centenas de linhas num espaço comum de referência. Assim sendo, o presente trabalho foi não só essencial para confirmar o padrão de expressão relatado, aumentando assim o grau de confiança no mesmo, como também um importante passo para a integração destas linhas num atlas internacional. Genes associados a doenças neurológicas são conservados no peixe-zebra, logo a disponibilidade desta informação poderá contribuir para o estudo de distúrbios neurológicos e para a possível identificação de alvos moleculares.

Palavras chave: peixe-zebra, proteína Kif5c^{560}, microscopia confocal, atlas cerebrais

CONTENTS

List of Figures

LIST OF TABLES

ABBREVIATIONS

ABBE	Advanced Bio-imaging and Bio-optics Experimental
A, C, G, T	Adenine (A), Cytosine (C), Guanine (G), and Thymine (T) - DNA base pairs
ANOVA	Analysis of variance
ANTs	Advanced Normalization Tools algorithm
ATP	Adenosine 5'-triphosphate
BACs	Bacterial Artificial Chromosomes
BSA	Bovine Serum Albumin
ccu	Champalimaud Centre for the Unknown
CF	Champalimaud Foundation
CLS	Centralized Life Support
cmlc2	cardiac myosin light chain 2
CMTK	Computational Morphometry Toolkit
CNS	Central Nervous System
CoPA	Commissural Primary Ascending neurons
CRISPR	Clustered Regularly Interspaced Palindromic Repeats
DMSO	Dimethyl sulfoxide
DNA	Deoxyribonucleic Acid
DsRed	*Discosoma* coral red fluorescent protein
EDTA	Ethylenediaminetetraacetic Acid

e.g.,	exempli gratia, meaning "for example"
EGFP or GFP	(Enhanced) Green Fluorescent Protein
elavl3	ELAV like neuron-specific RNA binding protein 3
ERK1, ERK2	Extracellular signal-Regulated Kinase 1 and 2, respectively
EYFP or YFP	(Enhanced) Yellow Fluorescent Protein
E3	Embryonic medium
fabp10a	Fatty acid binding protein 10a
GABA	ɣ-aminobutyric acid
gap43	growth associated protein 43
GFF	GAL4FF
GLYT1, GLYT2	Glycine Transporter 1 and 2, respectively
HCRTR2	Hypocretin Receptor 2
isl2b	islet2b (ISL LIM homeobox 2b)
Kif5c^{560}	Truncated version of Kinesin-1 family member 5c protein
LCSM	Laser Confocal Scanning Microscope
LMPA	Low-Melting Point Agarose
LoxP	Locus X-over P1
mapZebrain	Max Planck Zebrafish Brain
M-cells	Mauthner cells
MHB	Midbrain-Hindbrain Boundary
mitfa	microphthalmia-associated transcription factor a
mRFP	membrane-bound red fluorescent protein

mRNA	messenger Ribonucleic Acid
mpeg1	macrophage expressed 1 gene
NA	Numerical Aperture
NGS	Normal Goat Serum
NP	Neuronal Polarization
nucMLF	Nucleus of the Medial Longitudinal Fasciculus
nucMLFp	Nucleus of the Medial Longitudinal Fasciculus projections
PBS	Phosphate-Buffered Saline
PCR	Polymerase Chain Reaction
PFA	Paraformaldehyde
pitx2	paired-like homeodomain 2
pSAM	-6.7Tru.Hcrtr2
PTU	1-phenyl 2-thiourea
RNA	Ribonucleic acid
slc6a3, slc6a5	Solute carrier family 6 member 3 and member 5, respectively
TALENs	Transcription Activator-Like Effector Nucleases
t-ERK	Total Extracellular signal-Regulated Kinases
TeO	Optic Tectum
Tg	Transgenic
Tricane	Ethyl 3-aminobenzoate methanesulfonate
Tris-HCl	Tris(hydroxymethyl)aminomethane hydrochloride
TILLING	Targeting-Induced Local Lesions in the Genome
TU	Tübingen

UAS	Upstream Activating Sequence
vglut2a	Vesicular-glutamate transporter 2a
ViBE-Z	Virtual Brain Explorer for Zebrafish
wt	wild type
ZBB	Zebrafish Brain Browser
ZFIN	Zebrafish Information Network
ZFNs	Zinc Finger Nucleases
3D	three-dimensional
~	around
<	inferior

UNITS

bp	base pair
dpf	days post-fertilization
g	grams
h	hours
hpf	hours post-fertilization
Kb	kilobase
L	Litre
M	molar
mg	milligram
mg / mL	milligram per millilitre
min	minutes
mL	millilitre
mm	millimetre
mM	millimolar
ms	meter per second
ng / µL	nanogram per microlitre
nl	nanolitre
nm	nanometre

ppm	parts per million
psi	pound per square inch
V	Volt
w / v	weight / volume
º C	degree Celsius
%	percentage
µL	microlitre
µM	micromolar
µm	micrometre
µS	microsecond

1

INTRODUCTION

One of the central goals of neuroscience is to understand the dynamics, organization, and functioning of the brain, in order to decipher how sensory information is recognized, processed and translated into behaviour (Gahtan et al., 2005). However, to address this goal, it is first necessary to attain a good understanding of neurons' morphology and connectivity, as a requirement to comprehend the complex neural network (Feierstein et al., 2015).

Over the last decades, zebrafish has become a model of excellence to neuroscience, with the creation and characterization of several transgenic lines used to study neuronal populations, in a relatively simple nervous system (Feierstein et al., 2015). Its genetic tractability has made it a well-suited organism to study a wide range of subjects, from developmental biology, to regeneration, neurophysiology, toxicology and so many more (Cassar et al., 2020; Spence et al., 2008).

1.1 Zebrafish as an animal model

Danio rerio, commonly known as zebrafish, is a small omnivorous teleost fish native to the floodplains of Southern Asia, being found in shallow, slow-flowing waters with aquatic vegetation and a silty substratum (Spence et al., 2008). The Asian continent is characterized by its monsoon climate with a wide seasonal variation, resulting in a broad tolerance of zebrafish to a vast range of breeding protocols (Cassar et al., 2020).

Its conserved vertebrate biology, easy husbandry and low-cost maintenance compared to other vertebrate models, high fecundity, a fully annotated genome, and small size are just some of the attractions in the use of zebrafish as an alternative to mammals (e.g., mice) (Arjmand et al., 2020; Spence et al., 2008). Moreover, it presents a 70% homology with the human genome and 82% of orthologous human disease-related genes (Cassar et al., 2020).

Successful mating results in hundreds of transparent externally fertilized eggs that develop quite rapidly (two to three months until adulthood), allowing scientists to reduce the overall duration of their experiments while applying non-invasive *in vivo* techniques (Cassar et al., 2020). Although there are some major differences related to anatomy and physiology, most zebrafish organs are already formed between 48- to 72-hours post-fertilization (hpf) and perform the same functions as their human counterparts (Cassar et al., 2020).

Lastly, in comparison to mammals, the use of fish raises far fewer ethical concerns, since experiments with the earliest life-stages of zebrafish are not regulated as animal studies, according to the European Commission Directive 63/2010. The autonomous feeding just begins around 5 days post fertilization (dpf), the time considered as the first stage subjected to regulation. As a result, working with zebrafish embryos and/or larvae under 5 dpf is considered, at least in Europe, an alternative to animal experimentation (Cassar et al., 2020).

1.2 Genetic tractability of zebrafish

Zebrafish external development allied with the optical clarity of the embryo were some of the main features that first attracted scientists. With the opportunity to perform manipulation at such early stages, researchers were given the power to create genetically-modified animals, using a wide variety of gene-editing tools, and easily track under the microscope fluorescent molecules, organelles, cells, and tissues, in real time and *in vivo* (Choe et al., 2021; Pei & Burgess, 2019).

Among these technologies, it is possible to highlight, as mutagenic methods, the morpholino-mediated gene knockdowns and targeting-induced local lesions in the genome (TILLING), as reverse genetic approaches applied to study gene deletion, either transiently or permanently, respectively; fixed-point shear enzymes, such as zinc finger nucleases (ZFNs) and transcription activator-like effector nucleases (TALENs), that target specific sequences and introduce DNA double-strand breaks; and more recently the clustered regularly interspaced short palindromic repeats (CRISPR) technology, used to generate tissue-specific knockouts (Li et al., 2021; Sertori et al., 2016). Regarding the transgenic approaches is important to mention the transposon systems, such as the Tol2 and the Sleeping Beauty, used for highly efficient integration of foreign genetic material into a host genome (Li et al., 2021).

1.2.1 Transgenic approaches

DNA microinjection into one-cell stage embryos remains the most simple and reliable method to generate a stable line of transgenic animals, being based on the use of a small glass needle to introduce foreign genetical material into fertilized eggs. The needle is filled with a DNA solution and attached to an air pump, penetrates the cell membrane, and delivers the fluid inside the nucleus (Dean, 2013). There, the gene is amplified and integrated into the genome, and then transmitted to every subsequential cells, including the germline cells, allowing a further propagation of the transgene to the next generation (Xu, 1999).

Many years ago, transgenic animals were generated by microinjection of naked DNA, in which a DNA plasmid or bacterial artificial chromosomes (BACs), was linearized by a

restriction enzyme, purified, and then injected into the host. However, researchers quickly realized that the integration efficiency and the frequency of transmission to the next generation were very low. Moreover, the multi-exogenous plasmid copies lead to an abnormal development and a difficulty in detecting the integration site. To solve this issue scientists started to rely on transposable elements, such as the tol2 transposon (Li et al., 2021; Suster et al., 2009).

1.2.1.1 Tol2-mediated transgenesis

The tol2 transposon, described for the first time in the medaka fish, is a DNA sequence of 4.7 kilobases (kb) that encodes for a functional transposase enzyme, with the ability to change the insertion position of any DNA fragment cloned between two Tol2 cis-sequences (Kawakami, 2007; Li et al., 2021). A DNA plasmid containing the gene of interest, trapped between those two sequences, and a synthetic transposase mRNA are co-injected into fertilized zebrafish embryos. The mRNA is translated into a functional transposase enzyme that recognizes the two Tol2 cis-sequences and excise them. Therefore, the trapped DNA is excised from the donor plasmid and integrated in the host genome, through a cut-and-paste mechanism (Figure 1.1) (Kawakami, 2007).

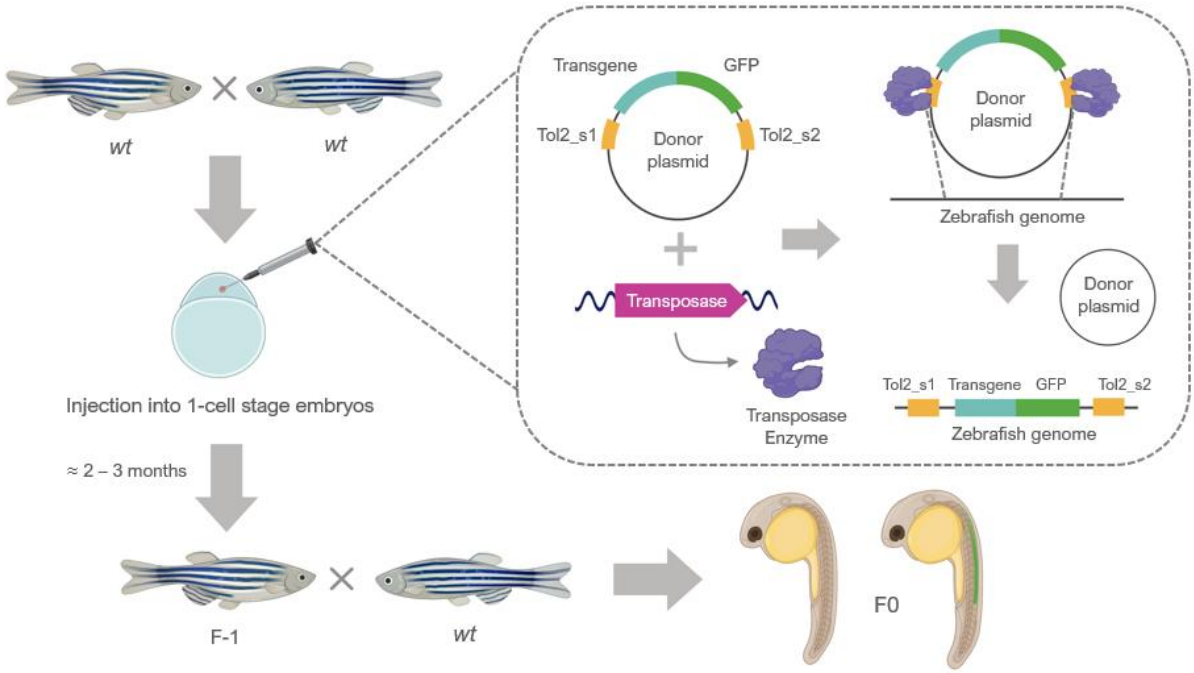

Figure 1.1 - Tol2-mediated transgenesis. Zebrafish fertilized embryos are obtained by a genetic cross of two wildtype (*wt*, as for non-transgenic) fish. A synthetic transposase mRNA and a Tol2 construct (donor plasmid), containing two tol2 cis-sequences (Tol2_s1 and Tol2_s2) and the transgene that drives the expression of a specific reporter (e.g. GFP), are co-injected into zebrafish eggs. The Tol2 construct is excised from the donor plasmid and integrated into zebrafish genome. The injected embryos will give rise to the F-1 generation that when crossed with a *wt* fish, will give rise to non-transgenic fish and transgenic fish, heterozygous for the Tol2 insertions (F0 generation). In this example, the transgene codifies for a spinal cord protein, depicted in green. Adapted from Kawakami (2007), with modifications, and created with Biorender.com.

The Tol2 transposase can transpose a DNA insert as large as 11 kb, without any reduction on transposition activity. It does not cause any gross rearrangement or modification at the target site, except for the creation of an 8-base pair (bp) duplication at each site of integrated Tol2 elements (Halpern et al., 2008; Kawakami, 2007).

This genome editing approach presents a high genomic integration in the germ line and it was already proved to be active in all vertebrate cells tested so far, including zebrafish, xenopus, chicken, mouse, and human (Kawakami, 2007; Suster et al., 2009).

1.2.2 Important transgenic systems

The fluorescent reporters used in the creation of transgenic lines function as *in vivo* markers that facilitate genetic screens. To control where and when these markers are expressed within the animal, sophisticated control techniques, such as the Gal4-UAS and the Cre-loxP systems, are useful to analyse gene's function (H. Kim et al., 2018; Marquart et al., 2015). These systems have not been applied to vertebrates for a long time, mainly due to the lack of an efficient transgenesis method, but when the tol2-mediated transgenesis was discovered, in 2004, it was finally possible to use them more efficiently (Asakawa & Kawakami, 2008; Mukherjee & Liao, 2018).

1.2.2.1 Gal4-UAS transactivation system

A relevant step in the acceptance of zebrafish as a biomedical model was the refinement of transgene introduction by using the Gal4-UAS transactivation system. The Gal4 protein is a yeast transcription activator, with a DNA-binding domain and a transcription activation domain. Gal4 binds to DNA as a dimer and specifically recognizes the Upstream Activating Sequence (UAS) (Asakawa & Kawakami, 2008; Scott, 2009).

It is used as a two-component gene expression system, in which one line expresses the Gal4 protein and another line carries the reporter gene located downstream of the UAS sequence. In a double transgenic progeny, obtained from a cross of the two lines, Gal4 is expressed, binds to the UAS, and activates the expression of the reporter gene (Figure 1.2) (Asakawa & Kawakami, 2008). Gal4 can also cooperatively bind to multiple tandem UAS sites, for further enhancement of gene expression, and the positive cells can be identified by the fluorescence emitted by the reporter's gene-encoded protein (Halpern et al., 2008).

This system allows a spatiotemporal control of any construct adjacent to the UAS through the binding of the right promoter to which Gal4 is bound. Gal4 will be expressed when and where the selected promoter is active, consequently manipulating when and where the UAS reporter is expressed (Scott, 2009).

The binary nature of the Gal4-UAS system enables the creation of several driver and reporter lines that can be combined in different ways to generate a wide variety of zebrafish transgenic lines (Halpern et al., 2008; Scott, 2009).

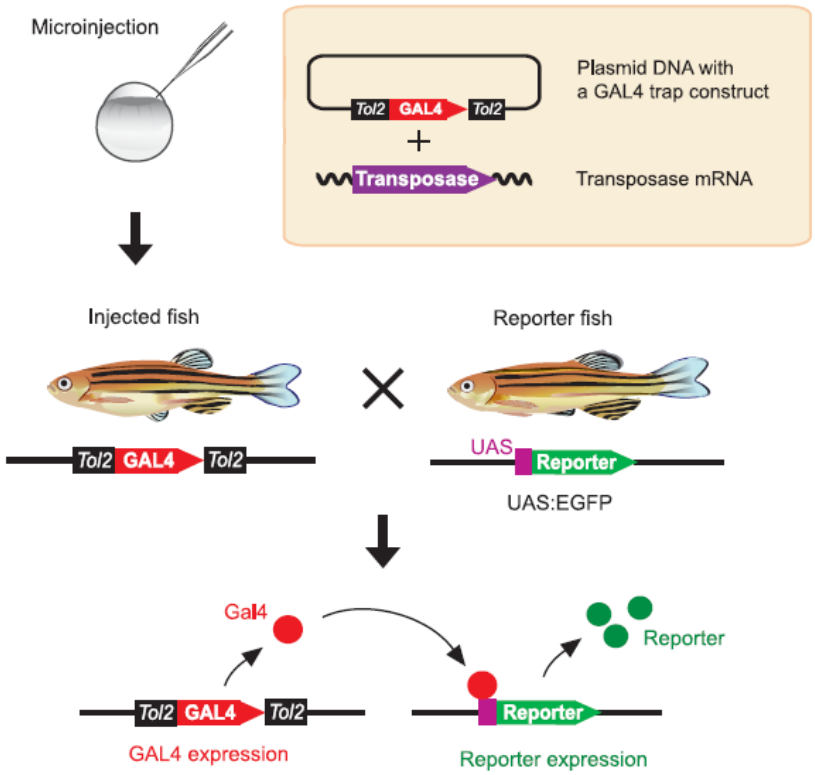

Figure 1.2 - Tol2-mediated Gal4 enhancer trap. A transposon donor plasmid, containing the Gal4 gene trapped between two Tol2 cis-sequences and a synthetic transposase mRNA are co-injected into fertilized zebrafish eggs. The trap Gal4 gene is excised from the donor plasmid, by the transposase enzyme, and integrated into zebrafish genome, including the germline cells, originating the so-called injected fish. By a genetic cross of the injected line and a reporter line, containing the Upstream Activating Sequence (UAS) upstream of the reporter enhanced green fluorescent protein gene (EGFP), the Gal4 is expressed and links specifically to the UAS sequence, activating the reporter gene transcription. Gal4 expressing cells can be visualized by the fluorescence emitted from the reporter's gene-encoded protein. Adapted from Asakawa & Kawakami (2008).

1.2.2.2 Cre-LoxP-mediated recombination system

The Cre-loxP-mediated recombination system is a powerful gene-editing tool, mainly applied to investigate tissue-specific overexpression or to perform lineage tracing during embryogenesis (Mukherjee & Liao, 2018). The Cre enzyme, named for causing recombination, is a tyrosine site-specific recombinase with a DNA breaking-rejoining ability. It is encoded by the cre gene from the bacteriophage P1 and recognizes specific DNA fragment sequences called locus X-over P1 (loxP) (H. Kim et al., 2018; McLellan et al., 2017).

Like the Gal4-UAS, the Cre-loxP works as a two-component system (Figure 1.3) in which one line expresses the Cre recombinase, and the other expresses the gene of interest flanked by two loxP sites. The Cre enzyme recognizes the two loxP and mediates a site-specific deletion

by the creation of a circular DNA fragment, containing the excised and inactivated gene (referred as gene Y) (H. Kim et al., 2018; McLellan et al., 2017).

Although this system is mostly used for gene deletion, it can also cause inversion or translocation of the flanked DNA, depending on the orientation of the loxP sites. If they are in the same direction deletion occurs; in opposite directions the gene is inverted and in the case of intrachromosomal recombination translocation takes place (H. Kim et al., 2018).

The specificity of the recombination is controlled by the promoter and/or enhancer sequences that drive the Cre expression in the cell or tissue of interest (H. Kim et al., 2018).

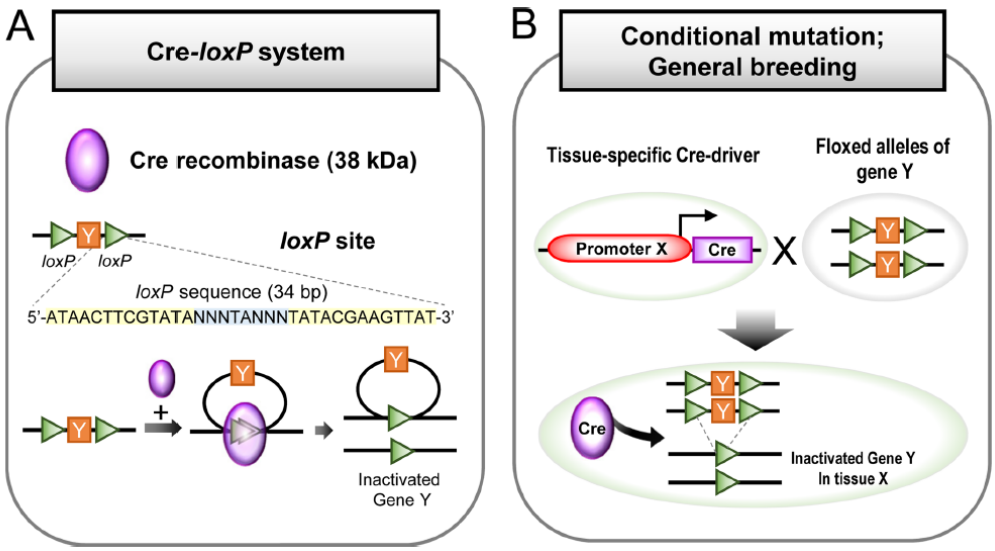

Figure 1.3 - Cre-LoxP-mediated recombination system. **(A)** A general overview of Cre-loxP system, in which the 38 kilodalton (kDa) Cre recombinase recognizes two loxP sites, each with 34 base pair (bp), flanking the target gene Y. After recognition, the Cre recombinase generates a circular DNA fragment, containing the excised and inactivated gene Y and another fragment containing one loxP site. **(B)** General breeding strategy for conditional mutation using the Cre-LoxP system, in which the Cre driver line expresses the Cre recombinase in a tissue-specific manner, and another line possess loxP flanked (floxed) alleles of the interest gene Y. By a genetic cross of the two lines, the Cre recombinase excises the "floxed" loci and inactivates gene Y. Adapted from Kim et al. (2018).

1.2.3 Transgenic zebrafish lines and the biomedical research revolution

The possibility of creating transgenic animals carrying additional or modified copies of genes, deliberately inserted into their genomes, was firstly reported in 1988 (Choe et al., 2021; Dean, 2013). Nine years later, the creation of a zebrafish transgenic line that expressed a fluorescent protein in a cell-specific manner - the Tg(gata1a:GFP) - was described for the first time, which completely revolutionized biomedical research (Choe et al., 2021).

Since then, multiple transgenic lines expressing fluorescent reporters have been created to study a wide range of subjects. For example, the Tg(mpeg1:EGFP) line was engineered to track macrophages and study their interaction with neutrophils during inflammation; the

Tg(fabp10a:DsRed) line was design to study the patterning and differentiation of the hepato-pancreatic ductal system and the Tg(slc6a3:EGFP) line can be used to study dopaminergic neurons, whose loss is associated with various neurological disorders (Choe et al., 2021).

Until now zebrafish was used as a vertebrate model organism in more than 40,000 biomedical studies, existing so far around 49,000 transgenic zebrafish lines registered in the Zebrafish Information Network (ZFIN) (Choe et al., 2021).

1.3 The use of zebrafish transgenic lines in neuroscience

1.3.1 Neuroscience challenges and the use of zebrafish

To study brain's functional organization it is essential to characterize distinct neuronal populations and perceive their involvement in specific circuits. Over the years, zebrafish has become a promising model organism to do this, given the possibility of using optical methods to record and manipulate neural activity throughout the brain (Feierstein et al., 2015).

Zebrafish central nervous system (CNS) organization is similar to that of other vertebrates and well described at multiple life-stages. In fact, the main structures, subdivisions and cell types of the human brain have equivalents in this model (Arjmand et al., 2020; Cassar et al., 2020). Zebrafish larvae possess a tiny brain, with less than half a cubic millimetre, containing around 100,000 neurons (Randlett et al., 2015) and a rapid neuronal development, as evidenced by larvae's ability to follow visual stimuli, capture small moving prey and avoid predators at 5 dpf, which ultimately reveals an already well-developed neuronal network (Feierstein et al., 2015). Furthermore, its reduced physical dimensions combined with its optical transparency allow the entire brain to be rapidly scanned at a cellular resolution, granting scientists the chance to perform neuronal analysis much more easily (Marquart et al., 2017).

The ease of manipulation of zebrafish has led to the creation of several neurologic transgenic lines that, in alliance with systems like the Gal-UAS and the Cre-LoxP, allowed the study of neurodevelopmental disorders such as autism; neuropsychiatric disorders including depression and anxiety; and neurodegenerative diseases such as Alzheimer's and Parkinson's disease. In addition, neurological disease-associated genes are conserved in zebrafish, enabling the identification of molecular drug targets (Cassar et al., 2020).

1.3.2 Zebrafish brain anatomy

Zebrafish CNS specification begins around 6 hpf, at the beginning of gastrulation, and at 24h the forebrain, midbrain, and hindbrain structures can already be easily distinguished. These

embryonic subdivisions provide the foundation from which cells differentiate and form the adult brain structures (Vaz et al., 2019).

The forebrain, in the most anterior part (Figures 1.4A and 1.5), is perhaps one of the most complex domains, subdivided into the telencephalon, diencephalon, hypothalamus, and retina (Figure 1.5A). These structures play a key role on the reception and processing of sensory information and its conversion into behaviour. For example, the pallium, sub pallium and the olfactory body (Figure 1.5B), parts of the telencephalon, are associated with the regulation of social behaviour, memory, and emotions. On the other hand, the thalamus, pineal body, and habenula (Figure 1.5B), sections of the diencephalon, are associated with attention, alertness, and circadian behaviours (Vaz et al., 2019).

The midbrain, located in a central position (Figures 1.4B and 1.5), is a small structure responsible for sight and hearing, from which derive the tectum and tegmentum (Figure 1.5), as the major structures. The tectum, also called optic tectum, is responsible for the visual processing and crucial for survival since it makes part of the startle and reflex response centre. For the tegmentum knowledge is still scarce, but research on mice have shown that the dorsal tegmentum receives the stimulus and the ventral tegmentum fires up neurons related to motivation and reward (Vaz et al., 2019).

On the posterior part, it is located the hindbrain (Figures 1.4C and 1.5), one of the most studied embryonic brain structures of zebrafish. The hindbrain is separated from the midbrain by the midbrain-hindbrain boundary (MHB) (Figure 1.5A), transient and not present in adult zebrafish brain, but essential for the patterning of neighbouring regions, such as the tectum and cerebellum. From the hindbrain arise motor neurons that control the movement of the eyes, jaw, head, and body, and neurons that innervate the branchial arches (Vaz et al., 2019).

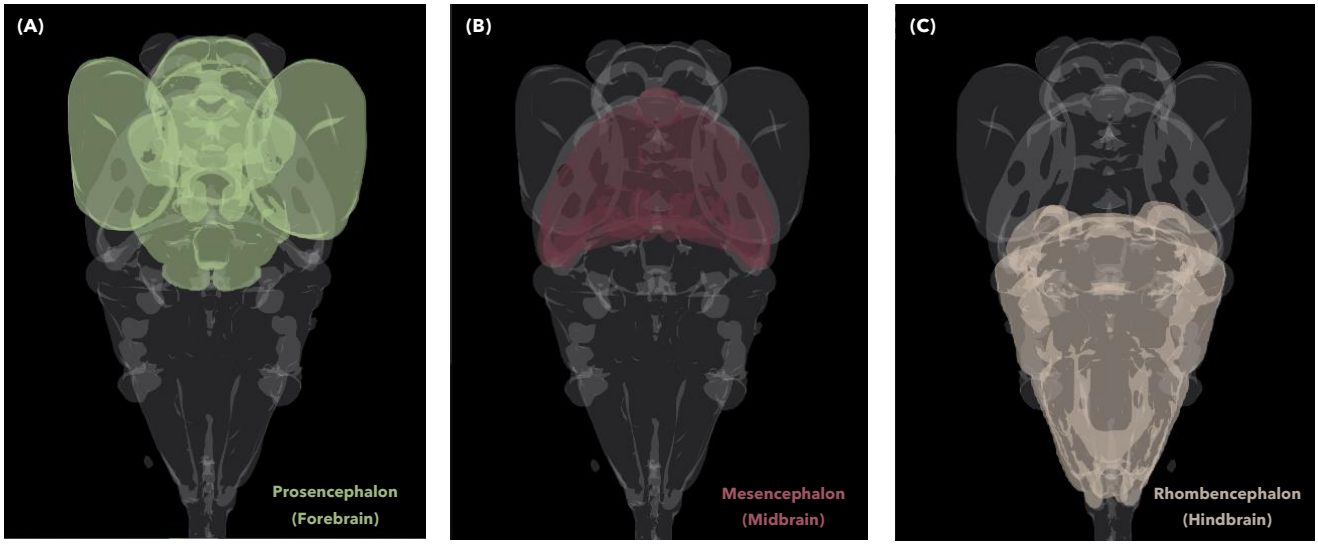

Figure 1.4 - Zebrafish brain anatomy overview. **(A)** - forebrain or prosencephalon, involved in the reception and processing of sensory information and its conversion into behaviour; **(B)** - midbrain or mesencephalon, responsible for vision and hearing functions; **(C)** - hindbrain or rhombencephalon, from which arise motor neurons that control the movement of the eyes, jaw, head, and body, and innervate the branchial arches. Adapted from mapZebrain Atlas (https://mapzebrain.org).

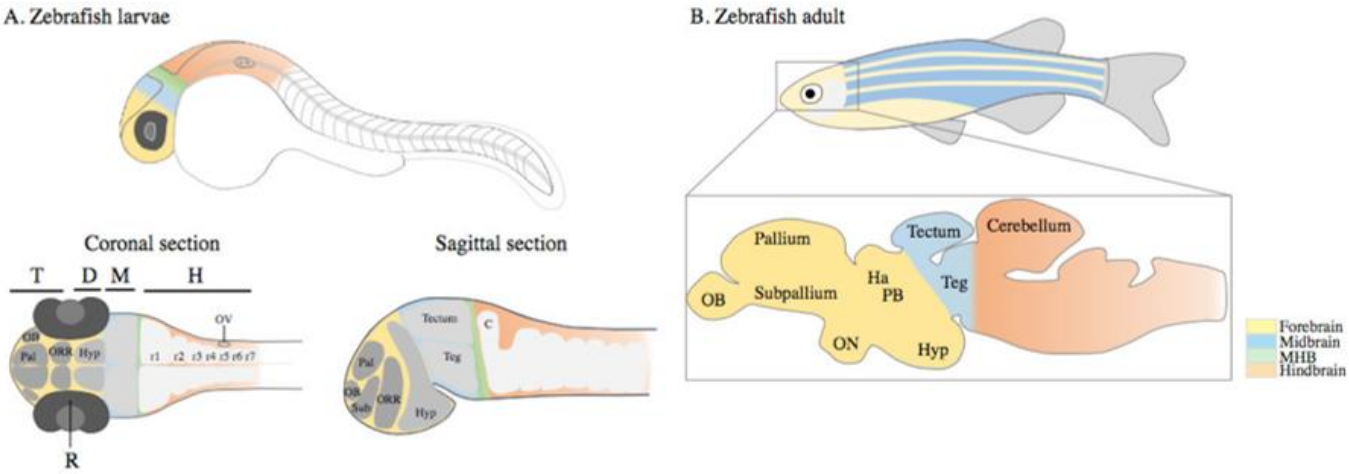

Figure 1.5 - Zebrafish brain development. **(A)** - Schematic representation of the embryonic brain (30 hpf), displaying the forebrain (yellow), midbrain (blue), midbrain-hindbrain boundary (green), and hindbrain (orange). The forebrain is subdivided into the telencephalon (in darker gray) and the diencephalon, containing the hypothalamus (lighter grey). **(B)** - Simplified representation of the adult brain and its main domains. **Legend:** C: cerebellum; D: diencephalon; M: midbrain; MHB: midbrain-hindbrain boundary; H: hindbrain; Ha: habenula; Hyp: hypothalamus; OB: olfactory bulb; ON: optic nerve; ORR: optic recess region; OV: optic vesicle; Pal: pallium; PB: pineal body; R: retina; r1–r7: rhombomeres 1 to 7; Sub: sub pallium; T: telencephalon; and Teg: tegmentum. Adapted from Vaz et al. (2019).

1.3.3 The use of Kif5c^{560} protein to study neuronal polarization

To create a functioning neural network, neurons must migrate to their final destinations and extend their axons toward their target in a process commonly known as neuronal polarization (NP). However, little is known about the mechanisms behind this phenomenon and how its coordinated *in vivo* (Breau et al., 2017).

NP can be defined as the establishment of distinct molecular structures to generate a single axon and multiple dendrites. Neurons work as complex computational units, with specific input and output sites. The electrical information is passed from neuron to neuron via action potentials, in which the input is collected by the dendrites, processed in the cell body and the resulting output is transmitted throughout the axon. For a good neural circuitry function and signal transmission, it is crucial that the extension of the axon and dendrites of an early neuron happens correctly (Randlett et al., 2011; Schelski & Bradke, 2017).

The process of NP has been studied for decades with dissociated hippocampal neurons, the most commonly used experimental system, and is divided into five stages. In stage 1 neurons develop a lamellipodium, from which small neurites emerge in stage 2. After that, in stage 3, alternating neurites extend in brief growth phases keeping similar lengths, until one of them breaks the symmetry. This neurite grows for an extended period of time and becomes the axon, while the growth of the others stops. After one week, during stage 4, the remaining neurites branch and later develop into dendrites. In the last stage of the process, stage 5, the axon is further matured and synapses are formed (Schelski & Bradke, 2017).

The earliest intracellular marker of axonogenesis, during hippocampal neuron polarization, is the constitutively active motor domain of Kinesin-1 family member 5c (Kif5c) (Randlett et al., 2011). The truncated version of Kif5c, Kif5c^{560}, is composed of amino acids 1 to 560 and selectively accumulates in axons microtubules (Jacobson et al., 2006). When fused to the Yellow Fluorescent Protein (YFP), Kif5c^{560}-YFP expression can be visualized as a transient yellow fluorescence in one or few neurites, during stage 2. As the neuron progresses to Stage 3, Kif5c^{560}-YFP accumulates specifically and permanently in the axon terminals, remaining there during all axon extension and lateral movements (Breau et al., 2017; Jacobson et al., 2006; Randlett et al., 2011). The use of this YFP-tagged protein makes it possible to know when neuronal polarity first emerges and to visualize axonal differentiation in real time (Jacobson et al., 2006).

1.3.4 Transgenic zebrafish lines studied: what is known so far

In order to better envisage the brain dynamics, it is important to increase the variability of neuronal markers currently available. The zebrafish lines studied on this project were chosen based on this assumption, presenting distinct drivers that induce expression on different neuronal populations. The characterization of these lines will ultimately allow their use in a wide variety of *in vivo* functional studies, crucial to increase the scientific knowledge on the complex neuronal network.

1.3.4.1 Tg(gata1a:GFP)

In 1997, the Lin group, at the Medical College of Georgia, created the transgenic zebrafish line gata1a:GFP, by the injection of a linearized construct comprising the GATA-1 and the green fluorescent protein (GFP) genes (Choe et al., 2021).

The GATA-1 gene encodes for the GATA binding protein 1a, an erythroid-specific transcription factor that functions as a key regulator of haematopoiesis and myeloid cell differentiation. Since this gene is strictly expressed in erythroid progenitor cells, the gata1a protein can function as an early marker of erythrocytes and used to study embryonic erythropoiesis (Bradford et al., 2022; Choe et al., 2021). Expressed in connection with the GATA-1 gene is the GFP reporter, a fluorescent protein derived from the jellyfish *aequorea victoria*, that emits green fluorescence when exposed to ultraviolet light (Kong et al., 2020).

In previous studies for this gene, GFP positive cells were observed at 16 hpf in the intermediate cell mass, the earliest hematopoietic tissue in zebrafish; into circulating blood between 24 hpf and 2 months; in the heart at 2 dpf; in the eyes and in some spinal cord neurons. Additionally, a high fluorescence was noted in the head kidney of 1-month-old fish, which suggested this structure as the primary localization of adult erythropoiesis (Long et al., 1997).

Even though hematopoiesis occurs in different anatomical sites, in comparison to mammals, the molecular mechanisms behind it are highly conserved in zebrafish, making it a powerful vertebrate model system to study hematopoietic disorders (Gore et al., 2018). Human orthologs of the GATA-1 gene were already associated with blood disorders such as beta thalassemia, hematologic abnormalities in Down syndrome and with some bone marrow cancers, like leukaemia and multiple myeloma (Bradford et al., 2022; Choe et al., 2021).

1.3.4.2 Tg(aldoca:gap43-Venus)

The Tg(aldoca:gap43-Venus) line was created by the Hibi group, at the Graduate School of Science, Nagoya University, Japan, where zebrafish embryos were injected with a construct comprising the aldoca, gap43 and Venus genes, taking advantage of the tol2 transposon system (Bradford et al., 2022; Tanabe et al., 2010).

Zebrafish has two copies of the aldolase C gene, the aldoc or aldolase c, that encrypts for a fructose-bisphosphate aldolase enzyme, and the aldocl, aldolase Ca or just aldoca, which encodes for the zebrin II glycolytic enzyme. Zebrin II is specifically expressed in Purkinje cells of the vertebrate cerebellum and plays an important role in adenosine 5'-triphosphate (ATP) biosynthesis (Lin et al., 2020; Tanabe et al., 2010). Working as the reporter marker of this line is the fusion protein gap43-Venus, comprising the growth associated protein 43 (gap43), a neurite elongation and synapse formation indicator highly expressed in early stages of

development (Rosskothen-Kuhl & Illing, 2014), and the Venus as an improved mutated version of YFP, which exhibits a greater speed and efficiency of maturation and a superior tolerance to acidosis, thus showing a more stable fluorescence (Nagai et al., 2002).

In previous studies, gap43-Venus expression was observed from 72 hpf and confirmed in the axons, dendrites, soma and the cerebellovestibular tracts of cerebellar Purkinje cells, from 3 dpf until adulthood (Takeuchi et al., 2015).

The cerebellum is one of the most important structures of the hindbrain, associated with functions like motor control, reception and processing of sensory stimuli, and learning (Vaz et al., 2019). Using the Tg(aldoca:gap43-Venus) line was already proven that zebrin-positive Purkinje cells are resistant to excitotoxicity and cell injury, degenerating much slower, allowing the brain to compensate the disrupted function by increasing the cerebrocerebellar connectivity. In fact, several studies have shown an enhanced cerebrocerebellar connectivity in chronic neurodegenerative diseases, such as spinocerebellar ataxias, Alzheimer's and Parkinson's disease and multiple sclerosis (Lin et al., 2020).

1.3.4.3 Tg(pitx2c:GFP)

The Tg(pitx2c:GFP) line was generated by the Yost group, at the University of Utah, through the injection of a construct comprising the pitx2c and GFP genes (Wolman et al., 2008).

The pitx2 gene encodes for the paired-like homeodomain 2, a bicoid transcription factor capable to bind to both DNA and RNA targets simultaneously, implicated in the control of the left-right asymmetry during organogenesis. This gene exhibits two isoforms, pitx2a and pitx2c, with distinct functions and non-overlapping expression patterns. The pitx2c isoform is expressed symmetrically in the presumptive mesendoderm, during late blastula and in the prechordal plate, during late gastrula (Bradford et al., 2022; Essner et al., 2000). The mesendoderm is a population of cells only present during gastrulation, that gives rise to the mesoderm and the definitive endoderm. (Boumelhem et al., 2015). The prechordal plate gives rise to the head cavities and participates in the patterning of the cranial neural tube (Adelmann, 1922). Linked to the pitx2c gene is the GFP, as a reporter marker of the line.

In previous studies, GFP fluorescence was detected in several structures including the developing gut, digestive system, dental epithelium, and brain, more specifically in the dorsal diencephalon and in the nucleus of the medial longitudinal fasciculus (nucMLF) (Bradford et al., 2022; Essner et al., 2000; Wolman et al., 2008). The nucMLF are the first neurons to differentiate and extend their axons in the midbrain, during zebrafish neuronal development (Wolman et al., 2008).

Mutations on the pitx2 gene have already been reported in patients with Axenfeld–Rieger syndrome, a rare autosomal dominant disorder characterized primarily by developmental abnormalities of the eye (Tümer & Bach-Holm, 2009).

1.3.4.4 Tg(pSAM:Gal4), Tg(UAS:mCherry)

The Tg(-6.7Tru.Hcrtr2:Gal4-VP16) construct was generated by the Schier group, at the Department of Molecular and Cellular Biology, Harvard University, comprising the 6.7 kb DNA fragment upstream (-) of the *takifugu rubripes* hcrtr2 gene (-6.7Tru.Hcrtr2 or pSAM) and a Gal4 DNA fragment linked to a portion of the herpes simplex virus protein VP16. This construct was ultimately used to create the Tg(-6.7Tru.Hcrtr2:Gal4-VP16), Tg(UAS:GCaMP5) zebrafish line, similar to the one studied during this project but with a different reporter (Bátora et al., 2021; Lacoste et al., 2015; Sadowski et al., 1988). The mCherry marker is a protein derived from the stony-coral *discosoma sp.*, with a fast maturation and high photostability (S. Y. Kim et al., 2020).

The hcrtr2 gene encodes for the hypocretin receptor 2 (HCRTR2), that recognizes the orexin/hypocretin neurotransmitter. The orexin neuropeptide was discovered recently and added to the list of neurotransmitters involved in the control of sleep/wakefulness cycle, as well as the ɣ-aminobutyric acid (GABA), serotonin and norepinephrine. Orexin displays a specific activity pattern, in which orexinergic neurons are active during wakefulness and practically silent during normal sleep (Firouzabadi et al., 2020).

HCRTR2 polymorphisms have already been reported to cause a disfunction of the orexin system, contributing to various neurologic and neuropsychiatric disorders, such as narcolepsy and depression. Additionally, an aberrant activation of the orexin neurons during the night might also contribute to insomnia (Firouzabadi et al., 2020).

In previous studies, the expression of this gene was reported in the notochord cells, between 24 and 36 hpf; spiral fiber neurons on the hindbrain and their descending projections to the Mauthner cells (M-cells) axon cap, a bundle of spiral fiber neuron axons surrounding the M-cells axon; in the commissural primary ascending (CoPA) neurons of the spinal cord; in the anterior and posterior lateral line; statoacoustic and trigeminal ganglion; and a sparse labeling in the habenula and tegmentum. The spiral fiber neurons are a group of approximately ten neurons, located bilaterally in rhombomere 3, that excite the M-cells, involved in the short-latency escape response (Bátora et al., 2021; Lacoste et al., 2015).

1.3.4.5 Tg(glyt2:|R|-Gal4), Tg(UAS:GFP)

The Tg(glyt2:loxP-mCherry-loxP-Gal4, cmlc2:GFP), Tg(UAS:GFP) zebrafish line, shortened to Tg(glyt2:|R|-Gal4), Tg(UAS:GFP), was generated by the Higashijima group, at the Okazaki Institute for Integrative Bioscience, Japan, in which a mCherry reporter is expressed under

the control of the glycine transporter 2 (glyt2) gene, recently renamed to solute carrier family 6 member 5 (slc6a5). This line was created with both Cre-loxP and Gal4-UAS transgenic systems, and presents additionally the cardiac myosin light chain 2 (cmlc2) protein as a green heart marker (Bradford et al., 2022; Severi et al., 2018).

The glyt2 gene encodes for the glycine transporter 2 (GLYT2) protein, involved in the uptake of glycine across the plasma membrane of glycinergic neurons. Glycine is the main inhibitory neurotransmitter in the brainstem and spinal cord of vertebrates, participating in a wide variety of motor and sensory functions. The inhibitory activity is mediated by its action on glycine receptors, ligand-gated chloride channels whose opening leads to neurons hyperpolarization. Therefore, glycine transporters 1 and 2 (GLYT1 and GLYT2) play a key role in removing this neurotransmitter from the synaptic cleft, ceasing glycine inhibitory action (Barreiro-Iglesias et al., 2013; Bradford et al., 2022).

In previous studies, fluorescence was detected in the hindbrain, where glycinergic neurons were observed in the rhombencephalon, with descending projections from the reticular, raphe, and octavolateral neurons to the spinal cord (Barreiro-Iglesias et al., 2013).

Moreover, a considerable spatial overlap between this transgenic line expression pattern and the swim cluster was reported in prior experiments, which indicates an activation of the glycinergic cells during swimming. This discover was unexpected, since few hindbrain glycinergic neurons have been associated with locomotion functions (Barreiro-Iglesias et al., 2013). More research will be needed in the future, in which this line will present a big impact in the study of GLYT2 and its involvement in locomotor defects or neuromotor disorders, such as hyperekplexia (Carta et al., 2012).

1.3.5 Zebrafish brain atlases

After understanding the great impact that zebrafish transgenic lines had on the neuroscience field, researchers felt the need to find a way to combine all this useful information into a common reference space. With developments in imaging technology and computational methods, along with a wide variety of genetically encoded markers that reliably report neuronal firing and synaptic activity, it was finally possible to create 3D comprehensive brain atlases that made it so much easier to compare different transgenic lines and to have a clearer view of the anatomical organization of the zebrafish brain (Marquart et al., 2017; Randlett et al., 2015; Severi et al., 2018). Among the most commonly used atlases is relevant to highlight the Virtual Brain Explorer for Zebrafish (ViBE-Z), Z-Brain, Zebrafish Brain Browser (ZBB) and the Max Planck Zebrafish Brain (mapZebrain) as the most valuable ones (Kunst et al., 2019; Marquart et al., 2017).

ViBE-Z was the first comprehensive 3D digital brain atlas built specifically for zebrafish. It is an online software that maps gene expression data, with cellular resolution, and uses fluorescence-stained nuclei as reference for registration. Its appearance was a big change for the scientific community, since ViBE-Z enhanced the data quality available at the time through a fusion and attenuation correction of multiple confocal microscope scans of embryos/larvae with 2 to 4 dpf (Marquart et al., 2017; Ronneberger et al., 2012).

In contrast, the Z-Brain was created to be more focused on larvae with 6 dpf, containing information on gene expression and neural activity linked to a good neuroanatomical segmentation. The software allows a direct comparison between different zebrafish lines, each expressing different genes, revealing more clearly the functional connectivity of the brain (Marquart et al., 2017; Randlett et al., 2015).

The ZBB came next, as an improved version of Z-Brain, enabling a simpler visualization of the horizontal, sagittal, and transverse views simultaneously, and being specifically useful to look for target neurons and their projections (Marquart et al., 2015).

Although Z-Brain and ZBB were robust datasets on their own, researchers saw an opportunity to merge both, in a new and more reliable version - the ZBB1.2. Both atlases reflected the same developmental timepoint (6 dpf) and images were acquired at similar resolutions (0.8×0.8×2 µm for Z-Brain and 1×1×1 µm for ZBB) and orientation (dorsal to ventral horizontal scans). Despite using distinct brain references (total ERK for Z-Brain and vglut2a for ZBB) and acquisition processes (immunohistochemical stains for Z-Brain and live scans for ZBB), the combination was enriching, adding a large number of transgenic lines to Z-Brain and bringing to ZBB the manual segmentation of Z-Brain (Marquart et al., 2017; Randlett et al., 2015).

Lastly, the mapZebrain appeared as an interactive cellular-resolution atlas for 6 dpf larvae, working as a multifunctional database. It allows: 1) to visualize the expression pattern of hundreds of transgenic lines, together with their spatial coordinates; 2) to use the 3D neuroanatomical model to better understand the segmentation of zebrafish brain and visualize more clearly its regional boundaries; and 3) to take advantage of a huge catalogue of neuron's morphology and better understand their role in the neural network (Kunst et al., 2019).

1.4 Project goals

The recognition and characterization of neuronal populations, as well as the perception of their involvement in specific circuits, remains crucial to expand our scientific knowledge about the complex brain dynamics and its organization. To achieve this purpose, it is possible to resort to transgenic zebrafish lines designed to express specific neuronal markers and image their brains through confocal microscopy. The collected information can then be used as an

anatomical map of the nervous system and incorporated into comprehensive digital brain atlases. These open-source databases are an important tool for the scientific community, becoming even more powerful as more labels and activity maps are registered, with the characterization of more and more transgenic lines.

With that in mind, this project had two main goals:

1) Generate a new and stable transgenic zebrafish line, through DNA microinjection of the 10xUAS:Kif5c^{560}-EYP construct into one-cell stage zebrafish embryos, taking advantage of the tol2 transposon system. The creation of this line aims to contribute, in the future, to a better understanding of when neuronal polarity first emerges and how it is coordinated *in vivo*.
2) Characterize and confirm the spatial and temporal expression of five previously-established transgenic zebrafish lines, with the purpose of incorporating this new information into a well-established international zebrafish brain atlas. Although the expression of the genes studied had already been described in previous findings, to the best of our knowledge none of the exact lines had been registered into the most commonly used atlases. Therefore, the present project was not only useful to confirm the expression pattern previously reported, increasing the degree of confidence in it, but was also a step towards the integration of these lines into ZBB1.2 atlas. Since the lines studied mark different neuronal populations and that neurological disease-associated genes are conserved in zebrafish, the availability of this information may contribute to future studies on neurological disorders and the identification of molecular drug targets.

2

MATERIALS AND METHODS

2.1 Animal handling and welfare

In vivo experiments were performed using zebrafish, from the Fish Platform at Champalimaud Foundation (CF). Fish were handled in accordance with the European Directive on animal experimentation and standard protocols, following the Champalimaud Fish Platform program (Martins et al., 2016; Monteiro et al., 2018) and Direção Geral de Alimentação e Veterinária-approved procedures.

Fish holding rooms were maintained at a controlled temperature of 25ºC, with a 50%-60% humidity level and under a 14h light/10h dark photoperiod cycle, with a light intensity of 200-300 lux at the water surface. Zebrafish were typically kept in 3.5L tanks (Tecniplast®), under the control of Centralized Life Support (CLS) recirculating systems (Tecniplast®), with a maximum density of 10 fish per litre. Since water chemistry directly impacts fish physiology, parameters such as temperature (~28ºC), pH (~7.4), conductivity (~1300 µS), dissolved gases, total ammonia (<0), nitrites (<0), and nitrates (<0) were monitored regularly (Martins et al., 2016).

Embryos and larvae under 6 dpf were housed in dedicated incubators (Memmert) at 28ºC and a photoperiod cycle of 14h light/10h dark. Adult zebrafish were fed twice a day, with a live feed in the morning - *Artemia nauplii* - and a nutritionally complete dry powder (Zebrafeed®Sparos) in the afternoon. In substitution to artemia, rotifers were used for early stages of development, until 60 dpf, and fish were fed four times a day (Martins et al., 2016; Monteiro et al., 2018).

2.2 Zebrafish lines

During this project, ten different zebrafish lines were used:

- Tübingen (TU), a well-known wild type (*wt*) line.
- nacre$^{-/-}$, a recessive mutant line that shows a complete absence of melanophores due to a single-base mutation in the microphthalmia-associated transcription factor a (mitfa) gene. Nonetheless, nacre$^{-/-}$ fish present a normal development of the retinal pigment epithelium (Lister et al., 1999).

- Tg(elavl3:GFF)ccu5, Tg(UAS:mCherry), a reporter line that triggers mCherry expression under the control of the ELAV-like neuron-specific RNA binding protein 3 (elavl3) promoter, commonly used as a pan-neuronal driver (Tallafuss et al., 2015). Additionally, the GFF (Gal4FF), is an engineered transcriptional activator comprising the DNA-binding domain of Gal4 fused to two transcription activation modules from VP16, being less toxic than Gal4-VP16 (Bradford et al., 2022).
- Tg(isl2b:Gal4), Tg(cmlc2:GFP), driver line that triggers Gal4 expression under the control of the ISL LIM homeobox 2b (isl2b) promoter, required for the anterior second heart field development in zebrafish. This lines presents a heart-specific green marker - cmlc2 - useful in the identification of fish with the isl2b:Gal4 construct (Huang et al., 2003; Witzel et al., 2017).
- Tg(isl2b:Gal4), Tg(10xUAS:GCaMP6fEF05)ccu2, a Gal4-UAS zebrafish line in which the GCaMP6fEF05 expression is driven under the control of the isl2b promoter.
- Tg(gata1a:GFP)
- Tg(aldoca:gap43-Venus)
- Tg(pitx2c:GFP)
- Tg(-6.7Tru.Hcrtr2:Gal4), Tg(UAS:mCherry), shortened to Tg(pSAM:Gal4), Tg(UAS:mCherry)
- Tg(glyt2:loxP-mCherry-loxP-Gal4, cmlc2:GFP), Tg(UAS:GFP), shortened to Tg(glyt2:|R|-Gal4), Tg(UAS:GFP)

The expression pattern of the last five lines was studied during this project and their respective import location for CF is represented in Table 2.1. Additionally, an eleventh line will be described - Tg(elavl3:GFF)ccu5, Tg(UAS:mCherry), Tg(10xUAS:Kif5c^{560}-EYFP) - whose establishment began during this project.

Table 2.1 - Transgenic zebrafish lines characterized during this project and their respective import location to Champalimaud Foundation (CF).

Transgenic line denomination	Imported to CF from
Tg(gata1a:GFP) and Tg(aldoca:gap43-Venus)	Emre Aksay-Cornell Lab (New York)
Tg(pitx2c:GFP) and Tg(pSAM:Gal4), Tg(UAS:mCherry)	Engert Lab (Cambridge)
Tg(glyt2:|R|-Gal4), Tg(UAS:GFP)	RIKEN Institute (Japan)

2.3 Generation of a new and stable zebrafish line

2.3.1 10xUAS:Kif5c^{560}-EYFP construct design

The 10xUAS:Kif5c^{560}-EYFP DNA construct (Figure 2.1) was generated by the Molecular and Transgenic Tools platform, at CF, using two available plasmids, the pCS2^{+} and an already available plasmid containing the Kif5c^{560}-EYFP cassette. The pCS2^{+} plasmid is a multipurpose expression vector, widely used for protein expression in xenopus and zebrafish embryos, or for a high-level transient expression in mammals and birds (Wang et al., 2016).

Both plasmids were firstly expanded and their sequence was verified. The Kif5c^{560}-EYFP cassette was then amplified, from the existent plasmid mentioned above, and directionally cloned into a 10xUAS backbone. The coding sequence of Kif5c^{560}-EYFP was subcloned into the BamH1 and EcoR1 sites of the pCS2^{+} plasmid, by a Polymerase Chain Reaction (PCR) amplification of the coding region from pBa-Kif5c^{560}-YFP (Jacobson et al., 2006), using the following primers: 5'-GGGGGATCCATGGCAGATCCAGCCGAATG-3' (forward) and 5'-CCCGAATTCTTA-GACGGTCCGCTTGTACAGCTC-3' (reverse). Lastly, the DNA construct was expanded and purified for further injection into zebrafish embryos.

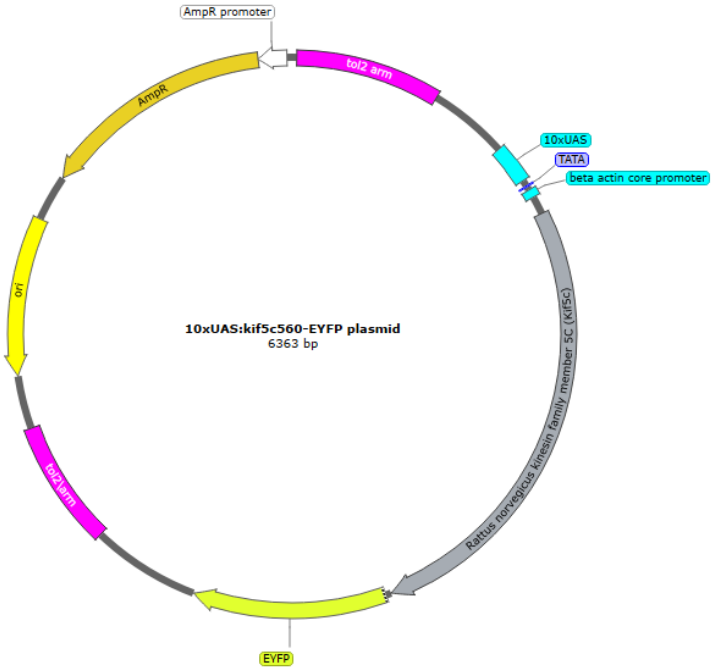

Figure 2.1 - 10xUAS:Kif5c^{560}-EYFP plasmid map. AmpR: Ampicillin resistance gene; bp: base pair; EYFP: Enhanced Yellow Fluorescent Protein; ori: origin of replication; UAS: Upstream Activating Sequence. Generated with SnapGene® software (from Insightful Science; available at snapgene.com).

2.3.2 Preparation of needles and injection plates

The microinjection needles were made from borosilicate glass capillaries (World Precision Instruments Inc.,TW100-4), with a Laser-Based Micropipette Puller (Sutter Instrument CO., Model P-2000), using the following settings:

heat = 400, filament = 4, velocity = 45, delay = 200 and pull = 100

Concerning the 1% (w/v) agarose microinjection plates (Figure 2.2), they were prepared by adding 1g of agarose to 100 mL of embryonic medium (E3) 1x and heating the mixture until all agarose was dissolved. The homogeneous solution was transferred to two petri dishes and a plastic mold was placed in the centre of both to create linear tranches later used to align the embryos. After the agarose had solidified, the mold was removed and E3 1x supplemented with methylene blue (Table 2.4), an antifungal agent, was added to the plates so that agarose does not dehydrate, crack, or gain mold. The plates were stored at 4°C until further use.

2.3.3 Fish outcross and embryo collection

Zebrafish embryos, used for the microinjection procedure, were obtained by outcrossing adult fish from the Tg(elavl3:GFF)ccu5, Tg(UAS:mCherry) line with the TU or nacre$^{-/-}$ lines, in a ratio of 3 females to 2 males. Crosses were set in 2L breeding tanks (Tecniplast®), that were assembled on the day prior to microinjection, by the combination of the outer and inner tank. The inner tank has a perforated bottom that allows the passage of the embryos and their accumulation on the outer tank, where adults cannot access thus preventing the eggs from being eaten by the progenitors that do not show any parental care behaviour (Spence et al., 2008). Additionally, a vertical plastic barrier was inserted in the middle of each tank, separating males and females, to guarantee a controlled and synchronous spawning.

In the following morning, the barrier was removed to allow the animals to mate. Ten to twenty minutes later, after spawning, fish were housed back to their original tanks, the embryos were collected using a strainer and transferred into petri dishes with E3 1x + methylene blue. The non-viable embryos were removed to a sodium hypochlorite (bleach) container, used for euthanasia of embryos/larvae under 6 dpf (Table 2.4).

For all crosses carried out during this project, a crossing frequency of once a week was maintained, to ensure the animals welfare, the quality, and the quantity of the offspring.

2.3.4 Microinjection into one-cell stage embryos

The injection mixtures were prepared on ice, comprising the Tol2 transposase mRNA, the 10xUAS:Kif5c^{560}-EYFP DNA construct, and the pH sensitive marker phenol red, as described on Table 2.2. These solutions remained on ice until further loading into the microinjection needle.

Table 2.2 - Injection mixtures composition - concentrations (in nanograms per microlitre - ng/µL) and volumes (in microlitres - µL) of the different components.

Stock solution	Volume of stock solution	Concentration in the injection mix
Tol2 mRNA (500 ng/µL)	1 µL	100 ng/µL
10xUAS:Kif5c^{560}-EYFP DNA construct (105 ng/µL)	1.19 µL	25 ng/µL
	1.42 µL	30 ng/µL
	2.38 µL	50 ng/µL
0.05% phenol red	Made up to a final volume of 5 µL	n/a

Abbreviation: n/a - not applicable.

The microinjection needle was then loaded with the injection mixture, using 20 µL Eppendorf Microloader™ tips (FISHER), and carefully attached to the PicoNozzle tip. The PicoNozzle tip is connected to a Pneumatic PicoPump (World Precision Instruments Inc., model PV 820), adjusted to the desired one-cell stage microinjection settings: pressure, vent, gated, a range of 100 ms, hold pressure of ~0.25 psi and eject pressure ~10 psi. The needle tip was broken under the stereoscope (Zeiss SteREO Discovery.V8), using a forceps (FST by DUMONT Biology) and the pressure was verified according to the desired volume to inject.

After egg collection, the embryos were transferred to the injection plate, using a plastic pipette, and aligned into its trenches (Figure 2.2). The surplus E3 medium was removed and the embryos were positioned with the 1-cell to the left, with the help of a plastic tip. Under the stereoscope, the injection mixture was delivered into the embryos by gently puncturing the chorion until reaching the cell, where the mixture was delivered through a short pulse of air pressure, activated by a foot paddle. Injection at the correct site was visually verified with the help of phenol red: loading into the embryo's perivitelline fluid results in a red spot with diffuse edges that fade over time; injection into the yolk results in a pH-induced colour shift from red to yellow and injection into the one-cell results in a red spot with defined edges (Erickson et al., 2016).

Once all embryos were injected, they were carefully transferred to a petri dish with fresh E3 medium 1x + methylene blue and incubated at 28°C. Non-injected embryos were also kept in the incubator for control purposes. The microinjection procedure was performed six times, in six different days.

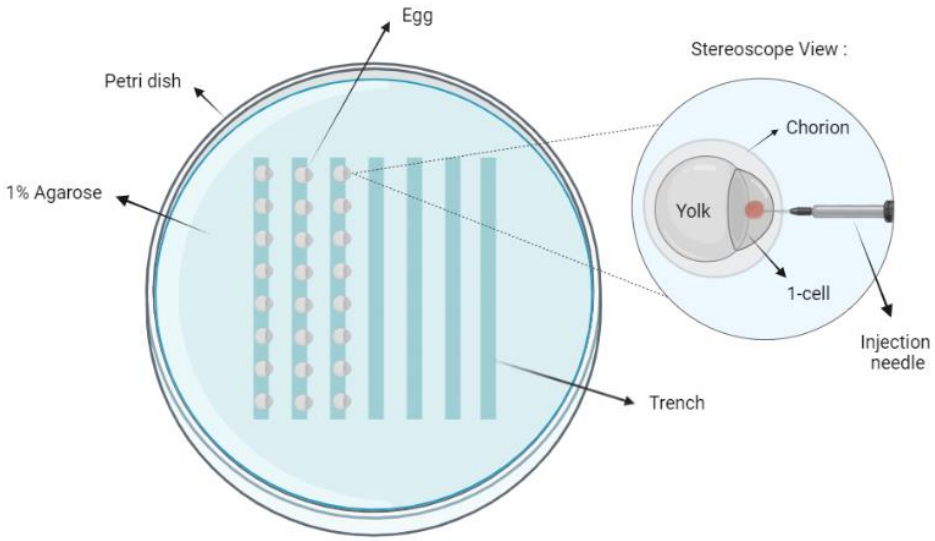

Figure 2.2 - Injection plate representation and stereoscope view during microinjection into one-cell stage embryos. The injection plates are composed by a 1% agarose matrix with perpendicular trenches, where the embryos were aligned with the 1-cell to the left. During the microinjection procedure, the needle softly perforates the embryo's chorion and the cell membrane, loading the DNA construct injection mixture (red spot) inside the cell, through a short air burst. Created with BioRender.com.

2.3.5 Embryo counting and bleaching

On the following day (1 dpf), the non-viable embryos were counted and removed from the plates to a bleach container, used for euthanasia of embryos/larvae under 6 dpf. The remaining ones were analysed regarding possible deficiencies. Both data was further used to calculate mortality and morbidity rates, to verify if any experimental condition (e.g., the injection volume and needle size) should be adjusted according to the results.

The embryos were subsequently bleached, according to Martins et al. 2016, in order to enter the water recirculation system at 5/6 dpf. The surface disinfection of embryos with sodium hypochlorite, also called bleaching, is crucial to minimize the risk of pathogen transmission within the fish population.

2.3.6 Screening for transient expression

To evaluate injections' success, the embryos were screened for Kif5c^{560}-EYFP transient expression (that accumulates on axons terminals) at 3 dpf, using the fluorescence stereoscope Axio Zoom V.16 (Zeiss) and the GFP filter. The normal and abnormal positive embryos were counted and the level of fluorescence was classified according to 4 levels of intensity: faded,

reasonable, bright, and very bright. The positive larvae presenting a bright or very bright fluorescence and a complete expression pattern, without any deficiency, were selected to be raised until reaching sexual maturity (6 to 12 weeks post-fertilization). These fish are the so-called F-1 generation.

2.3.7 Kif5c^{560}-EYFP expressing time

When screening any transgenic line, it is important to know which is the best timing to do it, in order to always selected the best positive larvae. Until here, the screens were performed at 3 dpf. However, we wanted to know if at 1 dpf there was already any visible fluorescence and if at 2 dpf it was possible or not to carry out the selection process.

In order to answer these questions, the time from which the Kif5c^{560}-EYFP protein fluorescence can be detected was study for one of the microinjection procedures, by screening the injected embryos at 1, 2 and 3 dpf. Images were acquired using the Axio Zoom V.16 fluorescence stereoscope, equipped with a Axiocam 512 mono CCD camera (Zeiss) controlled by the ZEN 2.5 2012 Blue Edition software (Zeiss), using a PlanNeoFluar Z 1x objective (NA = 0.25). The fluorescence stereoscope is set with the HXP200C fluorescence light source and fish were imaged at a 36x magnification for an overall lateral view, 82x for a brain amplified lateral view, 63x for a dorsal brain view and 85.2x for a dorsal amplified brain view.

2.3.8 Screening for stable expression

When the positive injected fish (F-1) reached sexual maturity, breeding tanks were assembled and each adult was crossed with a Tg(isl2b:Gal4), Tg(cmlc2:GFP) fish, with an opposite pigmentation to the fish of interest. On the following morning, the crossing pairs in which spawning did not occur were transferred back to their original tanks. For the pairs that generated offspring, the Tg(isl2b:Gal4), Tg(cmlc2:GFP) fish returned to the fish facility's system, whereas the F-1 fish were housed individually in 1.1L tanks (Tecniplast®) and given a unique identifier code. The embryos were collected to individual petri dishes, using different strainers, and the plates were labelled with the same identifier code as the progenitor.

The progeny was screened for stable expression, at 3 dpf, using the fluorescence stereoscope, to evaluate the germline transmission of the construct to the offspring. A total number of 200 embryos per couple, from at least two obligatory different crosses, were screened. Positive progeny was selected to be raised until adulthood, based on their fluorescence intensity (high), expression pattern (complete) and percentage of stable transgene integration (lower

percentage of positives, to ensure a higher probability of a single insertion into the genome), and gave rise to the F0 generation. Three additional larvae were selected for a confocal analysis.

At the end of this thesis, the F0 generation was growing. When these fish reach sexual maturity, the screening process described for F-1 will be repeated by the fish platform technicians to select the best founders and finally establish a stable Tg(elavl3:GFF)ccu5, Tg(UAS:mCherry), Tg(10xUAS:Kif5c^{560}-EYFP) zebrafish line, by raising the F1 population. The steps to follow for establishing a stable transgenic line are summarized in Figure 2.3.

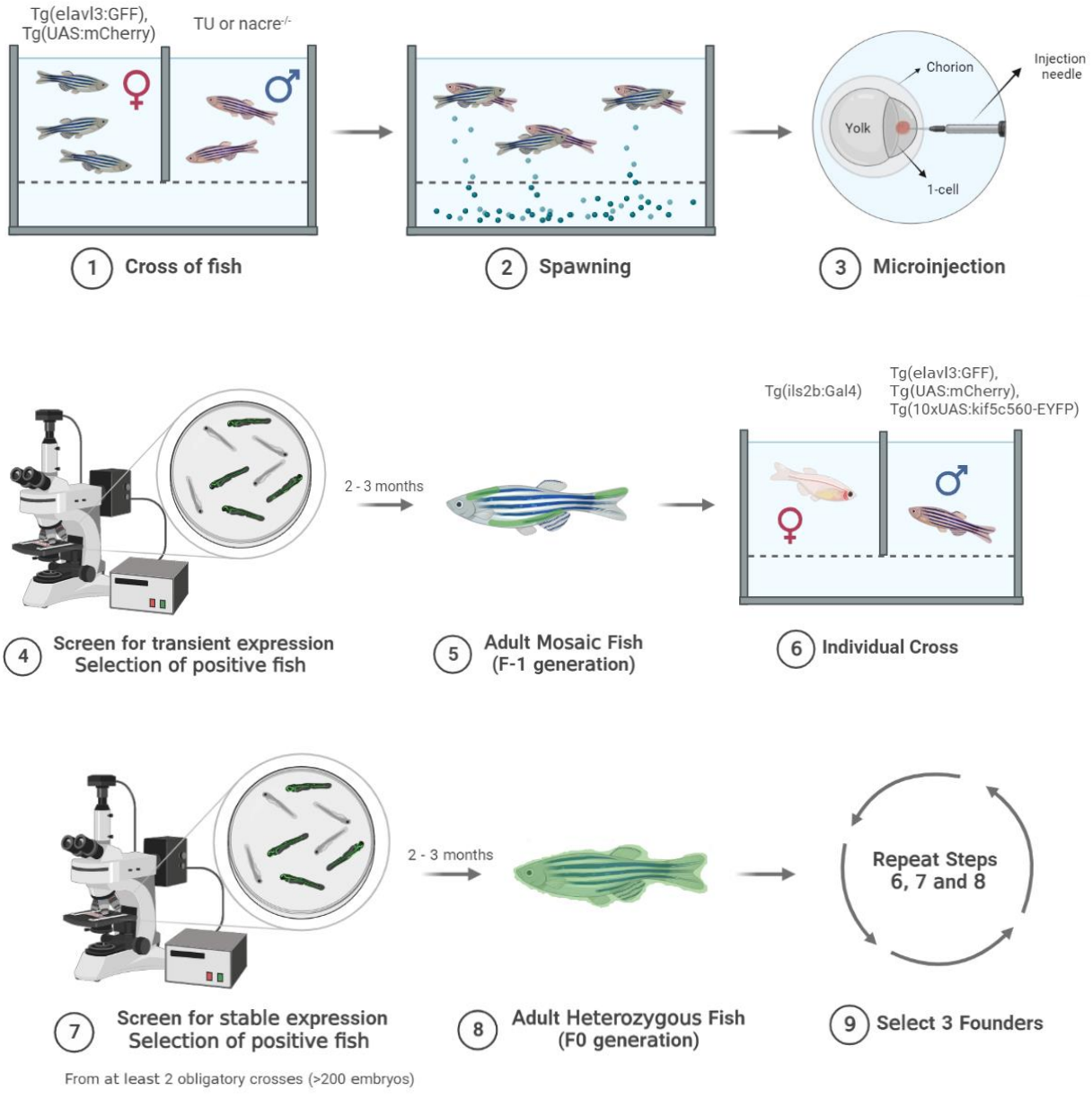

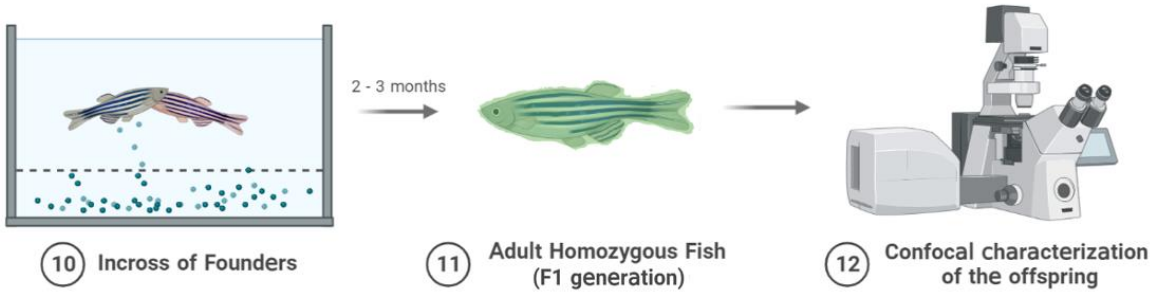

Figure 2.3 - Establishment of the Tg(elavl3:GFF)ccu5, Tg(UAS:mCherry), Tg(10xUAS:Kif5c^{560}-EYFP) transgenic zebrafish line. Firstly, Tg(elavl3:GFF)ccu5, Tg(UAS:mCherry) fish were crossed with TU or nacre$^{-/-}$, the embryos were collected and further used for 1-cell stage microinjection of the DNA construct mix (Steps 1, 2 and 3). Embryos were screened, at 3 dpf, and positive fish were selected to grow until adulthood (Steps 4 and 5). When reached sexual maturity, the F-1 generation was individually crossed with the Tg(isl2b:Gal4), Tg(cmlc2:GFP) line and the offspring, from at least two obligatory crosses, was screened for stable expression (Steps 6 and 7). Fish were raised until adulthood (Step 8). In the future, steps 6, 7 and 8 will be repeated, to select three good founders (F0) (Step 9), which will be crossed between each other (Step 10). The offspring obtained will grow until adulthood, giving rise to the F1 generation (Step 11). This line will be then completely stablished and the F1 offspring will be characterized by confocal microscopy (Step 12). Created with Biorender.com.

2.3.9 Confocal microscopy analysis

2.3.9.1 Fixation, mounting and imaging

At 3 dpf, the three selected larvae mentioned above were anesthetised in 3-amino benzoic acidethylester (tricaine) 0.6 mM (Table 2.4) and fixed in paraformaldehyde (PFA) 4% in PBS, for thirty minutes at room temperature. The samples were then rinsed two times and washed another two for five minutes, in PBT 0.25% (Table 2.4). The purpose of this step was not to perform a confocal characterization, as it was done for the other five previously-stablished transgenic lines studied on this project, but to confirm that the injected fish (F-1) were in line with the needs of the research collaborator interested in this line generation.

To be imaged through confocal microscopy, larvae were mounted directly on a glass coverslip (24 x 60 mm, 170 ± 5 µm, No. 1.5H, Superior Marienfield), in a drop of 1.5% (w/v) low-melting point agarose (Table 2.4) in PBS 1x, as straight as possible and with their dorsal side against the coverslip. The larva within the drop of agarose, was surrounded by a high vacuum silicone grease (Dow Corning®), in a U shape, and a plastic spacer (Figure 2.4). The coverslip was glued to a glass slide (T/F Ground 0.8-1.0 mm, Fisher) correctly identified, and the space left between them was filled with two drops of PBS 1x, to avoid agarose dehydration.

Larvae were imaged with the laser confocal scanning microscope (LCSM) 980 upright (Zeiss), using the long-distance LCI Plan-Apochromat 25x/0.8 multi-immersion objective lens (Zeiss). The assembly apparatus (Figure 2.4) was placed on the microscope stage, with the coverslip faced up, and a drop of Milli-Q water was used as immersion medium. Using the ZEN

2010 software, the focal planes were selected and the acquisition parameters, such as the laser power, master gain, digital gain, and digital offset, were optimized according to each larva. Anatomical z-stacks were obtained, with a z-stack slice interval of 1 µm and a pixel size of 0.80 × 0.80 (x × y), with the Alexa Fluor 488 channel. To cover the entire brain, two adjacent tiles were obtained.

2.3.9.2 Image processing and zones attribution

All images were processed and analysed using FIJI, an open-source image analysis software based on ImageJ2 (Schindelin et al., 2012). The two adjacent tiles of each sample were stitched together into one final output image using the Pairwise Stitching plugin (Preibisch et al., 2009). The fluorescence intensity was optimized using the Brightness and Contrast tool, and a standard-sized scale bar was added to the images.

The anatomical zones attribution was carried out by a direct comparison of the z-stacks obtained with reference brains of zebrafish brain atlases, such as Z-brain (Randlett et al., 2015), ZBB1.2 (Marquart et al., 2017) and mapZebrain (Kunst et al., 2019).

2.3.10 Statistical analysis

Statistical analyses were executed with R (Ihaka & Gentleman, 1996). Embryo mortality and morbidity rates were tested for assumptions for parametric analyses, namely normality and homogeneity of variances, by Shapiro–Wilk's and Levene's tests, respectively. Following, data was analysed by F test-based analysis of variance (one-way ANOVA). For all statistical analyses, the significance threshold was set to 0.05. Post-hoc comparisons were performed using TukeyHSD test.

2.4 Neuronal characterization of zebrafish transgenic lines

The neuronal spatiotemporal fluorescence expression of the five previously-stablished transgenic zebrafish lines studied during this project was performed through a whole-mount immunostaining procedure followed by confocal microscopy imaging. All processes mentioned in this section were performed twice for each zebrafish line.

2.4.1 Fish crosses and embryo collection

Zebrafish embryos were obtained by crossing adult fish, with a ratio of 6 females to 4 males. 2L tilted breeding tanks (Tecniplast®) were assembled and filled with system water, and the best fish - rounder females and more pigmented males - were selected for spawning. The

tilted breeding boxes, provide a region of shallow water, which maximizes reproductive behaviour as it mimics the natural breeding preferences of zebrafish (Martins et al., 2016). For the Tg(gata1a:GFP), Tg(aldoca:gap43-Venus), Tg(pitx2c:GFP), and Tg(glyt2:|R|-Gal4), Tg(UAS:GFP) zebrafish lines the cross was performed with nacre or pigmented fish from the same tank (incross). Regarding the Tg(pSAM:Gal4), Tg(UAS:mCherry) line, an outcross with the Tg(isl2b:Gal4), Tg(10xUAS:GCaMP6fEF05)ccu2 line was made and only the Tg(pSAM:Gal4), Tg(10xUAS:GCaMP6fEF05)ccu2 progeny was used, with the green reporter offering a better confocal visualization.

Fish matting occurs on the next morning, with spawning activity coinciding with the first activity peak, that usually starts within the first minute of exposure to light after darkness (Spence et al., 2008). The eggs fell through the perforated bottom of the inner tank, were collected using a strainer and transferred into petri dishes with E3 1x + methylene blue. Visible non-viable/dead embryos were removed from the plates, which were ultimately incubated at 28ºC. The spawners were housed back into their holding tanks.

2.4.2 Embryo care

On the next day, at 24 hpf, the non-viable embryos were removed and trashed to a bleach container and the embryonic medium was replaced by a 0.2 mM 1-phenyl 2-thiourea (PTU) solution in E3 (Table 2.4). In zebrafish, pigmentation starts developing approximately at 24 hpf. In order to improve signal detection, during confocal microscopy, PTU is used to prevent the development of pigmentation on the embryos, by blocking all tyrosinase-dependent steps in the melanin pathway. This treatment must be initiated as soon as possible, because PTU does not remove already formed pigment (Karlsson et al., 2001). Until larval fixation, at 6 dpf, the E3 + PTU medium was refreshed daily.

2.4.3 Screening of larvae for stable expression

Before the immunostaining process, larvae were anesthetized in tricaine 0.6 mM and screened for their fluorescence, at 3 dpf. The screening process, performed with the Axio Zoom V.16 fluorescence stereoscope, was crucial to select positive larvae with a complete expression pattern and a good fluorescence.

The Tg(gata1:GFP), Tg(aldoca:gap43-Venus) and Tg(pitx2c:GFP) lines were selected using a GFP filter (excitation colour: blue/cyan) that emits at the green spectrum; the Tg(pSAM:Gal4), Tg(UAS:mCherry) line was screened using a mRFP filter (excitation colour: green/yellow) that

emits at red and the Tg(glyt2:|R|-Gal4), Tg(UAS:GFP) was screened using both filters. Thirty good larvae were selected, for further fixation.

2.4.4 Whole-mount immunostaining of zebrafish larvae

2.4.4.1 Sample preparation

The imaging of larvae through confocal microscopy involves a rigorous specimen preparation, whose main objective is to maximize the fluorescence signal while preserving the 3D structure of the sample. In the case of fixed samples, the most critical preparation steps include fixation, permeabilization and blocking (Jonkman et al., 2020; Smith, 2008).

At 6 dpf, zebrafish larvae were transferred to tricaine 0.6 mM and fixed in paraformaldehyde (PFA) 4% in PBS, for two hours at room temperature. Larvae were then rinsed two times and washed another two for 5 min, in PBT 0.25% and further washed another 2x, for 5 min, with 150 mM Tris-HCl, pH 9. The fixation step main goal is to maintain the physical integrity of the sample as close to its native conformation, through the use of chemical crosslinkers, such as PFA, that crosslink with proteins and preserve cellular morphology (Hoff, 2015; Jonkman et al., 2020; Smith, 2008).

Larvae were then incubated in 150 mM Tris-HCl, pH 9, for 15 min at 70°C, cooled on ice, washed 3x in PBT 0.25% for 5 min and permeabilized in 0.05% Trypsin-EDTA (Sigma) for another 5 min, on ice. The permeabilization stage creates small holes in the lipid membrane of cells, which are vital to insure a good antibody penetration during staining (Hoff, 2015; Jonkman et al., 2020).

At the end, larvae were washed 1x in PBT 0.25% and further blocked in a mix of PBT 0.25%, 1% bovine serum albumin (BSA), 2% normal goat serum (NGS) and 1% dimethyl sulfoxide (DMSO, ReagentPlus® ≥ 99.5%, Sigma-Aldrich), overnight at 4°C. The blocking phase is essential to minimize unspecific binding of the primary antibody, avoiding any background fluorescence during confocal acquisition (Hoff, 2015; Jonkman et al., 2020).

Furthermore, it is also important to note that all the washing steps are critical for a good sample preparation, since PBS is a standard wash buffer presumed to have a membrane-stabilizing effect, thus preventing the loss of cellular components. Detergents such as Triton X-100 are added to PBS to increase the binding specificity of the antibodies used during the immunofluorescence staining phase (Hoff, 2015; Jonkman et al., 2020).

2.4.4.2 Whole-mount immunofluorescence staining

The whole-mount staining of larvae was performed through an immunohistochemistry protocol that labelled the extracellular signal-regulated kinases (ERKs) 1 and 2, therefore called a total ERK (t-ERK) staining. ERKs are expressed in several zebrafish structures, including the brain and retina, being a good target for a homogeneous staining. The two isoforms are ubiquitously expressed without obvious regulatory differences or subcellular localization. This labelling is crucial for examining the spatiotemporal expression of endogenous fluorescent molecules, allowing a better visualization of the entire brain during image acquisition (NHI, 2022; Randlett et al., 2015; Santos et al., 2018).

Therefore, larvae were incubated for 3 overnights at 4°C with a primary antibody mix of PBT 0.25%, 1% BSA, 1% DMSO and 1:500 mouse anti-tERK. After that, samples were rinsed 3x and washed 3x, for 30 min, with PBT 0.25% and incubated 3 overnights at 4°C with a secondary antibody mix of PBT 0.25%, 1% BSA, 1% DMSO and 1:500 goat anti-mouse IgG Alexa^{TM} 568. In the case of the Tg(glyt2:|R|-Gal4), Tg(UAS:GFP) line it was not possible to transpose its endogenous mCherry fluorescence to a green reporter, as previously performed for the Tg(pSAM:Gal4), Tg(UAS:mCherry) line. It would have been necessary to use a Cre reporter line expressing a green fluorophore and such line was not available at CF fish platform. So instead of that, the t-ERK was stained with the goat anti-mouse IgG Alexa^{TM} 488 green secondary antibody. Complete information regarding the three antibodies used is presented in Table 2.3. To finish, larvae were rinsed 3x and washed another 3x, for 30 min, with PBT 0.25% and stored in a PBT 0.25% solution with 0.05% sodium azide, until the mounting process.

Table 2.3 - Antibodies complete information - full length denomination, manufacturer reference, isotype and concentration used on the final mix.

	Denomination	Manufacturer reference	Isotype	Dilution
Primary antibody	mouse anti-tERK, p44/42 MAPK (ERK1/2)	Cell signalling, 4696	IgG1	1:500
Secondary antibody	Goat anti-mouse polyclonal Alexa Fluor^{TM} 568	ThermoFisher, A-11004	IgG (H+L)	1:500
Secondary antibody	Goat anti-mouse polyclonal Alexa Fluor^{TM} 488	ThermoFisher, A-11001	IgG (H+L)	1:500

Abbreviations: ERK - Extracellular signal-Regulated Kinase; H+L - gamma immunoglobins Heavy and Light chains; IgG - Immunoglobulin G; MAPK - Mitogen-Activated Protein Kinase; t-ERK - total ERK.

2.4.5 Mounting of larvae

In order to be imaged on the confocal microscope, larvae were directly mounted on a glass coverslip, in a drop of 1.5% (w/v) low-melting point agarose in PBS 1x, as straight as possible and with their dorsal side against the coverslip. Agarose mounting is commonly used when a specific orientation is desired, and/or when the structures to be imaged impose a naturally unstable orientation, such as a dorsal orientation for imaging the brain (Renaud et al., 2011). The larva within the drop of agarose, was surrounded by a high vacuum silicone grease, in a U shape, and a plastic spacer (Figure 2.4). Using the silicone grease, the coverslip was glued to a glass slide correctly identified, and the space left between them was filled with ~2 drops of PBS 1x, to avoid agarose dehydration. The samples were stored at 4ºC, until further analysis.

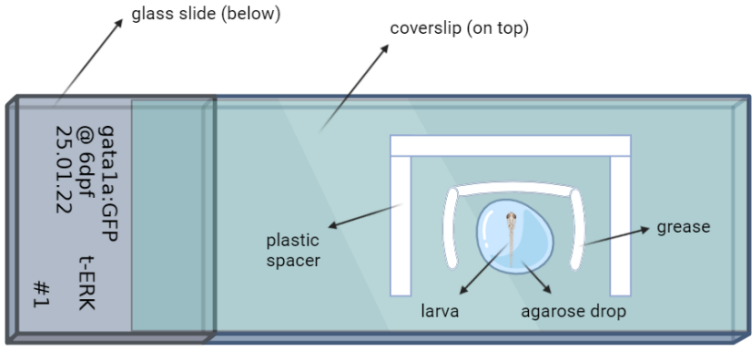

Figure 2.4 - Representation of larval mounting. Zebrafish larva was mounted directly in the coverslip, on a 1.5% (w/v) low-melting point agarose drop, surrounded by a silicone grease and a plastic spacer. The coverslip was then glued to a glass slide, previously identified with the line name (e.g., gata1a:GFP), development stage (6 dpf), date (e.g., 25.01.22), immunohistochemistry labelled protein (t-ERK), and larva identification (#1). t-ERK: total extracellular signal-regulated kinase; @: "at". Created with Biorender.com.

2.4.6 Confocal imaging

Larvae were imaged with the laser confocal scanning microscope (LCSM) 980 upright, using a long-distance LCI Plan-Apochromat 25x/0.8 multi-immersion objective lens, specialized in deep tissue imaging. Using the confocal microscope, it is possible to obtain high-contrast images used to investigate the spatial arrangement of fluorescent markers, without the need of physically slice the specimen. By scanning the sample on the z-axis, the image is obtained, pixel by pixel, by recording the fluorescence intensity at each position. The LCSM takes a series of single confocal images, called 'slices', which are then used to reconstruct the entire volume of the sample by the production of a 3D dataset, or 'z-stack' (Jonkman et al., 2020; Sanderson et al., 2016; Smith, 2008).

The assembly apparatus (Figure 2.4) of each sample was placed on the microscope stage, with the coverslip faced up, and a drop of Milli-Q water was used as immersion medium. Using the ZEN 2010 software, the focal planes were selected and the acquisition parameters,

such as the laser power, master gain, digital gain, and digital offset, were optimized according to each larva. Anatomical z-stacks were obtained, with a slice interval of 1 µm and a pixel size of 0.80 × 0.80 (x × y), with two different channels - Alexa Fluor 488 (for GFP detection) and Alexa Fluor 568 (for t-ERK detection). To cover the entire brain, two adjacent tiles were obtained. Since the imaging was performed with larvae's dorsal side up, the image quality may be lower in the most ventral areas of the brain.

2.4.7 Image processing using FIJI

All images were processed and analysed using FIJI. The two adjacent tiles were stitched together into one final output image using the Pairwise Stitching plugin (Preibisch et al., 2009). After that, the pixel size was verified and corrected, if needed, to the same value as the .czi original file. The fluorescence intensity of each channel was optimized using the Brightness and Contrast tool, and a standard-sized scale bar was added to all images.

For the Tg(gata1a:GFP), immunohistochemistry round 2 and the Tg(aldoca:gap43-Venus), on both rounds, an insufficient permeabilization of larvae led to a poor antibody penetration and its consequent accumulation on larvae's skin. Therefore, the samples were processed using the Segmentation Editor plugin (Schindelin et al., 2012), used to remove the high marked superficial skin.

2.4.8 Lines characterization

The anatomical characterization of the five previously-stablished transgenic lines studied on this project was carried out by a direct comparison of the obtained z-stacks with reference zebrafish brain atlases, such as Z-brain, ZBB1.2 and mapZebrain, and bibliography concerning similar lines. The anti-t-ERK pattern was crucial as reference for the identification of zones presenting fluorescence, since it allowed a better visualization of each structure boundary. Additionally, this staining is necessary for the registration of our images into a well-established zebrafish brain atlas, as this pattern is used to ensure a more accurate merging of the different samples from the same line.

2.4.9 Registration of images on ZBB atlas

The registration of whole brain images into reference atlases (Figure 2.5) is crucial to expand the scientific knowledge about the complex brain dynamics and its organization. However, the biological variability of the samples must be considered before, so images need to suffer important transformations during the registration process.

Firstly, images (pixel size = 0.8 x 0.8) were transformed, using the size function of FIJI, to match the reference pixel size of ZBB1.2 atlas (pixel size = 1 x 1). The two channels were split, and two output images were obtained - one for the GFP, gap43-Venus or mCherry channel and another for the t-ERK channel.

Previous to this project, six good t-ERK confocal stacks were obtained and used to create a reference t-ERK brain model, by an average of all stacks. This model was used in the ANTs (Advanced Normalization Tools) algorithm applied by Ruth Diez del Corral to the images obtained for the lines under study.

In summary, the ANTs algorithm compares the t-ERK channel images of each line to the reference t-ERK brain model and transform them to be as similar as possible to the reference. These transformations must be kept to a minimum to avoid local distortions and loss of precious information, which continues to be a challenge in brain registration. It is important to preserve cell morphology, but some deformation is also required to overcome biological variability between individual brains or malformations due to tissue processing (Marquart et al., 2017). After that, the ANTs algorithm uses the transformation matrix applied to the t-ERK images to also transform the GFP, gap43-Venus or mCherry channel images so that they undergo to the exact same changes. Finally, an average is calculated by a merge of the best images of each line, and a reference model for the expression pattern is obtained.

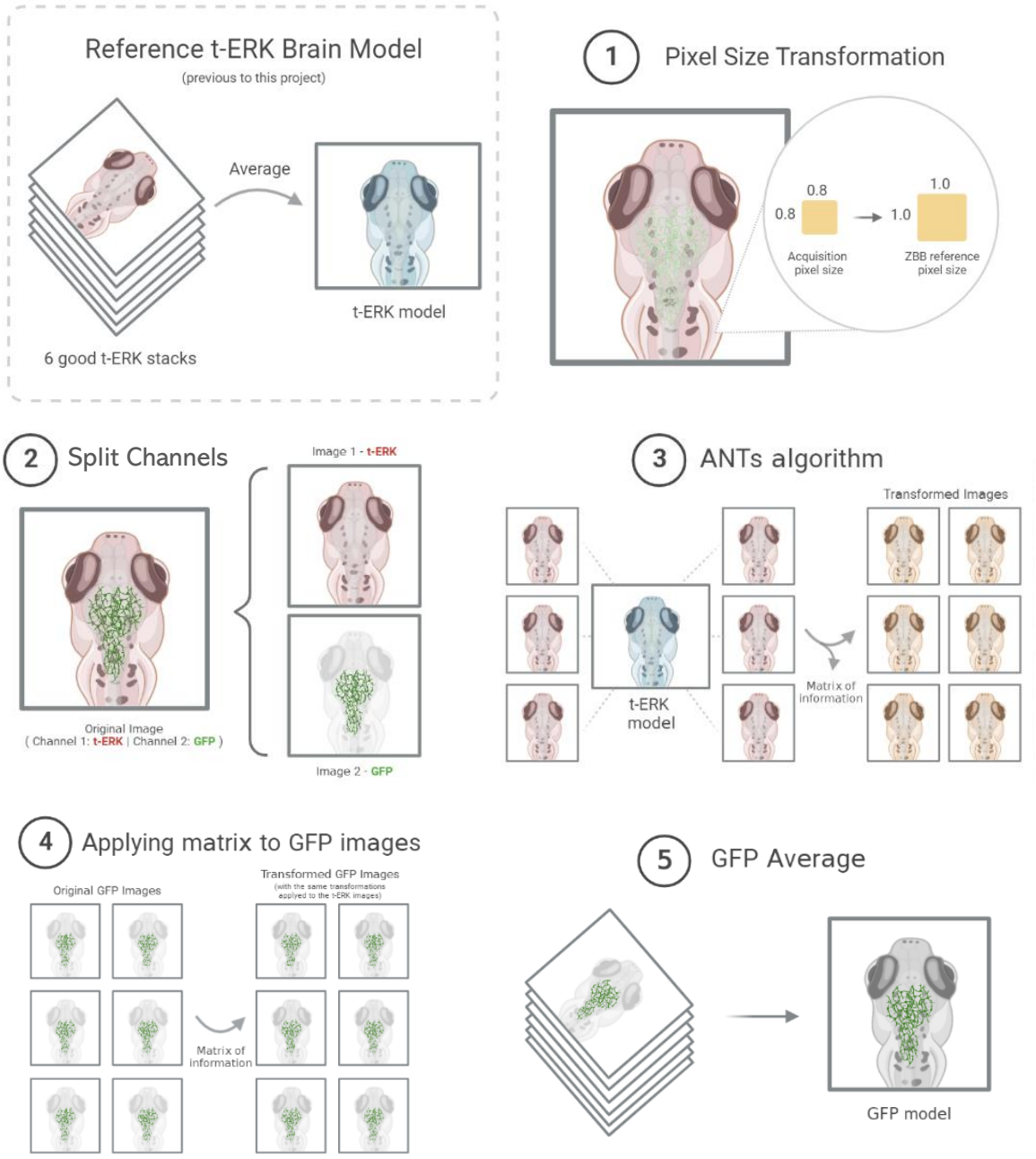

Figure 2.5 - Atlas registration workflow. Previously to this project, six good t-ERK confocal stacks were obtained and used to create a reference t-ERK brain model. On stage 1, the images of the lines under study passed through a pixel size transformation (0.8 x 0.8 to 1 x 1) to match the reference pixel size of ZBB1.2 atlas. On stage 2, the channels were split and two output images were obtained (one for the GFP channel (for example) and another for the tERK). On stage 3, the reference model was used in the ANTs algorithm, that compared the t-ERK channel images to the reference t-ERK brain model, transforming them to be as similar as possible to the reference. This algorithm stored the transformations employed into a matrix. On stage 4, this matrix was applied to the GFP images, so that they undergo to the exact same changes as the t-ERK. Finally, on stage 5, an average was calculated by a merge of all GFP images, and a GFP reference model was obtained. ANTs: Advanced Normalization Tools; GFP - Green Fluorescent Protein; t-ERK: total Extracellular signal-Regulated Kinases; ZBB1.2 - Zebrafish Brain Browser 1.2. Created with Biorender.com.

2.5 Reagents and chemicals

All reagents and chemicals used during this project were of standard practical grade (P.A.) and the most significant are presented in Table 2.4.

Table 2.4 - Reagents and chemicals used, their composition, and manufacturer.

Solution name	Composition	Manufacturer
Embryonic medium (E3 - 50x stock solution)	146.9 g NaCl ; 6.3 g KCl ; 24.3 g $CaCl_2.2H_2O$; 40.7 g $MgSO_4.7H_2O$; 10L Milli-Q water (Concentrations: 0.25 M NaCl, 8.45 mM KCl, 16.5 mM $CaCl_2.2H_2O$ and 0.16 M $MgSO_4.7H_2O$)	n/a
Embryonic medium + methylene blue (E3 - 1x working solution)	400 mL of E3 50x (stock solution) ; 60 mL 0.01% methylene blue solution ; Filled to 20 L with system water (Concentrations: 5 mM NaCl; 0.17 mM KCl; 0.33 mM $CaCl_2$; 0.33 mM $MgSO_4$; $3x10^{-5}$ % Methylene Blue)	n/a
0.3 mM Methylthioninium chloride (methylene blue stock solution)	0.05 g methylene blue powder ; 500 mL Milli-Q water	Sigma
0.5% Phenol Red solution (stock solution)	n/a	Sigma Lot # RNBF2888
0.05% Phenol Red solution (working solution)	100 µL of 0.5% Phenol Red (stock solution) ; 900 µL Milli-Q water	n/a
Phosphate-Buffered Saline (pH 7.2) (PBS - 1x)	8 g NaCl ; 0.2 g KCl ; 1.44 g Na_2HPO_4 ; 0.245 g KH_2PO_4 ; 1L Milli-Q water (Concentrations: 0.137 M NaCl; 2.70 mM KCl; 0.01 M Na_2HPO_4 and 1.80 mM KH_2PO_4)	n/a
4% paraformaldehyde (PFA) in PBS	40 g of PFA powder ; 800 mL of PBS 1x solution	n/a
10% Triton X-100 (stock solution)	100 mL of Triton X-100 ; 900 mL of Milli-Q water	n/a
0.25% PBT (PBS 1x + Triton 0.25%)	1,250 mL of Triton 10% ; 48,75 mL of PBS 1x solution	n/a
1.5% (w/v) low-melting point agarose	0.75 g of UltraPure™ low-melting point agarose ; 50 mL of PBS 1x solution	Invitrogen

1 M Tris-HCl (pH 9.0) (stock solution)	12.11 g Tris base ; 80 mL Milli-Q water ; Adjust pH to 9.0 with HCl ; 100 mL Milli-Q water	n/a
150 mM Tris-HCl (pH 9.0) (working solution)	15 mL of 1 M Tris-HCl (stock solution) ; 85 mL of Milli-Q water	n/a
Sodium hypochlorite (Bleach - working solution for surface disinfection of embryos)	36 ppm 10%	Sigma
15 mM Ethyl 3-aminobenzoate methanesulfonate (Tricaine - 25x stock solution)	2 g Tricaine powder ; 500 mL reverse osmosis water (pH 7.0) ; 10 mL of 1 M Tris (1M Tris: 121.14 g Trizma base ; in 1 L reverse osmosis water; pH 9.0)	Sigma
0.6mM Ethyl 3-aminobenzoate methanesulfonate (Tricaine - 1x working solution)	20 mL of 15 mM Tricaine (stock solution) ; 480 mL system water or 1x embryo medium	n/a
60 mg/mL Pronase (100x stock solution)	1 g Pronase ; 16.7 mL Milli-Q water	Roche Lot # 10165921001
6 mg/mL Pronase (1x working solution)	100 µL of 100x Pronase (stock solution) ; 9.9 mL 1x E3 medium (working solution without methylene blue)	n/a
10 mM 1-phenyl 2-thiourea (PTU - 50x stock solution)	152 mg PTU powder ; 100 mL Milli-Q water	Sigma
0.2 mM 1-phenyl 2-thiourea (PTU - 1x working solution)	1 mL of PTU 50x (stock solution) ; 1 mL 50x E3 (stock solution) ; 48 mL system water	n/a

Abbreviations: n/a - not applicable.

3

RESULTS

3.1 Generation of a new and stable zebrafish line

3.1.1 F-1 population

3.1.1.1 Mortality and morbidity rates

To generate the Tg(elavl3:GFF)ccu5, Tg(UAS:mCherry), Tg(10xUAS:Kif5c^{560}-EYFP) zebrafish line, six rounds of microinjections were performed. The number of aborted embryos was counted and the living ones were analysed for malformations. Non-injected embryos were kept for control purposes, being vital to assess what was the baseline mortality of the line and what was the mortality associated with the microinjection technique (Figure 3.1).

Although no statistically significant differences were found between different injection rounds (ANOVA F-test, $p > 0.05$), mortality and morbidity were variable, which can be associated with stochastic factors during the injection process *per se*, besides inter-individual variation. Round 1 (Figure 3.1A) caused higher mortality, in general, in both control and injected groups (~51% for the control and ~88% for both plasmid concentrations), so in the following rounds, the microinjection volume was decreased as part of the optimisation process.

There were no abnormal embryos among the control groups, whereas among the injected groups the rate ranged between 3-44%, also presenting clear variations between different rounds. Overall, the mean morbidity rate tended to be higher in round 1. The needle tip diameter was checked in posterior sessions to ensure a small enough size to deliver the payload with minimal disruption of the embryos.

Microinjection with different DNA concentrations was hypothesised to be important to investigate the toxicity of the construct. Still, no significant effect on concentration was found in any round (ANOVA F-test, $p > 0.05$). Nonetheless, in most cases, a tendency for a decrease in the number of abnormal embryos was recorded when higher concentrations of plasmid were delivered.

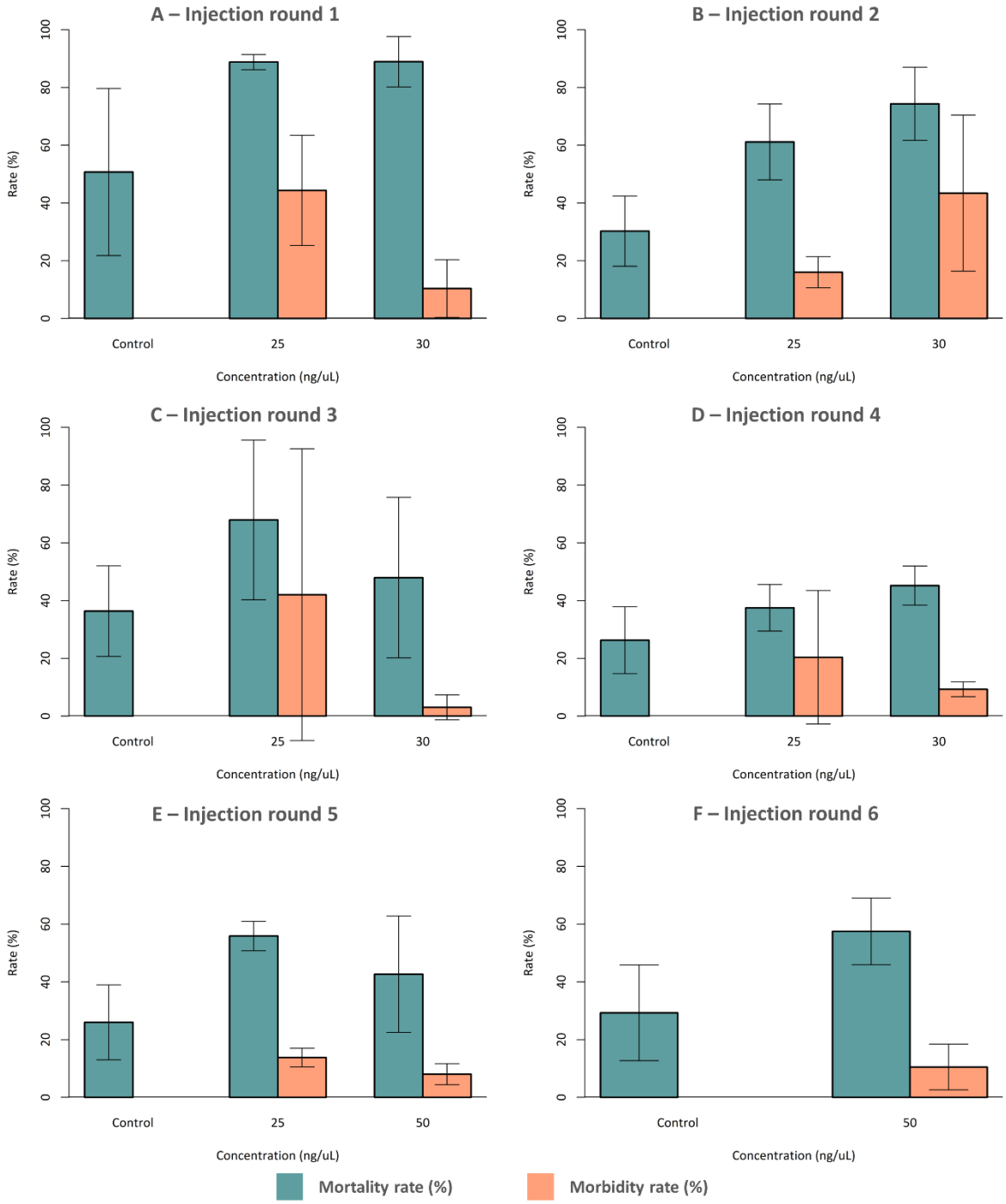

Figure 3.1 - Zebrafish embryo mortality and morbidity rates at 24 hpf, after injection of a mix comprising 25, 30 or 50 ng/µL (concentration in nanograms per microlitre) of the 10xUAS:Kif5c^{560}-EYFP DNA construct and 100 ng/µL of tol2 mRNA. Non-injected embryos were used as control. A - microinjection round 1; B - microinjection round 2; C - microinjection round 3; D - microinjection round 4; E - microinjection round 5; F - microinjection round 6. Data are presented as mean ± standard deviation. No significant effect of concentration was found in any individual round (F test-based ANOVA, $p > 0.05$). See also Appendices 1-7 in Supplementary Information for further details.

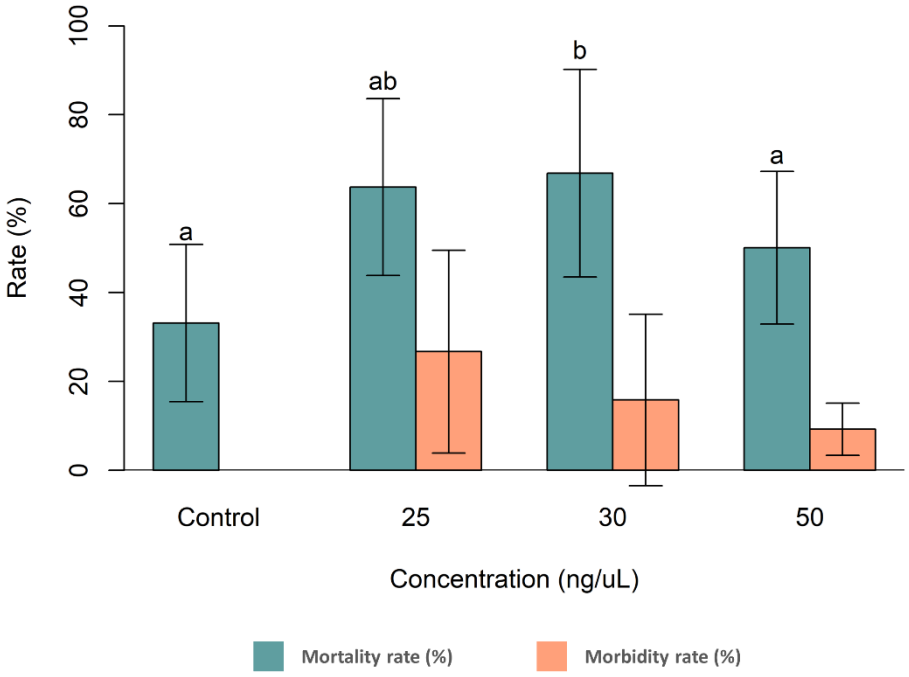

Figure 3.2 - Combined mortality and morbidity rates of zebrafish embryos from the six microinjection rounds. Embryos were injected with an injection mix comprising 25, 30 or 50 ng/µL (concentration in nanograms per microlitre) of the 10xUAS:Kif5c^{560}-EYFP DNA construct and 100 ng/µL of tol2 mRNA. Non-injected embryos were used as control. Data are presented as mean ± standard deviation. A significant effect of concentration was found (TukeyHSD Test, $p < 0.05$), indicated by different letters (a and b).

Only when the six rounds data were combined was replication enough to overcome variability and increase statistical power (Figure 3.2), which resulted in significant variations in mortality between treatments (TukeyHSD Test, $p < 0.05$). Regarding morbidity, such differences were not found (TukeyHSD, $p > 0.05$). Comparing the mortality of the control (~33%) and the injected groups (between 50-67%), statistical differences were not observed for a concentration of 50 ng/µL and were observed for a concentration of 30 ng/µL. The lowest concentration (25 ng/µL) showed no significant differences when compared to any other group. As these results were inconclusive in terms of concentration optimization, this aspect needed to be further evaluated according to the number and quality of positives obtained.

3.1.1.2 Screen for transient expression

To evaluate injections' success (integration of the construct into the fish genome), the embryos were screened for Kif5c^{560}-EYFP transient expression at 3 dpf. The normal and abnormal positive embryos were counted and the level of fluorescence was classified according to four levels of intensity: faded, reasonable, bright, and very bright (Figure 3.3).

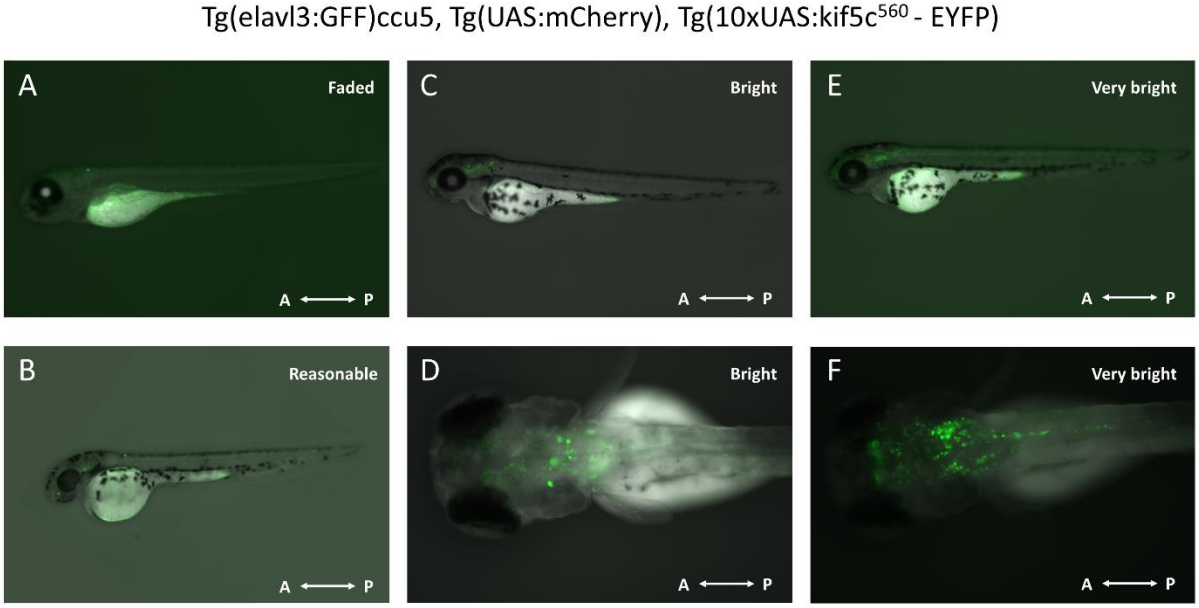

Figure 3.3 - Transient expression at 3 dpf of the Tg(elavl3:GFF)ccu5, Tg(UAS:mCherry), Tg(10xUAS:Kif5c^{560}-EYFP) zebrafish line - fluorescence intensity levels: faded, reasonable, bright, and very bright. A - faded expression pattern (lateral view); B - reasonable expression pattern (lateral view); C - bright expression pattern (lateral view); D - bright expression pattern (dorsal view); E - very bright expression pattern (lateral view); F - very bright expression pattern (dorsal view). Images acquired on Zeiss Axio Zoom.V16 fluorescence stereoscope, equipped with the Zeiss Axiocam 512 mono CCD camera and controlled by the Zeiss ZEN 2.5 2012 Blue Edition software, using a PlanNeoFluar Z 1x objective (NA = 0.25) and the GFP filter. All images present an anterior (A) - posterior (P) axis.

The Tg(elavl3:GFF)ccu5, Tg(UAS:mCherry), Tg(10xUAS:Kif5c^{560}- EYFP) line presented a characteristic elavl3 pan-neuronal expression pattern, homogenous throughout the brain, with a localized fluorescence on the axon terminals characteristic of the Kif5c^{560} protein.

The fluorescence intensity level designated as faded (Figure 3.3A) was described by either a very low fluorescence intensity and/or an incomplete expression pattern, in which few neurons presented green fluorescence. The second level of intensity (Figure 3.3B) was defined by a low fluorescence and/or an almost complete expression pattern. Bright (Figure 3.3C and D) and very bright (Figure 3.3E and F) levels were characterized by a complete expression pattern and a high green fluorescence, with the latter being brighter.

The positive larvae presenting a bright or very bright fluorescence and a complete expression pattern, without any deficiency, were selected to be raised until adulthood, giving rise to five F-1 lines - 3407, 3419, 3425, 3424, and 3446 (Table 3.1).

Table 3.1 - Screen for transient expression of the Tg(elavl3:GFF)ccu5, Tg(UAS:mCherry), Tg(10xUAS:Kif5c^{560}- EYFP) F-1 population, at 3 dpf. The embryos were obtained from a cross of the Tg(elavl3:GFF)ccu5, Tg(UAS:mCherry) line with a TU or nacre$^{-/-}$ line and injected, at one-cell stage, with a mix comprising 25, 30 or 50 ng/µL (nanograms per microlitre) of the 10xUAS:Kif5c^{560}-EYFP DNA construct and 100 ng/µL of Tol2 mRNA.

F-1 population screen results														
Injection ID	Concentration (ng/µL)	Number of injected embryos	Number of screened larvae	Number of positive fish			Integration rate (%) at 3dpf [(a)]	Fluorescence classification				Number of raised larvae	Number of surviving larvae	F-1 line number
				T	N	A		VB	B	R	F			
1	25	163	20	3	1	2	15.0	2	1	0	0	1	0	-
	30	129	15	1	1	0	6.67	1	0	0	0	1	0	-
2	25	215	82	21	12	9	25.61	0	0	3	9	0	-	-
	30	155	45	12	7	5	26.67	1	1	3	2	0	-	-
3	25	103	25	12	7	5	48.0	0	2	1	9	0	-	-
	30	148	66	10	7	3	15.2	2	0	3	5	2	2	3407
4	25	132	85	14	9	5	16.5	0	2	6	6	1	1	3419
	30	125	71	25	24	1	35.2	0	1	9	15	0	-	-
5	25	587	249	54	41	13	21.7	3	4	30	17	4	4	3425
	50	334	196	42	36	6	21.4	11	9	10	12	12	11	3424
6	50	404	186	64	55	9	34.4	8	13	17	26	14	9	3446

Abbreviations: A - abnormal; B - bright; F - faded; ID - identification; N - normal; R - reasonable; T - total; VB - very bright; [(a)] - (Number of total positive fish / Number of screened larvae) x 100

Although a large number of embryos were injected (a total of 2,495), only ~42% (1,040 embryos) survived until the screen time point, at 3 dpf, and even fewer (~25%) exhibited fluorescence (258 positives). Among the positive, ~22% (58 larvae) presented an abnormal development and were not selected to be raised. All microinjection rounds were successful for the presence of fluorescence, with a construct integration rate between ~7% to 48%.

The highest integration rate (48%) was obtained in round 3, for a concentration of 25 ng/µL. However, only 9% of the embryos injected in that round (corresponding to 2 embryos) presented a bright fluorescence and were not selected to be raised due to the presence of some development abnormalities in the eyes and jaw. It is also important to mention that a high integration rate does not necessarily mean the presence of good positive larvae (the ones with a bright or very bright and complete expression), as this case emphasizes. In fact, the highest numbers of good positive larvae were obtained in microinjection rounds 5 and 6, where the integration rate ranged between 21% and 34%.

Evaluating the effect of plasmid concentration in obtaining "good" larvae (classified as bright and very bright), the concentration of 30 ng/µL revealed poor results (6 embryos), followed by the dose of 25 ng/µL (13 embryos). A better outcome was verified for the 50 ng/µL concentration, where the number of "good" larvae practically tripled (41 embryos). As there were no statistically significant differences in terms of mortality between the control group and the 50 ng/µL injected one (Figure 3.2), this concentration can be considered as a reference for future microinjections of the 10xUAS:Kif5c^{560}-EYFP DNA construct.

Overall, from the "good" larvae obtained, only 57% (35 larvae) entered the fish facility's main system, since the remaining ones presented malformations and were euthanized. Of the healthy ones, 8 larvae did not survive, possibly due to some malfunction caused by the injection technique that was not detected before or was not physically visible, or even due to a natural cause. In fact, larvae from round 1 died the day after entering the system from some development abnormality that was not previously detected. For that reason, from injection round 2 onwards, all larvae were checked under the stereoscope before entering the system. Twenty-seven healthy larvae were raised until adulthood as F-1 lines, with designated numbers (Table 3.1).

3.1.1.3 Kif5c^{560}-EYFP expressing time

The time from which the Kif5c^{560}-EYFP protein could be detected was study by screening, under the fluorescence stereoscope, injected embryos at 1, 2 and 3 dpf.

At 1 dpf (Figure 3.4A) it was already possible to visualize a localized fluorescence in the brain and at 2 dpf (Figure 3.4B and C) Kif5c^{560}-EYFP fluorescence was detected by a sparse, incomplete, and less bright pattern, in comparison to the 3 dpf. At 3 dpf (Figure 3.4D and E), the fluorescence was brighter, with a pan-neuronal pattern characteristic of the elavl3 promoter, but with a localized/dotted expression due the accumulation of the Kif5c^{560} protein in axon terminals. Additionally, larvae's yolk size and its natural curvature at 2 dpf made it difficult to position the specimen for a clear dorsal view, which ultimately complicates the screen process. In conclusion, the results showed that it is possible to screen larvae for Kif5c^{560} at 2 dpf but it is advisable to carry out the selection at 3 dpf.

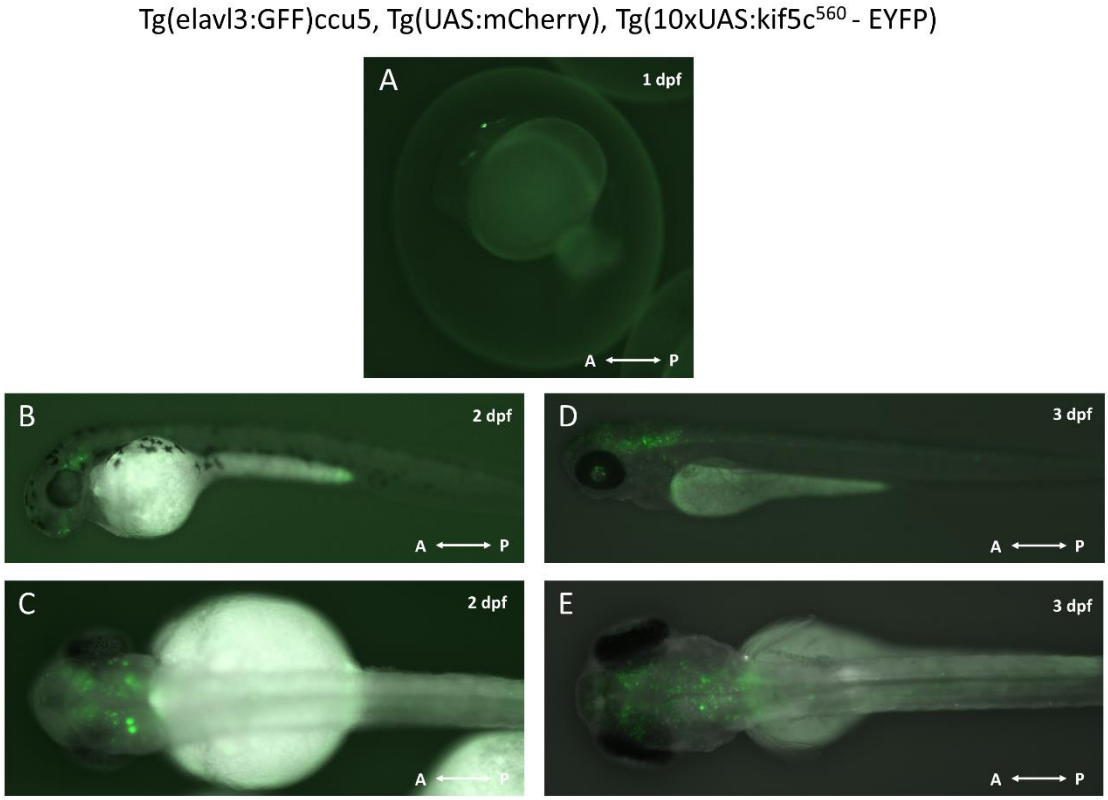

Figure 3.4 - Expression pattern, during development, of the Tg(elavl3:GFF)ccu5, Tg(UAS:mCherry), Tg(10xUAS:Kif5c^{560}-EYFP) zebrafish line. A - embryonic view at 1 dpf; B and C - lateral and dorsal view at 2 dpf, respectively; D and E - lateral and dorsal view at 3 dpf, respectively. Images acquired on Zeiss Axio Zoom.V16 fluorescence stereoscope, equipped with a Zeiss Axiocam 512 mono CCD camera and controlled by the Zeiss ZEN 2.5 2012 Blue Edition software, using a PlanNeoFluar Z 1x objective (NA = 0.25) and the GFP filter. All images present an anterior (A) - posterior (P) axis.

3.1.2 F0 population

3.1.2.1 Assessment of germline transmission

Once the F-1 generation reached sexual maturity, the progeny was screened to confirm which injected fish presented germline transmission (Table 3.2).

Positive larvae were selected and raised as F0 populations, based on their fluorescence intensity (bright and very bright) and expression pattern (complete). Other criteria considered for the F0 selection was a low percentage of positives, to ensure a higher integration efficiency. A lower percentage of positives is normally indicative of a higher probability of a single integration event into the genome, which favours stable expression over generations.

All the F-1 populations presented germline transmission, and just 5 out of the 27 injected fish raised were negative - 3419.1, 3424.2, 3424.3, 3424.8 and 3446.9. The results were inconclusive for the 3425.4, 3424.10, 3424.11 and 3446.8 that did not follow the established premise regarding the need to screen 200 embryos from at least two obligatory crosses. For

that reason, they are highlighted in red on Table 3.2. Fish 3446.4 and 3446.6 also did not respect that premise so were not used to stablish the F0 generation, despite presenting germline transmission. In the future, more crosses must be carried out for all the six fish, in order to infer with certainty their nature (positive or negative) and/or their germline transmission efficiency.

From the sixteen confirmed positive fish that respected the screens criteria, the germline transmission varied between 0.80% and 28.82%. This high variability is frequent and may be related to a different quality of the injected embryos or their exact development phase within the one-cell stage, upon injection.

The 3424.4, 3424.7, 3424.9, 3446.1, 3446.3 fish stood out due to a low integration rate of their progeny, but were not further used for line establishment since the 3424.4, 3424.9 and 3446.3 did not present any progeny with a bright or very bright expression pattern and the positive progeny of 3424.7 and 3446.1 did not include any larvae scored as very bright. Therefore, they were not selected to grow as F0.

As for 3425.2 and 3425.3, their progeny stood out from the rest due to a low number of positives coupled to a high quality, namely a complete pan-neuronal expression pattern and a high fluorescence intensity. Therefore, they were selected for further steps towards the establishment of the new stable transgenic line, giving rise to two F0 populations. Fish 3424.6 was also considered for the same purposes and its progeny was screened by one of fish platform technicians. Two good positive larvae were selected to be raised as another F1 promising line - 3790 (data not shown). Due to some possible silencing effects, is recommended to select at least three independent fish for the establishment of each generation, from F0 onwards.

Table 3.2 - Screen for stable expression of the Tg(elavl3:GFF)ccu5, Tg(UAS:mCherry), Tg(10xUAS:Kif5c^{560}-EYFP) F0 population, at 3 dpf. Embryos were obtained from crosses with the Tg(isl2b:Gal4), Tg(cmlc2:GFP) line and the progeny was labelled with a unique individual ID. A total of 200 embryos per couple, from at least two obligatory crosses, were screened. In red are identified the fish that need to be crossed again, to follow this assumption. In bold are highlighted the fish selected for further steps towards line establishment.

F0 population												
F-1 line number	Individual ID	Number of screened larvae	Number of positive	Germline transmission rate (%) at 3dpf [a]	Expression pattern			Fluorescence classification			Number of larvae raised	F0 line number
					C	I	VB	B	R	F		
3407	3407.1	1358	75	5.52	7	68	1	6	33	35	0	-
	3407.2	919	90	9.79	32	58	14	18	35	23		
3419	3419.1	303	0	0.00	-	-	-	-	-	-	-	-
3425	3425.1	303	47	13.82	12	35	7	5	15	20	-	-
	3425.2	**457**	11	2.41	6	5	2	4	2	3	2	3637
	3425.3	**281**	7	2.49	2	3	2	1	1	2	1	3701
	3425.4	2	0	0.00	-	-	-	-	-	-	-	-
3424	3424.1	312	76	24.36	5	71	1	4	23	48	0	-
	3424.2	222	0	0.00	-	-	-	-	-	-	0	-
	3424.3	457	0	0.00	-	-	-	-	-	-	0	-
	3424.4	720	9	1.25	0	9	0	0	0	9	0	-
	3424.5	288	83	28.82	17	66	1	16	32	34	0	-
	3424.6	336	4	1.19	3	1	3	0	1	0	0	-
	3424.7	459	10	2.18	2	8	0	2	5	3	0	-
	3424.8	402	0	0.00	-	-	-	-	-	-	0	-
	3424.9	500	4	0.80	0	4	0	0	0	4	0	-
	3424.10	227	0	0.00	-	-	-	-	-	-	0	-
	3424.11	0	-	-	-	-	-	-	-	-	-	-
3446	3446.1	475	7	1.47	3	4	0	3	0	4	0	-
	3446.2	356	12	3.37	1	11	1	0	3	8	0	-
	3446.3	327	5	1.53	0	1	0	0	0	1	0	-
	3446.4	151	9	5.96	7	2	7	0	2	0	0	-
	3446.5	-	-	-	-	-	-	-	-	-	0	-
	3446.6	45	7	15.56	2	5	0	2	3	2	0	-
	3446.7	348	12	3.45	0	12	0	0	1	11	0	-
	3446.8	306	0	0	-	-	-	-	-	-	0	-
	3446.9	322	0	0	-	-	-	-	-	-	0	-

Abbreviations: B - bright; C - complete; F - faded; I - incomplete; R - reasonable; VB - very bright; [a] - (Number of positives / Number of screened larvae) x 100

3.1.2.2 Confocal microscopy analysis of F0 larvae

To confirm that the injected (F-1) fish were in line with the needs of the research collaborator interested in this line generation, the F-1 offspring (F0) underwent a quick confocal analysis for a more detailed view of the line expression pattern. The best representative sample is displayed below as a z-maximum intensity projection (Figure 3.5A) and z-stack planes of the regions of interest (Figure 3.5A1 to A4). Zones attribution was performed by a direct comparison with reference brain atlases.

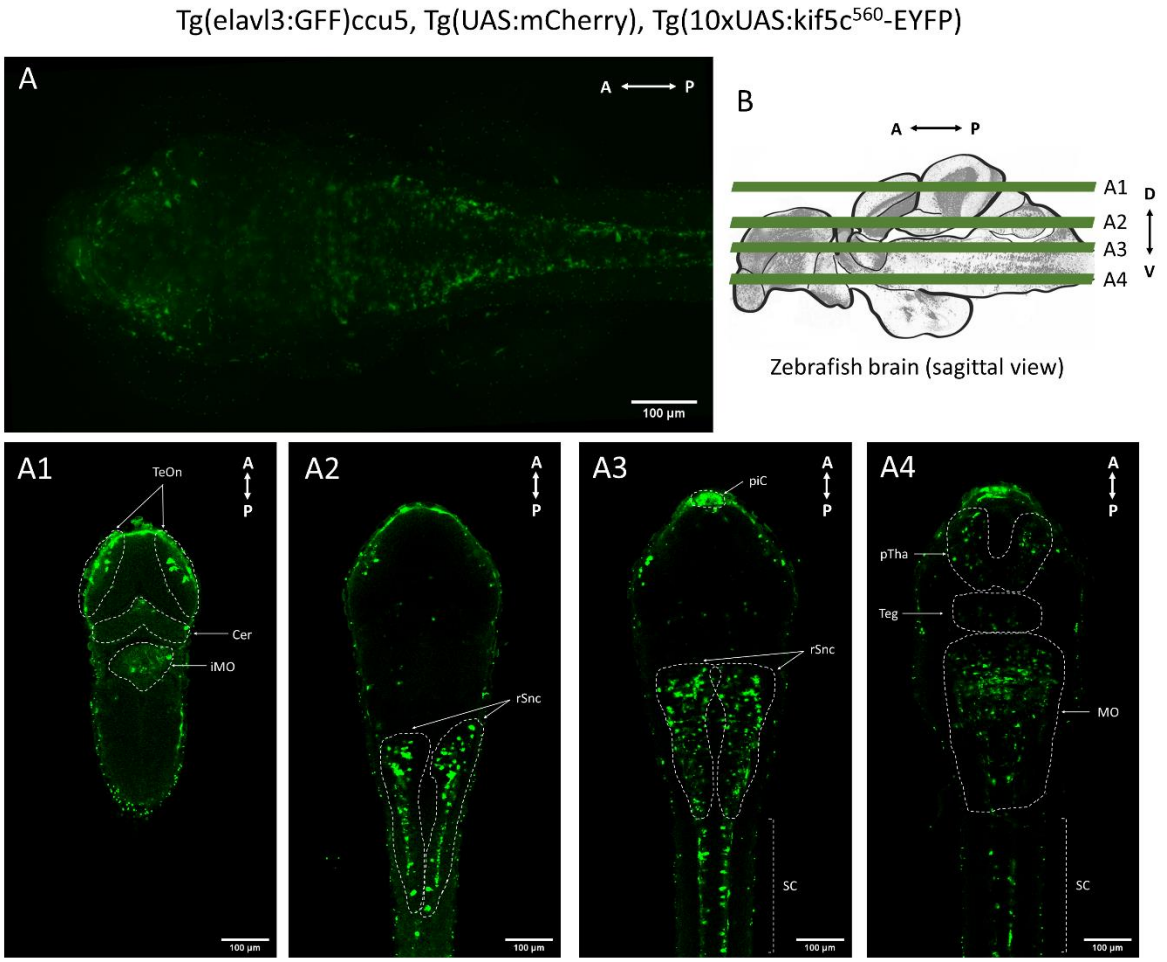

Figure 3.5 - EYFP expression, at 3 dpf, of the Tg(elavl3:GFF)ccu5, Tg(UAS:mCherry), Tg(10xUAS:Kif5c^{560}- EYFP) zebrafish line - progeny from the 3424.1 fish (F0 generation). Annotations of the EYFP expression (in green) have been made using abbreviations of the corresponded brain areas. A - z-maximum projection, obtained from the combination of 248 z-stack planes; B - zebrafish brain sagittal view, with identification of A1 to A4 z-stack planes, dorsal (D) to ventral (V). A1 to A4 - z-stack planes presenting regions of interest from the 43, 92, 124 and 150 planes, respectively. Panels go from dorsal to ventral, left to right. All images present an anterior (A) - posterior (P) axis and a scale bar with a 100 µm size. Abbreviations: Cer - cerebellum; iMO - intermediate medulla oblongata; MO - medulla oblongata; pTha - prethalamus; rSnc - reticulospinal neural clusters; SC - spinal cord; Teg - tegmentum; TeOn - optic tectum neuropil.

The F0 larvae displayed a characteristic elavl3 pan-neuronal expression pattern, homogenous throughout the brain, with a localized fluorescence on the axon terminals characteristic of the Kif5c^{560} protein. In the hindbrain, brighter fluorescence was observed in the reticulospinal neural clusters (rSnc) and their projections to the spinal cord (SC), in the cerebellum (Cer) and medulla oblongata (MO). In the midbrain, EYFP positive cells were detected in the tegmentum and optic tectum neuropil (TeOn). In the forebrain, fluorescence was observed in the prethalamus (pTha).

3.2 Neuronal characterization of five transgenic zebrafish lines

At 3 dpf, larvae were screened and positive fish with a complete expression pattern and a bright fluorescence (examples on Figure 3.6) were selected. For the Tg(gata1a:GFP) line (Figure 3.6A1 and A2) it was possible to visualize GFP fluorescence throughout the brain, in the olfactory epithelium (OE), optic tectum (TeO), cerebellum (Cer) and its eminentia granularis (EGr), and in the reticulospinal neural clusters (rSnc) and their projections to the spinal cord (SC). From a lateral perspective GFP expression was observed in the retina (R), in the heart (H), spinal cord (SC) and in the caudal aorta and venous plexus (CA&VP). The movement of erythrocytes in the bloodstream was observed during the screens.

Regarding the Tg(aldoca:gap43-Venus) line (Figure 3.6B1 and B2) the cerebellum (Cer) and the cerebellovestibular tracts (CVt) of Purkinje cells were easily observed.

As for the Tg(pitx2c:GFP) line (Figure 3.6C1 and C2) expression was detected in the thalamus (Tha) and tegmentum (Teg), the nucleus of the medial longitudinal fasciculus (nucMLF) and their projections (nucMLFp), and in the vagus motor neurons (VMn). Fluorescence was also detected in the developing gut, more specifically in the pharynx and esophagus (P&E), and as a round and speckled pattern spread across larval skin suggestive of being iridophore-pigmented cells (red arrows on Figure 3.6C1).

Concerning the Tg(pSAM:Gal4), Tg(UAS:mCherry) line (Figure 3.6D1 and D2) it was possible to observe the nucleus of the medial longitudinal fasciculus (nucMLF) and their projections (nucMLFp), the spiral fiber neurons (SFn), the mauthner cells (M-cells) and the reticulospinal neural clusters (rSnc) and respective projections to the spinal cord (SC).

Lastly, for the Tg(glyt2:|R|-Gal4), Tg(UAS:GFP) line (Figure 3.6E1 and E2) mCherry fluorescence was detected in the reticulospinal neural clusters (rSnc) and their projections to the spinal cord (SC) and in the retina (R). In the GFP channel, the cmlc2 fluorescence was observed in the heart (H).

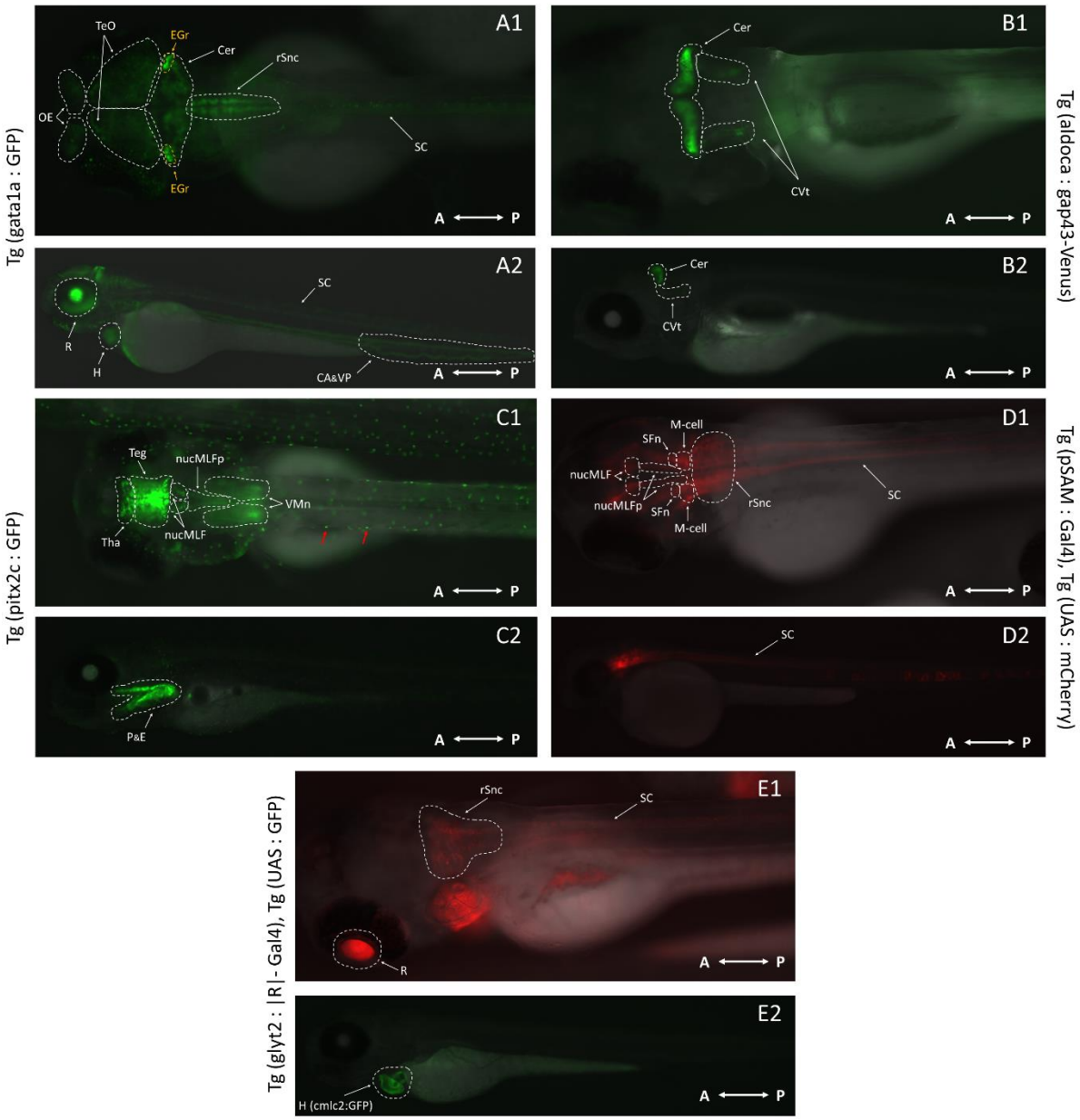

Figure 3.6 - Expression pattern, at 3 dpf, of the five previously-stablished zebrafish transgenic lines studied during this project, with identification of the main brain areas. A1 to E2 - Dorsal and lateral views of the Tg(gata1a:GFP) line (A1 and A2); Tg(aldoca:gap43-Venus) line (B1 and B2), Tg(pitx2c:GFP) line (C1 and C2), with red arrows indicating suggestive iridophore-pigmented cells (just two examples); Tg(pSAM:Gal4), Tg(UAS:mCherry) line (D1 and D2) and Tg(glyt2:|R|-Gal4), Tg(UAS:GFP) line (E1 and E2). Images acquired on Zeiss Axio Zoom.V16 fluorescence stereoscope, equipped with a Zeiss Axiocam 512 mono CCD camera and controlled by the Zeiss ZEN 2.5 2012 Blue Edition software, using a PlanNeoFluar Z 1x objective (NA = 0.25) and the GFP and mRFP filters. All images present an anterior (A) - posterior (P) axis. Abbreviations: CA&VP - caudal aorta and venous plexus; Cer - cerebellum; cmlc2 - cardiac myosin light chain 2; CVt - cerebellovestibular tracts; EGr - eminentia granularis of cerebellum; H - heart; M-cell - mauthner cell; nucMLF - nucleus of the Medial Longitudinal Fasciculus; nucMLFp - nucleus of the Medial Longitudinal Fasciculus projections; OE - olfactory epithelium; P&E - pharynx and esophagus (gut); R - retina; rSnc - reticulospinal neural clusters; SC - spinal cord; SFn - spiral fiber neurons; Teg - Tegmentum; TeO - optic tectum; Tha - Thalamus; VMn - vagus motor neurons.

3.2.1 Confocal microscopy

At 6 dpf, larvae were fixed and underwent a whole-mount immunohistochemistry protocol, where ERK1 and 2 were labelled for a t-ERK homogenous staining. For each of the five lines, the best representative samples were selected and are displayed below as z-maximum intensity projections and z-stack planes of the regions of interest. The anti-tERK pattern was used as reference for the identification of zebrafish brain structures, through direct comparison with reference brain atlases and gene expression literature. Since the imaging was performed with larvae's dorsal side up, image quality was lower in the most ventral areas of the brain.

For the Tg(gata1a:GFP) line (Figure 3.7), GFP expression was detected in the hindbrain in some reticulospinal neural clusters (rSnc), that project to the spinal cord, and in the cerebellum (Cer), being possible to visualize its different sub-regions: corpus cerebelli (cCer), valvula cerebelli (Va), eminentia granularis (EGr) and crista cerebellaris (CC). In the midbrain, fluorescence was observed in the optic tectum, divided into the optic tectum neuropil (TeOn) and optic tectum stratum periventriculare (TeOsp), and in the forebrain, a weak expression was noted in the pineal complex (piC) and in the olfactory epithelium (OE). Lastly, a bright signal was detected in the retina (R), in both retinal ganglion cells (RGC) and amacrine cells (AC) layers.

Regarding the Tg(aldoca:gap43-Venus) line (Figure 3.8), gap43-Venus expression was detected in the hindbrain, in all cerebellum (Cer) extension and its subdivisions - corpus cerebelli (cCer), valvula cerebelli (Va) and eminentia granularis (EGr). The cerebellovestibular tracts of Purkinje cells, that project to the neurons of the medial vestibular nucleus (mVestn) were also observed. The bright anti-t-ERK fluorescence in fish skin was likely caused by an insufficient permeabilization of larvae during the immunohistochemistry process, that ultimately led to a poor antibody penetration and its accumulation on larvae's skin.

Concerning the Tg(pitx2c:GFP) line (Figure 3.9), GFP signal was detected in the hindbrain, in the vagus motor neurons (VMn), superior raphe (sRa) and in the cerebellum (Cer) as a sparse labelling. In the midbrain, several distinct groups of tegmentum (Teg), such as the nucleus of the medial longitudinal fasciculus (nucMLF), the oculomotor nerve nucleus (OmNn), and the trochlear motor nucleus (tronuc) were visualized. In the forebrain, a localized fluorescence was observed in the tectum neuropil (TeOn), in the ventral thalamus (vTha), posterior tuberculum (PTub), preoptic area (pOa) and optic tract (Opt) af3, presumably. Additionally, a round and speckled pattern was observed on larvae's skin and retina suggestive of being iridophore-pigmented cells.

For the Tg(pSAM:Gal4), Tg(10xUAS:GCaMP6fEF05)ccu2 line (Figure 3.10), GFP expression was detected in the hindbrain, at the reticulospinal neural clusters (rSnc) and their

projections to the spinal cord (SC); in the spiral fiber neurons (SFn) and their descending projections to the mauthner cells (M-cells) and their serial homologs (MID2cm and MID3cm); and in the statoacoustic ganglion (SAG). In the midbrain, the projections from the nucleus of the medial longitudinal fasciculus (nucMLFp) were detected, in the tegmentum (Teg) region, and for the forebrain a sparse labeling was visualized in the habenula (Ha) and a bright fluorescence was detected in the pineal complex (piC).

Lastly, concerning the Tg(glyt2:|R|-Gal4), Tg(UAS:GFP) line (Figure 3.11), fluorescence was detected in the hindbrain, in the reticulospinal neural clusters (rSnc) and their descending projections to the spinal cord (SC). Glycinergic neurons were specifically visualized in the oculomotor nerve nucleus (OmNn), superior raphe (sRa), medial octavolateral nucleus (mOn) and in the MiD2cm and MiD3cm cells. In the forebrain, a sparse labeling was visualized in the pineal complex (piC) and a bright fluorescence was detected in the retina (R), in both retinal ganglion cells (RGC) and amacrine cells (AC) layers.

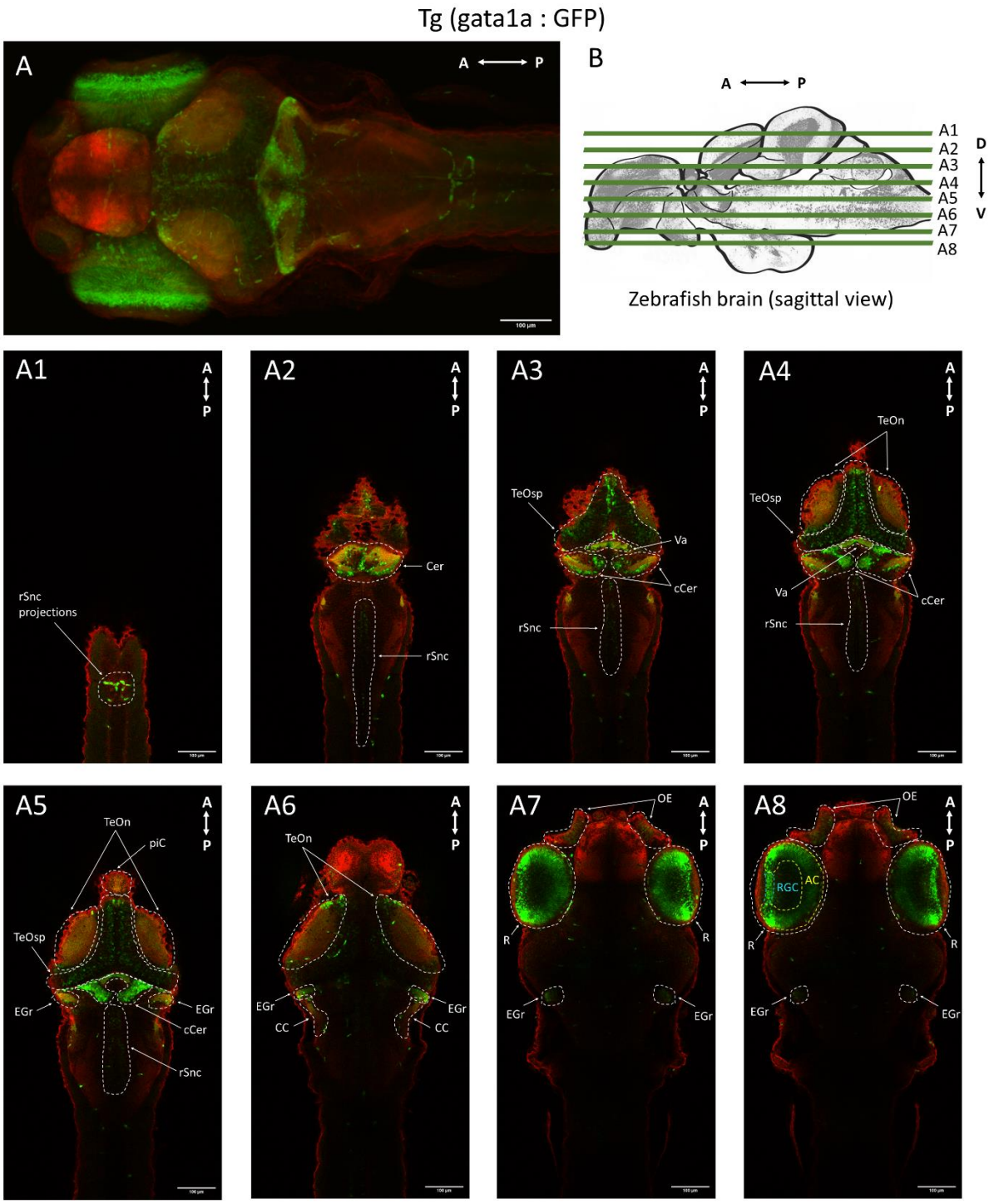

Figure 3.7 - GFP expression, at 6 dpf, of the Tg(gata1a:GFP) zebrafish line. Anti-tERK (in red) and GFP expression (in green). A - z-maximum projection (combination of 250 z-stack planes); B - zebrafish brain sagittal view, with identification of A1 to A8 z-stack planes, dorsal (D) to ventral (V). A1 to A8 - z-stack planes presenting regions of interest from the 15, 67, 78, 89, 99, 137, 197 and 208 planes, respectively. Panels go from dorsal to ventral, left to right. All images present an anterior (A) - posterior (P) axis and a 100 µm scale bar. Abbreviations: AC - amacrine cells layer; CC - crista cerebellaris; cCer - corpus cerebelli; Cer - cerebellum; EGr - eminentia granularis of cerebellum; OE - olfactory epithelium; piC - pineal complex; R - retina; RGC - retinal ganglion cell layer; rSnc - reticulospinal neural clusters; TeOn - optic tectum neuropil; TeOsp - optic tectum stratum periventriculare; Va - Valvula cerebelli.

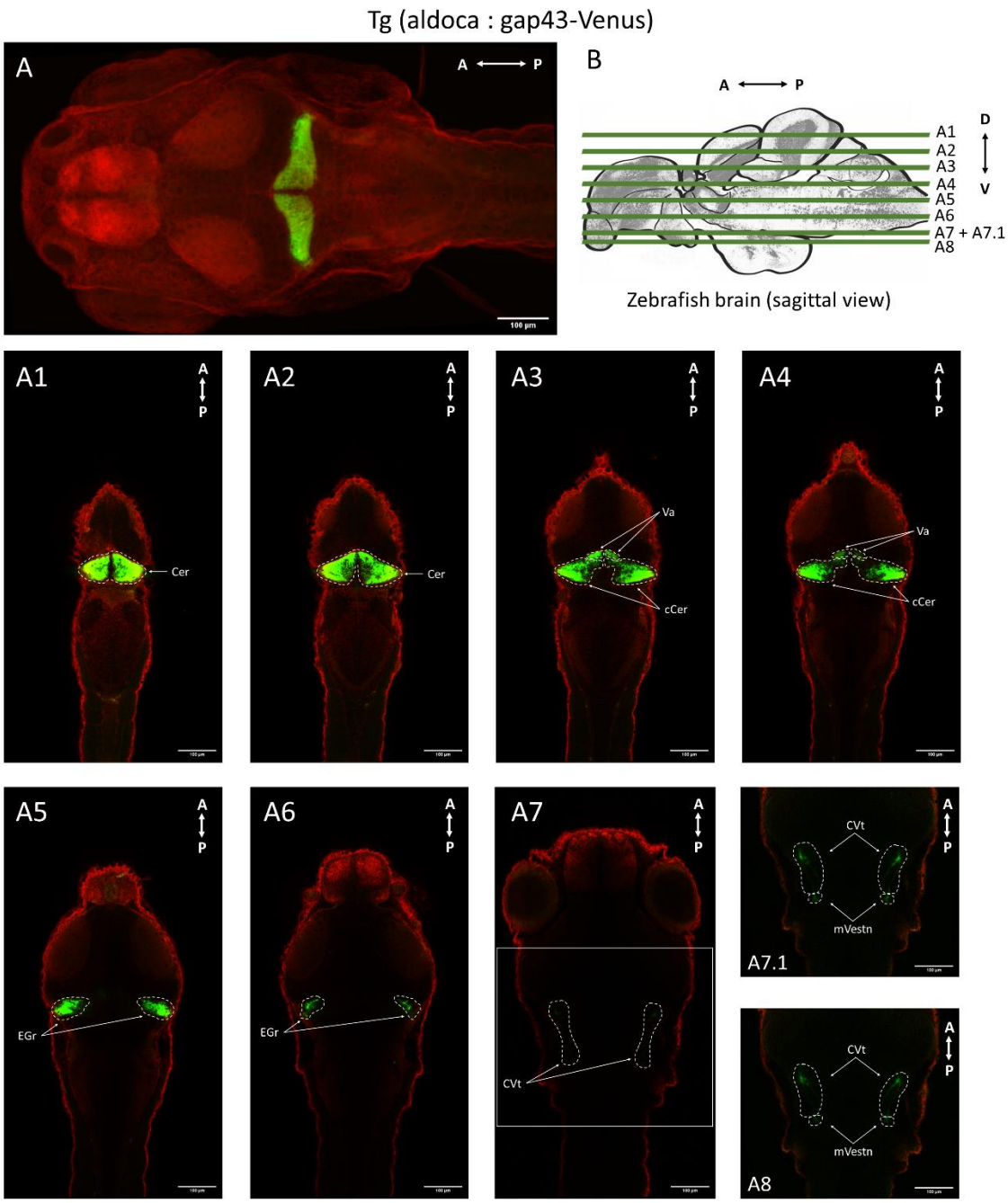

Figure 3.8 - gap43-Venus expression, at 6 dpf, of the Tg(aldoca:gap43-Venus) zebrafish line. Anti-tERK (in red) and gap43-Venus expression (in green). A - z-maximum projection (combination of 250 z-stack planes); B - zebrafish brain sagittal view, with identification of A1 to A8 z-stack planes, dorsal (D) to ventral (V). A1 to A8 - z-stack planes presenting regions of interest from the 33, 42, 55, 66, 84, 107, 164, 164 and 169 planes, respectively. Panels go from dorsal to ventral, left to right. All images present an anterior (A) - posterior (P) axis and a 100 µm scale bar. Abbreviations: cCer - corpus cerebelli; Cer - cerebellum; EGr - eminentia granularis of cerebellum; CVt - cerebellovestibular tracts; mVestn - medial vestibular nucleus; Va - Valvula cerebelli.

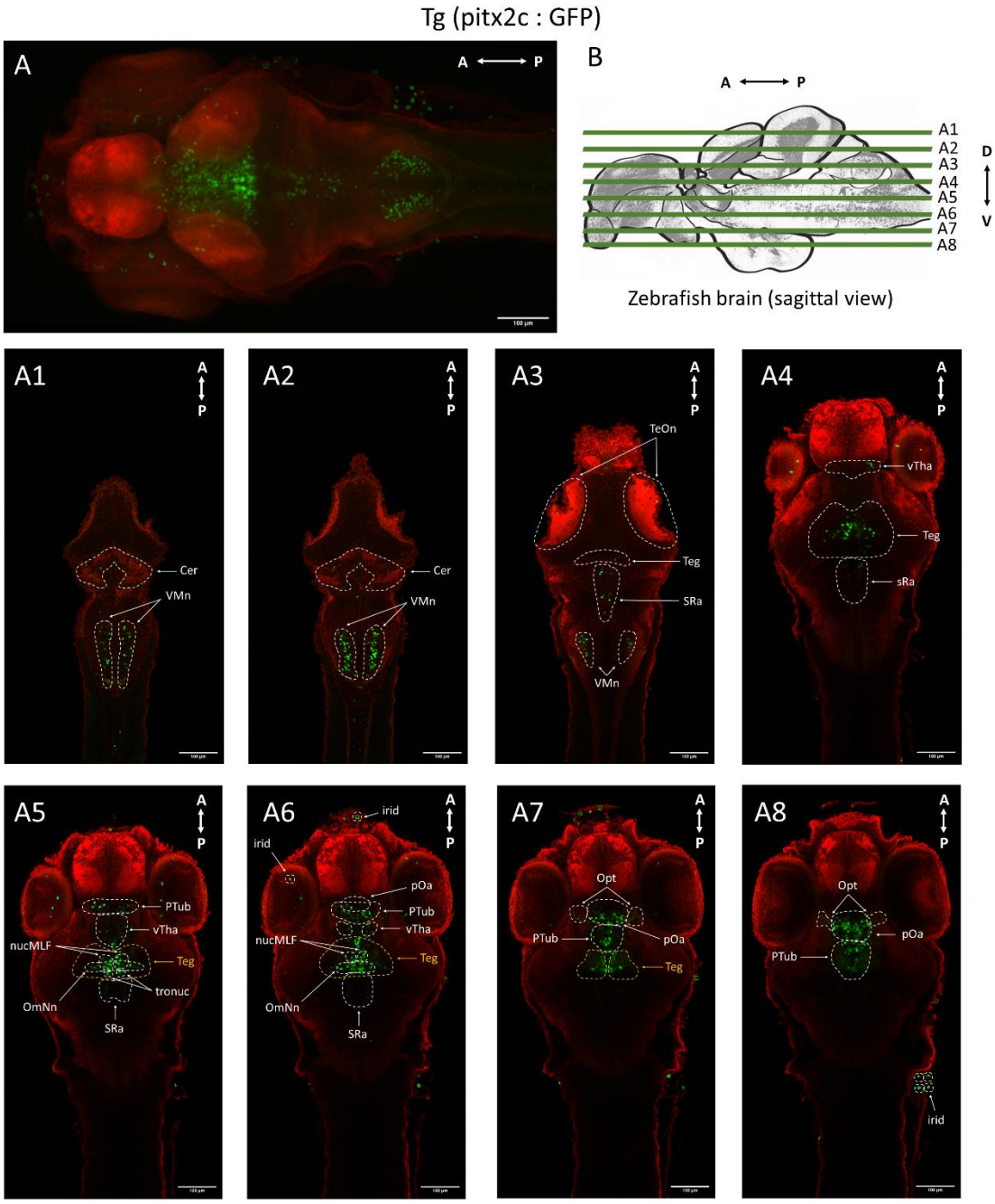

Figure 3.9 - GFP expression, at 6 dpf, of the Tg(pitx2c:GFP) zebrafish line. Anti-tERK (in red) and GFP expression (in green). A - z-maximum projection (combination of 198 z-stack planes); B - zebrafish brain sagittal view, with identification of A1 to A8 z-stack planes, dorsal (D) to ventral (V). A1 to A8 - z-stack planes presenting regions of interest from the 39, 49, 77, 129, 143, 150, 158 and 169 planes, respectively. Panels go from dorsal to ventral, left to right. All images present an anterior (A) - posterior (P) axis and a 100 µm scale bar. Abbreviations: Cer - cerebellum; irid - iridophore-pigmented cells; nucMLF - nucleus of the Medial Longitudinal Fasciculus; OmNn - oculomotor nerve

nucleus; Opt - optic tract af3; pOa - preoptic area; PTub - posterior tuberculum; sRa - superior raphe; Teg - tegmentum; TeOn - optic tectum neuropil; tronuc - trochlear nucleus; VMn - vagus motor neurons; vTha - ventral thalamus.

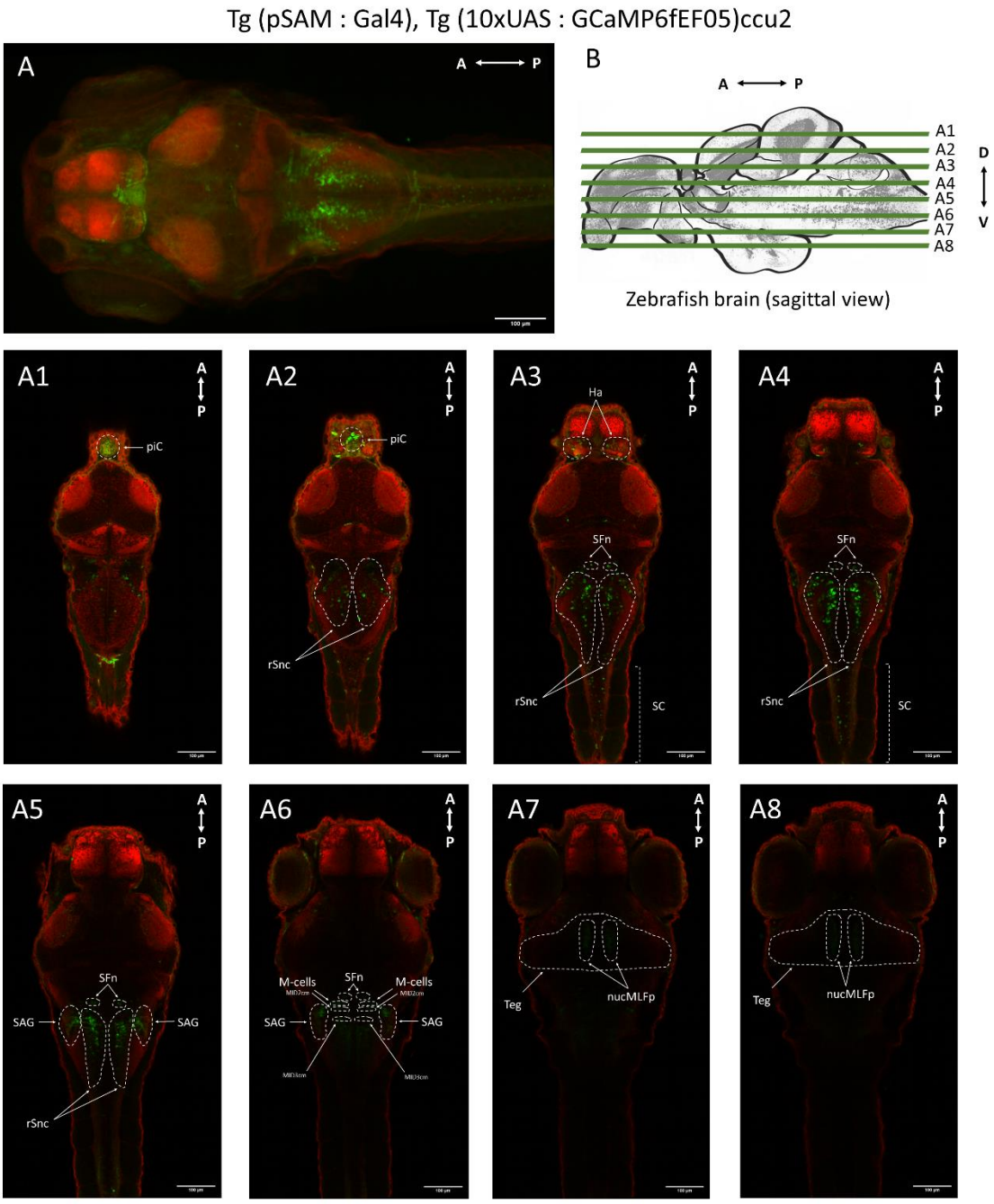

Figure 3.10 - GCaMP6fEF05 expression, at 6 dpf, of the Tg(pSAM:Gal4), Tg(10xUAS:GCaMP6fEF05)ccu2 zebrafish line. Anti-tERK (in red) and GCaMP6fEF05 expression (in green). A - z-maximum projection (combination of 182 z-stack planes); B - zebrafish brain sagittal view, with identification of A1 to A8 z-stack planes, dorsal (D) to ventral (V). A1 to A8 - z-stack planes presenting regions of interest from the 37, 50, 64, 76, 93, 116, 134, and 143 planes, respectively. Panels go from dorsal to ventral, left to right. All images present an anterior (A) - posterior (P) axis and a 100 µm scale bar. Abbreviations: Ha - habenula; M-cells - mauthner cells; MID2cm and MID3cm - serial homologs of mauthner cells; nucMLFp - nucleus of the Medial Longitudinal Fasciculus projections; piC - pineal complex; rSnc - reticulospinal neural clusters; SAG - statoacoustic ganglion; SC - spinal cord; SFn - spiral fiber neurons; Teg - tegmentum.

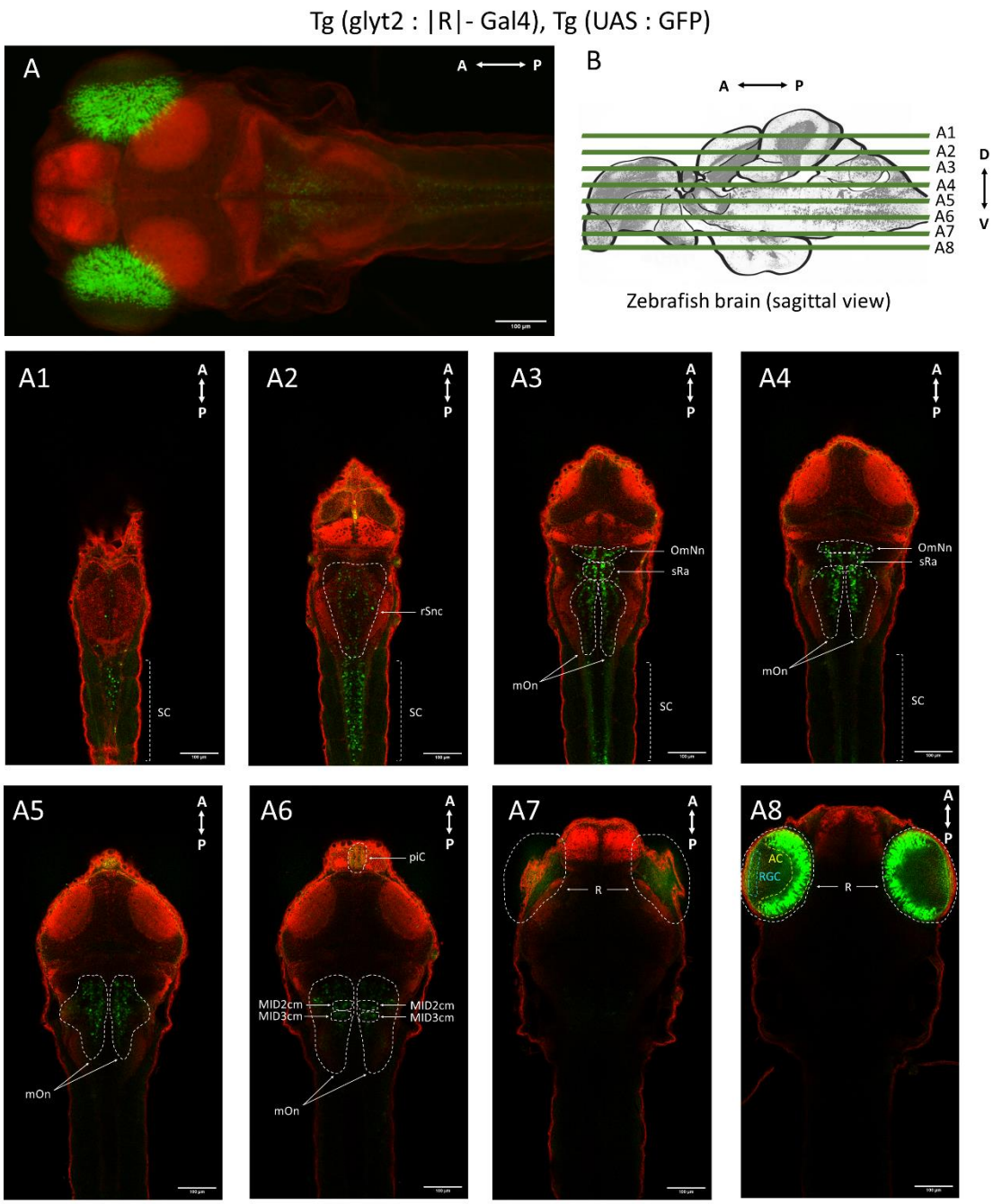

Figure 3.11 - mCherry expression, at 6 dpf, of the Tg(glyt2:|R|-Gal4), Tg(UAS:GFP) zebrafish line. Anti-tERK (in red) and mCherry expression (in green). A - z-maximum projection (combination of 247 z-stack planes); B - zebrafish brain sagittal view, with identification of A1 to A8 z-stack planes, dorsal (D) to ventral (V). A1 to A8 - z-stack planes presenting regions of interest from the 41, 59, 79, 98, 114, 132, 177, and 239 planes, respectively. Panels go from dorsal to ventral, left to right. All images present an anterior (A) - posterior (P) axis and a 100 µm scale bar. Abbreviations: AC - amacrine cells layer; MID2cm and MID3cm - serial homologs of mauthner cells; mOn - medial octavolateral nucleus; OmNn - oculomotor nerve nucleus; piC - pineal complex; R - retina; RGC - retinal ganglion cell layer; rSnc - reticulospinal neural clusters; SC - spinal cord; sRa - superior raphe.

3.2.2 Atlas registration results

After going through the ANTs algorithm, the GFP, gap43-Venus or mCherry channel images were merged and a reference model was obtained for each line. As the images shown are averages of several samples, some differences in terms of zones that present fluorescence may be observed, even if they may not be very significant. For the Tg(aldoca:gap43-Venus) line (Figure 3.12) there was just a difficulty in observing the medial vestibular nucleus (mVestn) for where the cerebellovestibular tracts of Purkinje cells project; for the Tg(pSAM:Gal4), Tg(10xUAS:GCaMPP6fEF05)ccu2 line (Figure 3.14) the spiral fiber neurons (SFn) and the mauthner-cells were difficult to identify and for the Tg(glyt2:|R|-Gal4), Tg(UAS:GFP) line (Figure 3.15) the pattern was almost the same. The MID2cm and MID3cm cells were not possible to distinguish in the latter two lines. The line that revealed more differences, presenting a much more complete expression pattern on the registration image was the Tg(pitx2c:GFP) line (Figure 3.13), which additionally showed fluorescence in the pineal complex (piC), optic tectum stratum periventriculare (TeOsp), vagal region (Vr), pallium (Pa) and sub pallium (subPa), pretectum (Pr), and thalamus (Tha). As for the Tg(gata1a:GFP) line, constraints were found in performing an average, due to a poor orientation of the samples.

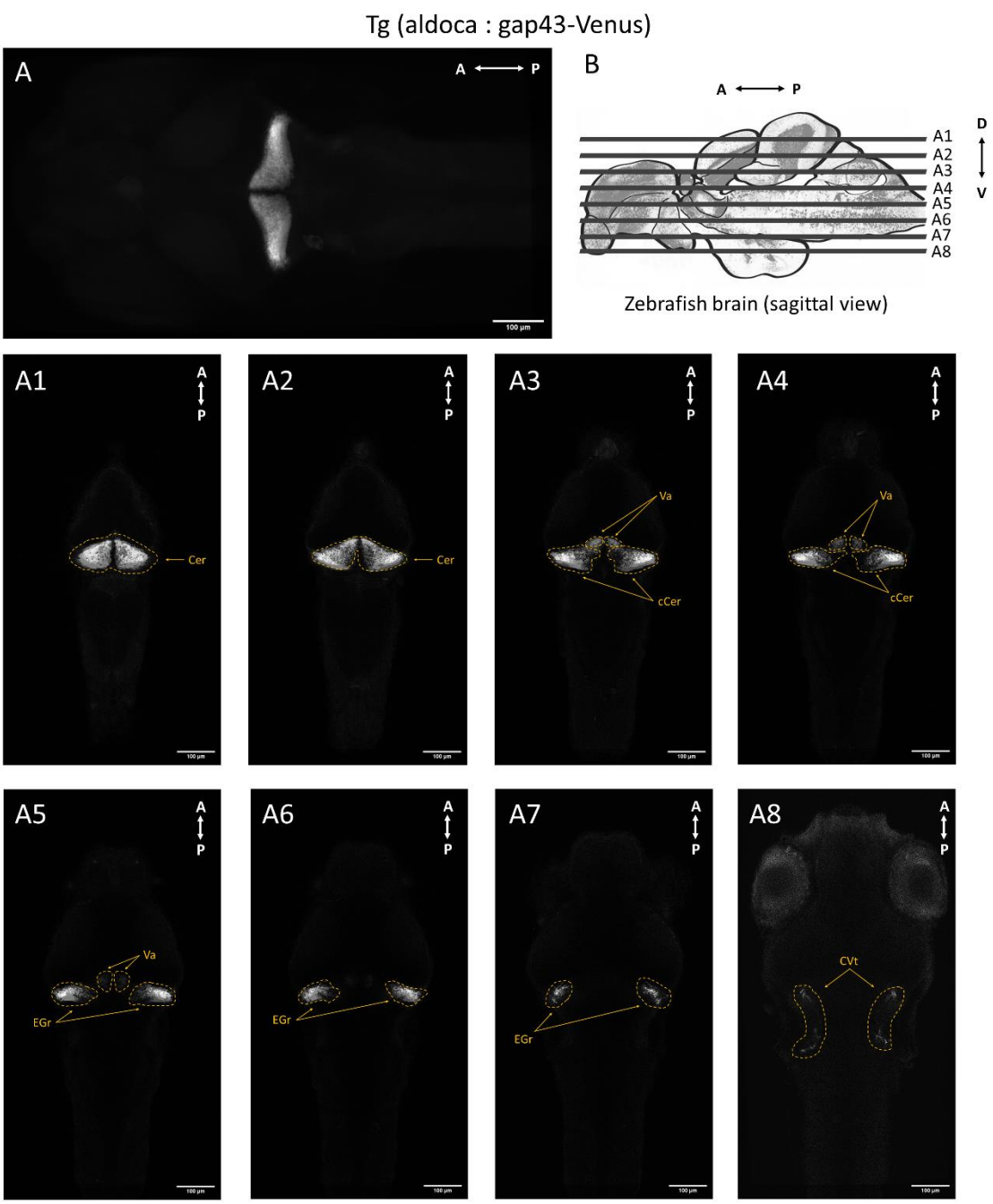

Figure 3.12 - gap43-Venus expression (average of three samples) obtained after the registration process for the Tg(aldoca:gap43-Venus) zebrafish line. Annotations of the gap43-Venus fluorescence (in white) have been made using abbreviations of the corresponded brain areas. A - z-maximum projection, obtained from the combination of the 370 z-stack planes; B - zebrafish brain sagittal view, with identification of A1 to A8 z-stack planes, dorsal (D) to ventral (V). A1 to A8 - z-stack planes presenting regions of interest from the 43, 55, 70, 82, 95, 104, 129 and 184 planes, respectively. Panels go from dorsal to ventral, left to right. All images present an anterior (A) - posterior (P) axis and a 100 µm scale bar. Abbreviations: cCer - corpus cerebelli; Cer - cerebellum; EGr - eminentia granularis of cerebellum; CVt - cerebellovestibular tracts; Va - Valvula cerebelli.

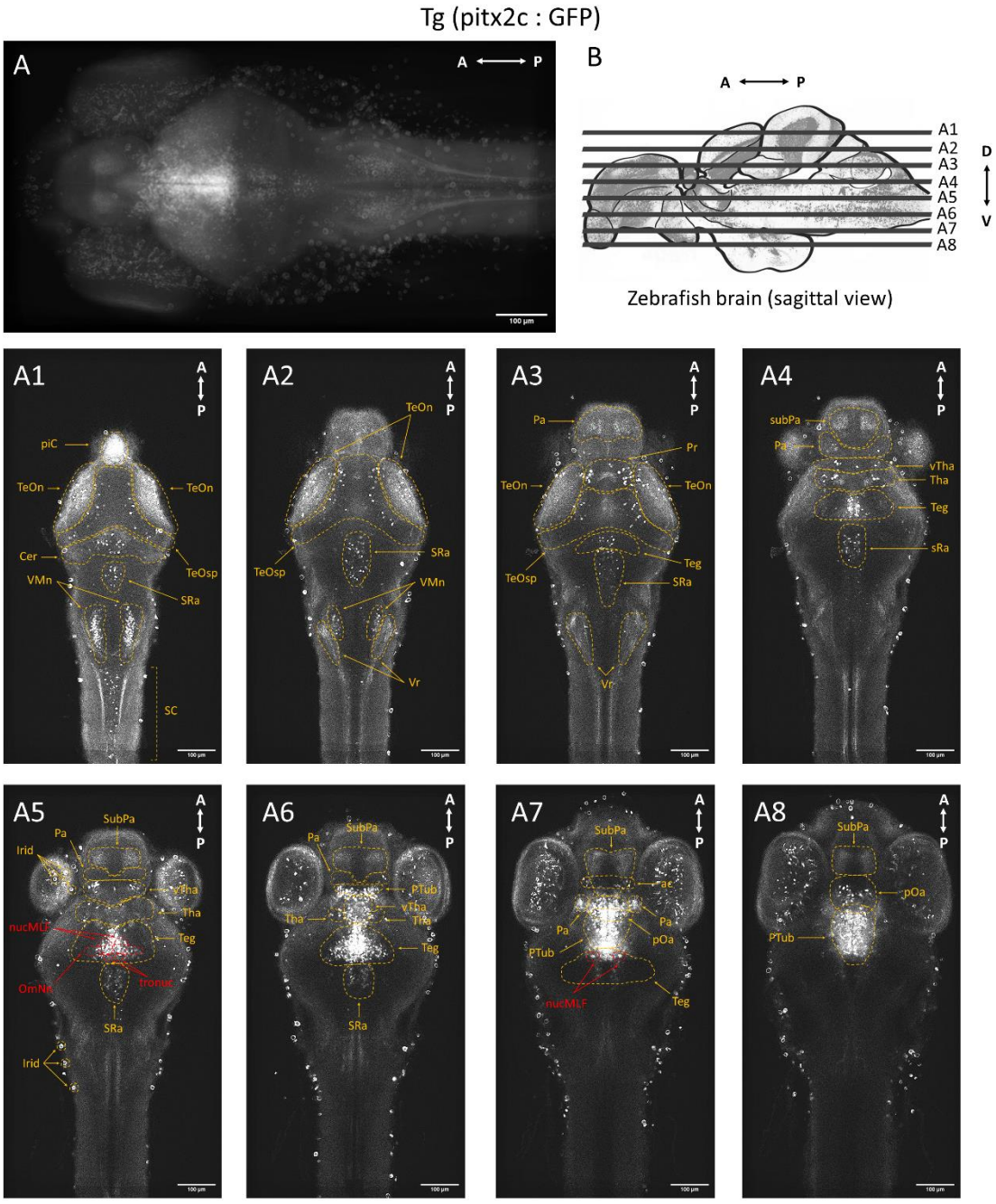

Figure 3.13 - GFP expression (average of nine samples) obtained after the registration process for the Tg(pitx2c:GFP) zebrafish line. Annotations of the GFP fluorescence (in white) have been made using abbreviations of the corresponded brain areas. A - z-maximum projection, obtained from the combination of the 370 z-stack planes; B - zebrafish brain sagittal view, with identification of A1 to A8 z-stack planes, dorsal (D) to ventral (V). A1 to A8 - z-stack planes presenting regions of interest from the 73, 103, 113, 126, 140, 161, 186 and 214 planes, respectively. Panels go from dorsal to ventral, left to right. All images present an anterior (A) - posterior (P) axis and a 100 µm scale bar. Abbreviations: ac - anterior commissure; Cer - cerebellum; irid - iridophore-pigmented cells; nucMLF - nucleus of the Medial Longitudinal Fasciculus; OmNn - oculomotor nerve nucleus; Pa - Pallium; piC - pineal complex; Pr - Pretectum; pOa - preoptic area; PTub - posterior tuberculum; sRa - superior raphe; subPa - sub pallium; Teg - tegmentum; Tha - Thalamus; TeOn - optic tectum neuropil; TeOsp - optic tectum stratum periventriculare; tronuc - trochlear nucleus; VMn - vagus motor neurons; Vr - Vagal region; vTha - ventral thalamus.

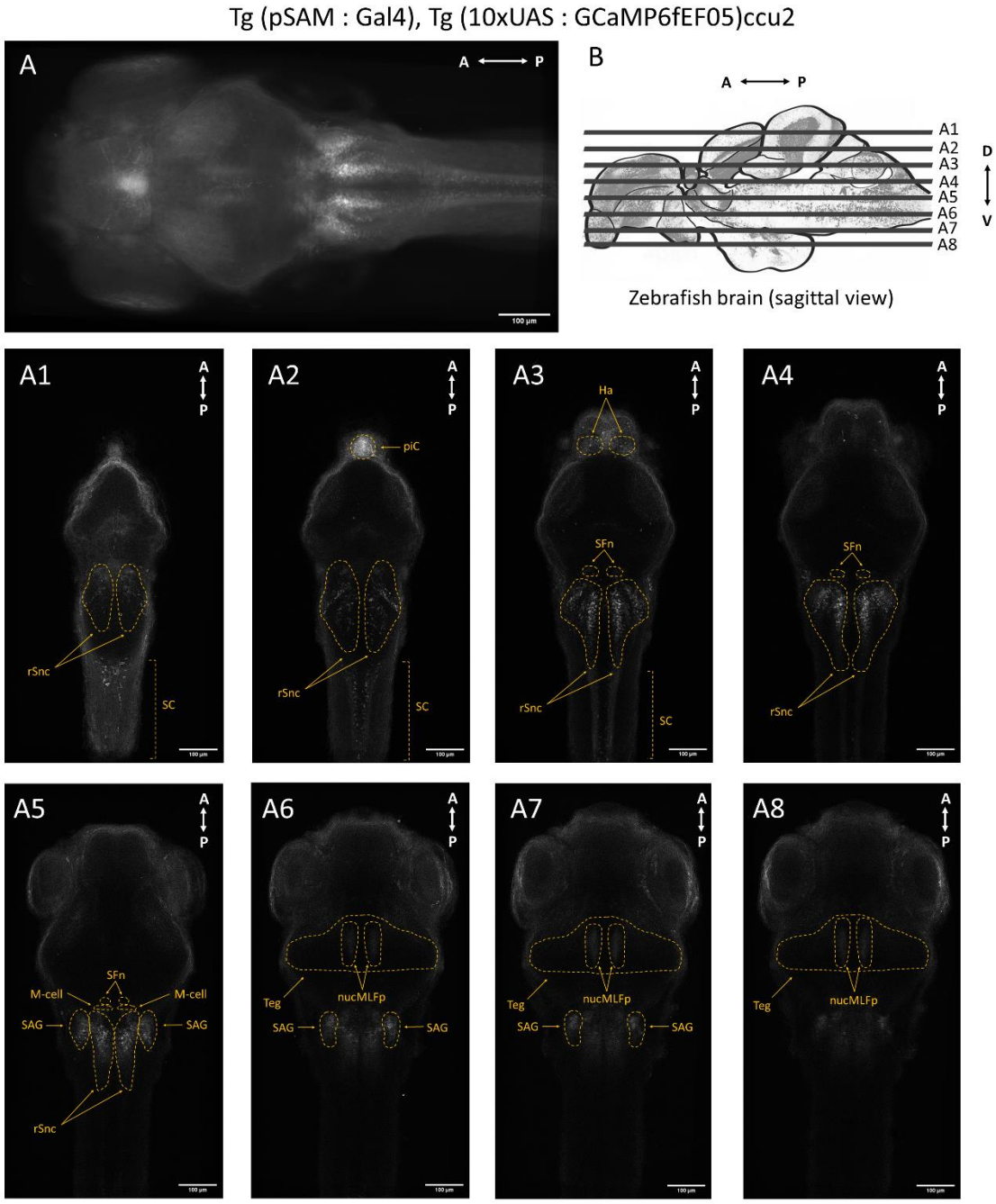

Figure 3.14 - GCaMP6fEF05 expression (average of twelve samples) obtained after the registration process for the Tg(pSAM:Gal4), Tg(10xUAS:GCaMP6fEF05)ccu2 zebrafish line. Annotations of the GCaMP6fEF05 fluorescence (in white) have been made using abbreviations of the corresponded brain areas. A - z-maximum projection, obtained from the combination of the 370 z-stack planes; B - zebrafish brain sagittal view, with identification of A1 to A8 z-stack planes, dorsal (D) to ventral (V). A1 to A8 - z-stack planes presenting regions of interest from the 56, 76, 103, 125, 154, 176, 191 and 196 planes, respectively. Panels go from dorsal to ventral, left to right. All images present an anterior (A) - posterior (P) axis and a 100 µm scale bar. Abbreviations: Ha - habenula; M-cells - mauthner cells; nucMLFp - nucleus of the Medial Longitudinal Fasciculus projections; piC - pineal complex; rSnc - reticulospinal neural clusters; SAG - statoacoustic ganglion; SC - spinal cord; SFn - spiral fiber neurons; Teg - tegmentum.

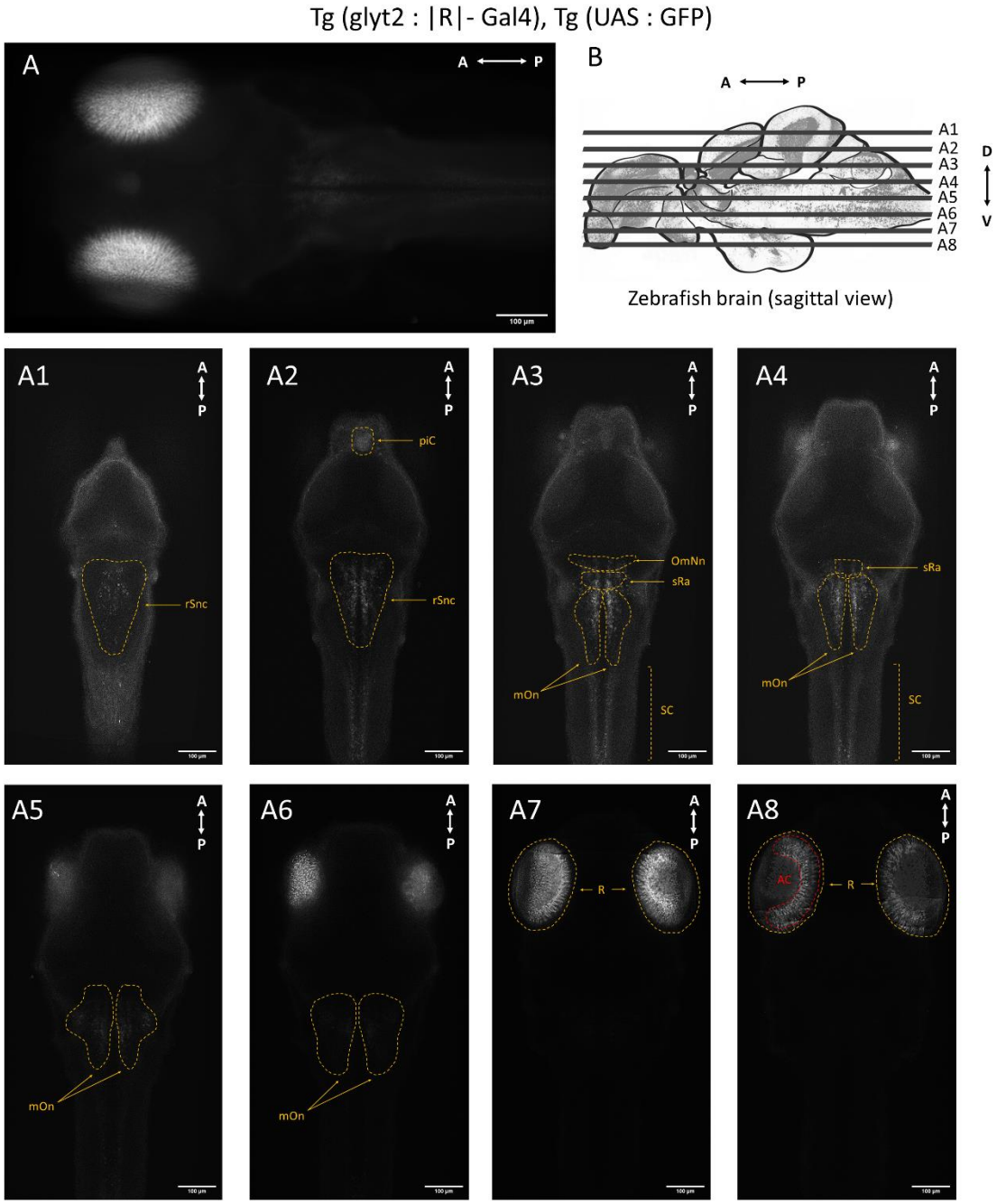

Figure 3.15 - mCherry expression (average of eight samples) obtained after the registration process for the Tg(glyt2:|R|-Gal4), Tg(UAS:GFP) zebrafish line. Annotations of the mCherry fluorescence (in white) have been made using abbreviations of the corresponded brain areas. A - z-maximum projection, obtained from the combination of the 370 z-stack planes; B - zebrafish brain sagittal view, with identification of A1 to A8 z-stack planes, dorsal (D) to ventral (V). A1 to A8 - z-stack planes presenting regions of interest from the 64, 100, 115, 130, 152, 170, 208 and 247 planes, respectively. Panels go from dorsal to ventral, left to right. All images present an anterior (A) - posterior (P) axis and a 100 µm scale bar. Abbreviations: AC - amacrine cells layer; mOn - medial octavolateral nucleus; OmNn - oculomotor nerve nucleus; piC - pineal complex; R - retina; rSnc - reticulospinal neural clusters; SC - spinal cord; sRa - superior raphe.

3.2.3 Expression pattern comparisons

Table 3.3 - Expression pattern summary - comparison between literature description and what was observed during the screens (at 3 dpf), confocal imaging (at 6 dpf) and after the registration process for ZBB1.2 atlas submission. In orange are highlighted the different zones observed when comparing confocal acquisition with the screens, and in blue the zones differences between the confocal images and after registration.

Expression pattern summary			
Literature (full larvae body)	Screens at 3 dpf (full larvae body)	Confocal microscopy of 6-day larvae (brain)	After registration process (brain)
Tg (gata1a:GFP)			
Brain ; Retina ; Spinal cord neurons ; Heart ; Circulating blood (24 hpf to 2 months)	OE ; TeO ; Cer (EGr) ; rSnc ; Retina ; Heart ; SC ; CA&VP ; Erythrocytes in blood circulation	OE ; TeO (TeOn, TeOsp) ; Cer (cCer, Va, EGr and CC) ; Retina (RGC and AC layers) ; rSnc ; piC	n/a
Tg (aldoca:gap43-Venus)			
Cerebellar Purkinje cells and their CVt	Cer and CVt of Purkinje cells	Cer (cCer, Va, EGr) ; CVt that project to the mVestn	Cer (cCer, Va, EGr); CVt
Tg (pitx2c:GFP)			
Developing gut ; Dental epithelium ; Dorsal diencephalon (after 19 hpf) ; nucMLF	Tha ; Teg (nucMLF and nucMLFp) ; VMn ; Developing gut (P&E)	vTha ; Teg (nucMLF, OmNn, tronuc) ; VMn ; sRa ; Cer ; TeOn ; PTub ; pOa and Opt	vTha ; Tha ; ac ; Teg (nucMLF, OmNn, tronuc) ; VMn ; sRa ; Cer ; TeOn; TeOsp ; PTub ; pOa ; Pa ; subPa ; piC ; Pr ; Vr
Tg (pSAM:Gal4), Tg (UAS:mCherry) / Tg (pSAM:Gal4), Tg(10xUAS:GCaMP6fEF05)ccu2			
SFn and their projections to the M-cells ; CoPA neurons on SC ; Anterior and posterior lateral line ; SAG ; Trigeminal ganglion ; Ha ; Teg	SFn ; M-cells ; rSnc and their projections to the SC ; nucMLF and nucMLFp	SFn ; M-cells ; MID2cm and MID3cm ; rSnc and their projections to the SC ; SAG ; Teg (nucMLFp) ; Ha ; piC	SFn ; M-cells ; rSnc and their projections to the SC ; SAG ; Teg (nucMLFp); Ha ; piC
Tg (glyt2:|R|-Gal4), Tg(UAS:GFP)			
Glycinergic neurons found in the rhombencephalon, with descending projections from the reticular, sRa, and mOn to the SC	mCherry fluorescence: rSnc and their SC projections ; Retina GFP fluorescence: Heart (due to cmlc2 marker)	rSnc and SC projections ; Retina (RGC and AC layers) ; OmNn ; sRa ; mOn ; MiD2cm and MiD3cm ; piC	rSnc and SC projections ; Retina (AC layer); OmNn ; sRa ; mOn ; piC

Abbreviations: ac - anterior commissure; AC - amacrine cells layer of retina; CC - crista cerebellaris; cCer - corpus cerebelli; Cer - cerebellum; CVt - cerebellovestibular tracts; EGr - eminentia granularis of cerebellum; Ha - habenula; M-cells - mauthner cells; MID2cm and MID3cm - serial homologs of mauthner cells; mOn - medial octavolateral nucleus; mVestn - medial vestibular nucleus; n/a - not applicable; nucMLF - nucleus of the Medial Longitudinal Fasciculus; nucMLFp - nucMLF projections; OE - olfactory epithelium; OmNn - oculomotor nerve nucleus; Opt - optic tract af3; Pa - pallium; piC - pineal complex; pOa - preoptic area; Pr - pretectum; PTub - posterior tuberculum; R - retina; RGC - retinal ganglion cell layer; rSnc - reticulospinal neural clusters; SAG - statoacoustic ganglion; SC - spinal cord; SFn - spiral fiber neurons; sRa - superior raphe; subPa - sub pallium; Teg - tegmentum; TeOn - optic tectum neuropil; TeOsp - optic tectum stratum periventriculare; Tha - thalamus; tronuc - trochlear nucleus; Va - Valvula cerebelli; VMn - vagus motor neurons; Vr - vagal region; vTha - ventral thalamus.

For the Tg(gata1a:GFP) and Tg(aldoca:gap43-Venus) lines, the expression pattern described in the literature corresponded the one observed during the screens and confocal acquisition, and also after registration for the second line (Table 3.3). Through confocal microscopy, it was possible to visualize, for both lines, the different subdivisions of cerebellum and optic tectum and, for the Tg(aldoca:gap43-Venus) line, to identify the medial vestibular nucleus (mVestn) to where the cerebellovestibular tracts project on the hindbrain.

Regarding the Tg(pitx2c:GFP) line some differences were noted when comparing the available bibliography with the obtained confocal images, with a pitx2c expression reported in the right dorsal diencephalon that was not detected by confocal microscopy. Instead GFP fluorescence was detected on other dorsal diencephalic regions, such as the preoptic area (pOa), the ventral thalamus (vTha) and the posterior tuberculum (PTub). After registration some differences were also observed, with GFP expression being detected in the thalamus (Tha), anterior commissure (ac), optic tectum stratum periventriculare (TeOsp), pallium and sub pallium (Pa and subPa), pineal complex (piC), pretectum (Pr) and vagal region (Vr).

Concerning the Tg(pSAM:Gal4), Tg(UAS:mCherry) line, in general the pattern matched between the literature, the screens, the confocal images and the registered ones, even if there wasn't signal detection on the anterior and posterior lateral line and in the trigeminal ganglion. During the screens it was possible to clearly identify the nucMLF and their projections, and during confocal visualization the MID2cm and MID3cm cells, habenula (Ha) and pineal complex (piC).

Lastly, for the Tg(glyt2:|R|-Gal4), Tg(UAS:GFP) line the expression pattern described on previous studies was in accordance with the one observed during the screens and the confocal imaging, with clearer visualization of the oculomotor nerve nucleus (OmNn), superior raphe (sRa), medial octavolateral nucleus (mOn) and pineal complex (piC) by confocal microscopy. After registration it was just difficult to observe the MID2cm and MID3cm cells.

4

DISCUSSION

At the end of this project, the establishment of the new zebrafish Tg(elavl3:GFF)ccu5, Tg(UAS:mCherry), Tg(10xUAS:kif5c^{560}-EYFP) line was considered successful, as five F-1 lines presented fluorescently-labelled larvae and germ line transmission was confirmed on the next generation (F0). According to the results obtained, the F0 lines currently growing demonstrated to be prone to give rise to promising F1 lines and continue the establishment of stable transgenic animals, featuring a predictable inherited transgene fluorescence.

Regarding the other five previously-established lines, the characterization process was successful for all, with just some small variations detected in comparison to the literature, and the registration process was successful for four of them. This represented a huge step towards the integration of these lines into a well-established international zebrafish brain atlas and the future study of several neurological disorders.

4.1 Generation of a new and stable zebrafish transgenic line

4.1.1 Mortality and morbidity rates

The microinjection procedure is a simple technique used to introduce foreign materials into newly fertilized embryos. It always involves a small disruption of membranes and an associated toxicity of the loaded substance, which affects embryo survival and its normal development. If high-quality needles and a good injection technique are employed, cell death can be kept to a minimum, but if the needles are a bit too large or present an irregular tip or if the technique is not perfect, cell death can occur shortly after the needle removal (Dean, 2013). For all rounds a tendency for a higher mortality in the injected embryos compared to the controls was noted (Results - Figure 3.1), confirming that the procedure itself and/or the operator's limited experience could have resulted in harming the embryos.

Since a uniform cutting of the injection needle is relevant to obtain an equal diameter and a consistency effect between different microinjections (Abdelrahman et al., 2021), the use of a microscope scale should be considered in future experiments. Additionally, cutting the

needle at a 45º angle is also important to guarantee better survival results, as a sharper tip is obtained and a lower mechanical force has to be applied (Abdelrahman et al., 2021).

The injection volume may also influence eggs survival and should be kept under 4.2 nl, 10% of the total embryo volume (Abdelrahman et al., 2021). Volume calibration is a requirement for the injection of substances such as morpholinos, used for gene knockdown, since variations of volume in quantitative experiments of this sort may lead to misinterpretations of the results, making it difficult to assess whether the embryo mortality is caused by a toxicity effect or by the gene knockdown (Eisen & Smith, 2008). In other cases, such as for the generation of transgenic lines, knowing the exact volume of DNA injected is not mandatory, so many experienced operators don't calibrate the needles, estimating the volume based on experience. However, the injections described here were done by an unexperienced operator, which may explain the inconsistency of results noted between different injection rounds. In the future, this step can be considered if more consistent results are needed.

Lastly, DNA concentration also influences embryo mortality and morbidity, as well as the integration success rate. High concentrations normally lead to high levels of toxicity, but lower concentrations are related to lower integration efficiencies. Injections started with a DNA concentration of 25 ng/µL, previously established by one of the fish platform technicians for a similar 10xUAS:Kif5c^{560} construct. Given the low number of "good" positives (Results - Table 3.1), classified as bright and very bright, the concentration was increased to 30 ng/µL and 50 ng/µL. A high mortality rate was obtained for 30 ng/µL but with 50 ng/µL the percentage of "good" positives improved, which indicated that the mortality increase when using 30 ng/µL was probably not related to the toxicity of the loaded substance itself but to other technical factors, such as the injected volume and/or the needle tip diameter.

4.1.2 Construct integration and silencing effects

Several variables influence DNA construct integration and transgene silencing over several generations, such as the injection stage, the use of tol2-mediated transgenesis and the number of UAS repeats.

Given rapid cell division, a delay in construct integration may lead to a mosaic expression, in which only a fraction of the embryo's cells inherit the injected DNA. With different genotypes within the same fish population, it would be difficult to ensure stable transgenic transmission across generations. For this reason, the injection procedure should be performed at the one-cell stage, for a higher probability of transgene integration in the genome and equal transmission to all succeeding cells, including the germline cells (Xu, 1999).

Furthermore, previous studies have shown that Tol2-mediated transgenesis exhibits a significantly higher germline transmission, with more than 50% of the injected fish passing the transgene insertions to their progeny (Kawakami, 2007). Additionally, transgenic animals generated based on this method demonstrate fewer silencing effects over several generations, since integration of tol2 elements does not cause any gross rearrangement at the target site (Akitake et al., 2011; Urasaki et al., 2006). The transgenic line created during this project was generated based on this principle and the results showed that ~82% of the injected fish transmitted the transgene to the next generation (Results - Table 3.2).

Lastly, we also took advantage of the Gal4-UAS transactivation system, in which the Gal4 protein recognizes the UAS sequence and drives the expression of any reporter gene located downstream. Gal4 can cooperatively bind to multiple tandem UAS sites, for a further enhancement of gene expression, however, the number of UAS repeats must be considered as it also influences the transgene silencing across generations. Each UAS repeat contains a 17 bp 5'-CGG-N_{11}-CCG-3' palindromic sequence, essential for Gal4 recognition and binding, but prone to DNA methylation. Although this silencing does not occur during the first screen for transient expression, when the transgene is stably integrated into the fish genome highly repetitive UAS constructs become more susceptible to CpG methylation. In previous studies, constructs with 14xUAS sequences shown higher levels of reporter expression but were more likely to suffer methylation than constructs with 4xUAS sequences, that also revealed good levels of expression. Thus, in order to strike a balance between both factors, our DNA construct was designed with a set of 10xUAS tandem sequences (Akitake et al., 2011).

4.1.3 Selection of fish for line establishment - Promising F-1 and F0 lines

The goal while establishing a new line is to generate stable transgenic animals, featuring a predictable inherited transgene fluorescence. To achieve this purpose, five F-1 promising lines (Results - Table 3.1) were selected based on a bright fluorescence intensity along with a complete and uniform expression pattern, more likely to correspond to an equal construct integration into all cells. After that, their progeny (F0 generation) was screened for stable expression and selected based on the same principles described above, in addition with a low number of "good" positives, indicative of a greater probability of integration into a single region. Since insertion of the transgene into the genome occurs randomly, a characteristic of tol2-mediated transgenesis, the number of insertions and/or the region(s) of integration will influence the observed expression. If the transgene integration occurs at more than one site, the progeny is more prone to present individuals with a mosaic expression, as shown by the four intensity levels obtained, generating heterogeneous populations and a greater

undesirable instability factor for line establishment. This mosaicism effect can be associated with an unequal distribution of the microinjected DNA during cells division, due to a delay in the microinjection procedure, or by the amount of injected DNA, with some injected fish receiving a higher volume of the construct and therefore presenting a higher probability of integration in more than one site (Amsterdam et al., 1995). However, is important to note that the four levels of fluorescence observed are normal in the first fish populations of any line establishment.

Even though the 3446 F-1 line presented a higher integration rate (34.4%) on the first screen (Results - Table 3.1), the progeny from the 3425 and 3424 F-1 lines presented better overall screen results for stable expression, with lower integration rates and a good number of positives (Results - Table 3.2). Of these, two 3425 fish and one 3424 fish stood out for the reasons already mentioned and will be screened when they reach sexual maturity. However, according to the results already obtained, these fish seem prone to give rise to promising F1 lines. The line will be considered stable when all transgenic fish comprise the same number and location of insertions. When possible, a single insertion is preferred as it is translated into a stronger and desirable integration stability. Insertions can be further confirmed, if desired, by a Southern blot analysis (Kikuta & Kawakami, 2009). It is important to note that a silencing effect due to methylation of CpG dinucleotides can always occur from the F0 generation onwards, the reason why it is recommended to establish at least three independent transgenic lines for any population.

4.1.4 Confocal analysis of F0 larvae

At 3 dpf, larvae were imaged through confocal microscopy, for a better expression pattern visualization, and the results showed a brighter fluorescence in the reticulospinal neural clusters (rSnc) and their projections to the spinal cord (Results - Figure 3.5). In fact, the first behavioural reactions appear at 3 days, with the rSnc being involved in larvae's turning movement, postural control, and cessation of the swimming activity. Sensory information, such as the sound, sight or movement of a predator may indicate a threat, and a rapid escape movement, known as the ''startle response'', is necessary. Thereby, the collected visual sensory information is transmitted to the rSnc populations, which generate the motor commands needed to excite the spinal cord neurons that drive the fish away from the detected threat (Berg et al., 2018; Feierstein et al., 2015; Gahtan et al., 2005). Thus, is possible to infer that the high fluorescence observed in the rSnc may be associated with the beginning of the establishment of the necessary neuronal connections, between the brain and the spinal cord, for the development of an effective ''startle response''. It is important to emphasize that this is just one hypothesis

to explain the high fluorescence observed, which would need to be confirmed through behavioral studies.

4.2 Neuronal characterization of five transgenic zebrafish lines

4.2.1 Mounting of larvae

For imaging of fixed immunostained samples, as performed in this project, the use of 1% low-melting point agarose (LMPA) remains the most appropriate matrix to achieve a firm and accurate sample immobilization. Its low melting temperature and lower gelling temperature (24 to 28°C) provide an easier manipulation for a longer period. Additionally, it also presents a good gel transparency, making the acquisition process easier, and when properly hydrated maintains its integrity for a few days. Larvae retrieval after image acquisition is also easy to accomplish with this matrix (Kleinhans & Lecaudey, 2019; Renaud et al., 2011).

Despite being the standard mounting, it has also proved to be a complex and time-consuming process that requires very good skills from the operator. The correct sample orientation is extremely important to ensure a good image quality, an accurate interpretation of the line expression pattern and also to register the output results into international zebrafish brain atlases. A practical example of a not so good assembly was seen for the Tg(pitx2c:GFP) line (Results - Figure 3.8A4), where the larva eyes are not perfectly symmetrical. However, the sample was chosen to be displayed, as it presented an expression pattern representative of the line in question.

In the future, a different mounting set up may be considered to facilitate the mounting process, to ensure a better sample orientation and, consequently, obtain better confocal stacks. One hypothesis would be to create an assembly apparatus with different wells that would have a standardized size for 6-days larvae. We would place the sample inside the well and then fill it with LMPA, just having to perform small adjustments for a perfect orientation.

4.2.2 Confocal microscopy and expression pattern comparisons

Although the performed anatomical characterization of the five previously-established lines was crucial for the purpose of incorporating this new information into an international zebrafish brain atlas, thus increasing the robustness of this type of databases, it was also vital to assess whether the expression pattern of the lines available in CF coincided or not with the ones previously reported. It is common to observe small differences, because even if the embryos are injected with the same construct, the establishment of lines in different laboratories

from different founders generate different fish populations with a distinct number and site(s) of insertion. A greater silencing may also occur in some lines which can be translated into an incomplete expression pattern. Additionally, some of the gene literature available is from *in situ* hybridization studies, which identifies positive cells based on their mRNA content and not on protein content as is the case of the immunohistochemistry technique (DeLellis, 1994). Therefore, discrepancies may be observed due to different time points of mRNA and protein expression and/or post-synthesis protein migration. Additionally, it is also relevant to mention that although mRNA is being synthesized in a cell, that does not necessarily mean that it gives rise to a functional and immunodetectable protein.

Regarding the Tg(pitx2c:GFP) line some variations were observed when comparing the available bibliography with the obtained confocal pattern (Results - Table 3.3). According to Essner et al., 2000, *in situ* hybridization studies showed an asymmetrical pitx2c expression in the right dorsal diencephalon, after 19 hpf, most likely to correspond to the future habenula. This structure is already developed at 6 dpf, however no expression was observed on this region. Instead GFP fluorescence was detected on other dorsal diencephalic regions, such as the preoptic area (pOa), the ventral Thalamus (vTha) and the posterior tuberculum (PTub). Possibly, at 6 dpf this protein ceases to be expressed in the habenula, which may explain why no signal was detected on this region. In addition, round and speckled cells were observed in larvae's skin and retina, a pattern not described in previous studies. According to the location and shape of these cells, they are suggestive of being iridophore-pigmented cells, present in zebrafish larvae after 3 dpf (Higdon et al., 2013; Lopes et al., 2008). The PTU treatment that these larvae were subjected to inhibits the formation of melanocytes, but it does not affect the formation of reflective platelets in white pigmented cells, such as iridophores (Fukuzawa, 2015). As such, iridophores develop normally in the presence of PTU, reinforcing our interpretation that pitx2c is labelling these cells. However, the connection between iridophores and the pitx2c gene is unclear, and future studies will be needed. One approach to confirm this hypothesis would be to perform an immunohistochemical co-labeling for the purine nucleoside phosphorylase 4a (pnp4a), a zebrafish iridophore marker, and verify whether this pattern corresponds to the one observed in the line (Kimura et al., 2017).

Concerning the Tg(pSAM:Gal4), Tg(UAS:mCherry) line, in general the pattern matched between the literature, screens at 3 dpf and confocal acquisition at 6 dpf (Results - Table 3.3), even if there was no signal detection on the anterior and posterior lateral line and in the trigeminal ganglion, as previously reported by Lacoste et at., 2015. These discrepancies may be explained by the fact that the lines are not exactly the same, as they were generated in different laboratories, or even due to a silencing effect, as explained above. Additionally, it was possible

to clearly identify the nucMLF and their projections during the screens at 3 dpf, but the same did not happen through confocal microscopy. This inconsistency may be explained not only by the different time points between both imaging techniques, but also by the transposition of the red endogenous mCherry fluorescence of this line to a green GCaMP fluorescence, with a better signal detection. This exchange may have not been 100% efficient, which can explain the differences found.

For the Tg(glyt2:|R|-Gal4), Tg(UAS:GFP) line (Results - Table 3.3) the expression pattern described on previous studies was in accordance with the one observed during the screens and the confocal imaging, with a predominant bilateral symmetric expression in the rhombencephalon. Additionally, it was possible to observe the MID2cm and MID3cm cells, belonging to the rSnc, and the oculomotor nerve nucleus (OmNn).

In relation to the Tg(gata1a:GFP) line, to the best of our knowledge, its neuronal expression is not sufficiently described on the literature, which further highlights the importance of this project and the incorporation of this new information into a zebrafish atlas.

To conclude, is important to note that the performed anatomical annotation is only tentative and that, in the future, the use of *in situ* hybridization or immunohistochemistry co-labelling for specific structures would help to confirm the zones assignments made.

4.2.3 Registration of images

To characterize any transgenic line, one of the main limitations of the process is the variability between different specimens. Although we expect to observe the same pattern in all samples, it is crucial to consider that they may present different levels of expression at the same fixation time, small distinctions in circuit assembly and few variations in the position of their neurons. So far, the best strategy to overcome this limitation is the image processing performed at the time of registration, in which all images are transformed taking as reference a common t-ERK model brain, mitigating the variability factor. This point highlights the importance of performing the t-ERK staining, a requirement if we seek for registration of our lines into the ZBB1.2 atlas, otherwise these transformations would not be possible. After this, we are able to perform an anatomical attribution of zones with a higher level of certainty, since the variability effect is reduced and the expression pattern of different samples is combined into one output z-stack.

Several algorithms are available to register confocal stacks such as the Computational Morphometry Toolkit (CMTK) and ANTs, however ANTs is now being the one used by us since it has been shown to supersede the CMTK as highlighted for the construction of ZBB1.2 atlas (Marquart et al., 2017).

The exact transgenic lines studied on this project are not registered in any of the most commonly used atlases, such as Z-Brain, ZBB1.2 and mapZebrain. Instead, and just for some of them, related lines are available: Tg(gata1:DsRed), registered on mapZebrain and ZBB1.2 with a different reporter marker; Tg(glyt2:GFP), present in all three atlases and with a direct expression independent of the Cre-LoxP system; or the Tg(6.7FRhcrtR-Gal4-uasKaede), published on Z-brain, and with an identical fluorescence to the Tg (pSAM:Gal4), Tg(UAS:mCherry) line. For the Tg(aldoca:gap43-Venus), Tg(pSAM:Gal4), Tg(UAS:mCherry) and Tg(glyt2:|R|-Gal4), Tg(UAS:GFP) characterized lines, we believe that the differences observed between the individual confocal images and the averages obtained after the registration process may not be very significant, suggesting that these populations have a stable and homogeneous expression. On the other hand, the Tg(pitx2c:GFP) line presented a broader expression pattern in the average reconstruction as compared to the selected individual fish, which may be related to a weak signal in the individual image, only detectable after the merging of several samples, or to an expression pattern that is neither uniform across the population nor complete in all fish. In fact, this line was established years ago at a different institution, and it is therefore possible that the screens during the line establishment were not executed according to the best practices. Silencing is also a possible explanation for the heterogeneous phenotypes, although silencing is much less frequent in inserts of the type direct promoter - final reporter, compared to dual systems such as GAL4/UAS. Unfortunately, it was not possible to execute and average for the Tg(gata1a:GFP) line, as the samples showed a bad orientation that made it impossible to perform an accurate merge. In the future, more samples will need to be acquired and the process repeated.

5

Conclusions and Future Perspectives

The creation of transgenic zebrafish lines expressing genetically encoded fluorescent proteins, together with the development of sophisticated imaging techniques, have created the opportunity to look at large neuronal populations with a very high resolution and spatial precision, which remains crucial to better understand the brain's functional organization.

The establishment of the Tg(elavl3:GFF)ccu5, Tg(UAS:mCherry), Tg(10xUAS:Kif5c^{560}-EYFP) zebrafish line showed promising results, with a clear success of the microinjection procedure confirmed by germline transmission to the next generation. In the future, more crosses will be carried out to confirm if the F0 fish whose number of screened embryos was not sufficient to draw a conclusion, carry or not the transgene in the germline. Furthermore, positive progeny from selected founders will be raised as F1 generation, completing the establishment of the line, that will be considered stable when all the positive progeny exhibits the same expression pattern. Since the kif5c^{560} protein was reported as the earliest intracellular marker of axonogenesis, this line will contribute to better comprehend the neuronal polarization phenomenon.

Regarding the other five previously-established lines studied during this project, it was possible to anatomically characterize their expression, that, in general, was in agreement with what was previously described on the literature. The execution of *in situ* hybridization and immunohistochemistry co-labelling for specific structures may help in the future to confirm the zones assignments suggested in this work. In addition, the official registration of the obtained images on the ZBB1.2 atlas will contribute to a greater robustness of this database and the possibility of using the collected information to study neurological disorders.

REFERENCES

Abdelrahman, D., Hasan, W., & Da'as, S. I. (2021). Microinjection quality control in zebrafish model for genetic manipulations. *MethodsX*, *8*, 101418. https://doi.org/10.1016/j.mex.2021.101418

Adelmann, H. B. (1922). The Significance of the Prechordal Plate: An Interpretative Study. *American Journal of Anatomy*. https://anatomypubs.onlinelibrary.wiley.com/doi/abs/10.1002/aja.1000310104

Akitake, C. M., Macurak, M., Halpern, M. E., & Goll, M. G. (2011). Transgenerational analysis of transcriptional silencing in zebrafish. *Developmental Biology*, *352*(2), 191–201. https://doi.org/10.1016/j.ydbio.2011.01.002

Amsterdam, A., Lin, S., & Hopkins, N. (1995). The Aequorea victoria green fluorescent protein can be used as a reporter in live zebrafish embryos. In *Developmental Biology* (Vol. 171, Issue 1, pp. 123–129). https://doi.org/10.1006/dbio.1995.1265

Arjmand, B., Tayanloo-Beik, A., Foroughi Heravani, N., Alaei, S., Payab, M., Alavi-Moghadam, S., Goodarzi, P., Gholami, M., & Larijani, B. (2020). Zebrafish for Personalized Regenerative Medicine; A More Predictive Humanized Model of Endocrine Disease. *Frontiers in Endocrinology*, *11*(July), 1–14. https://doi.org/10.3389/fendo.2020.00396

Asakawa, K., & Kawakami, K. (2008). Targeted gene expression by the Gal4-UAS system in zebrafish. *Development Growth and Differentiation*, *50*(6), 391–399. https://doi.org/10.1111/j.1440-169X.2008.01044.x

Barreiro-Iglesias, A., Mysiak, K. S., Adrio, F., Rodicio, M. C., Becker, C. G., Becker, T., & Anadón, R. (2013). Distribution of glycinergic neurons in the brain of glycine transporter-2 transgenic Tg(glyt2:Gfp) adult zebrafish: Relationship to brain-spinal descending systems. *Journal of Comparative Neurology*, *521*(2), 389–425. https://doi.org/10.1002/cne.23179

Bátora, D., Zsigmond, Á., Lőrincz, I. Z., Szegvári, G., Varga, M., & Málnási-Csizmadia, A. (2021). Subcellular Dissection of a Simple Neural Circuit: Functional Domains of the Mauthner-Cell During Habituation. *Frontiers in Neural Circuits*, *15*(March), 1–13. https://doi.org/10.3389/fncir.2021.648487

Berg, E. M., Björnfors, E. R., Pallucchi, I., Picton, L. D., & El Manira, A. (2018). Principles Governing Locomotion in Vertebrates: Lessons From Zebrafish. *Frontiers in Neural Circuits*, *12*(September), 1–18. https://doi.org/10.3389/fncir.2018.00073

Boumelhem, B. B., Assinder, S. J., Hammans, C., Tanudisastro, M. P., Le, D. T. M., Brigden, K. W. L., & Fraser, S. T. (2015). The Mesendoderm: A Wellspring of Cell Lineages for Regenerative Medicine. In *Frontiers in Stem Cell and Regenerative Medicine Research* (4th ed., pp. 36-100 (65)). https://doi.org/https://doi.org/10.2174/9781681084350117040004

Bradford, Y. M., Van Slyke, C. E., Ruzicka, L., Singer, A., Eagle, A., Fashena, D., Howe, D. G., Frazer, K., Martin, R., Paddock, H., Pich, C., Ramachandran, S., & Westerfield, M. (2022). *Zebrafish Information Network, the knowledgebase for Danio rerio research. Genetics. 220(4).* https://zfin.org/

Breau, M. A., Bonnet, I., Stoufflet, J., Xie, J., De Castro, S., & Schneider-Maunoury, S. (2017). Extrinsic mechanical forces mediate retrograde axon extension in a developing neuronal circuit. *Nature Communications*, *8*(1). https://doi.org/10.1038/s41467-017-00283-3

Carta, E., Chung, S. K., James, V. M., Robinson, A., Gill, J. L., Remy, N., Vanbellinghen, J. F., Drew, C. J. G., Cagdas, S., Cameron, D., Cowan, F. M., Del Toro, M., Graham, G. E., Manzur, A. Y., Masri, A., Rivera, S., Scalais, E., Shiang, R., Sinclair, K., … Harvey, R. J. (2012). Mutations in the GlyT2 gene (SLC6A5) are a second major cause of startle disease. *Journal of Biological Chemistry*, *287*(34), 28975–28985. https://doi.org/10.1074/jbc.M112.372094

Cassar, S., Adatto, I., Freeman, J. L., Gamse, J. T., Iturria, I., Lawrence, C., Muriana, A., Peterson, R. T., Van Cruchten, S., & Zon, L. I. (2020). Use of Zebrafish in Drug Discovery Toxicology. *Chemical Research in Toxicology*, *33*(1), 95–118. https://doi.org/10.1021/acs.chemrestox.9b00335

Choe, C. P., Choi, S.-Y., Kee, Y., Kim, M. J., Kim, S.-H., Lee, Y., Park, H.-C., & Ro, H. (2021). Transgenic fluorescent zebrafish lines that have revolutionized biomedical research. *Laboratory Animal Research*, *37*(1), 1–29. https://doi.org/10.1186/s42826-021-00103-2

Dean, D. A. (2013). Microinjection. *Brenner's Encyclopedia of Genetics: Second Edition*, 409–410. https://doi.org/10.1016/B978-0-12-374984-0.00945-1

DeLellis, R. A. (1994). In situ hybridization techniques for the analysis of gene expression: Applications in tumor pathology. *Human Pathology*, *25*(6), 580–585. https://doi.org/https://doi.org/10.1016/0046-8177(94)90222-4

Eisen, J. S., & Smith, J. C. (2008). Controlling morpholino experiments: Don't stop making antisense. *Development*, *135*(10), 1735–1743. https://doi.org/10.1242/dev.001115

Erickson, P. A., Ellis, N. A., & Miller, C. T. (2016). Microinjection for transgenesis and genome editing in threespine sticklebacks. *Journal of Visualized Experiments*, *2016*(111), 1–13. https://doi.org/10.3791/54055

Essner, J. J., Branford, W. W., Zhang, J., & Yost, H. J. (2000). *Mesendoderm and left-right brain, heart and gut development are differentially regulated by pitx2 isoforms*. *1093*, 1081–1093.

Feierstein, C. E., Portugues, R., & Orger, M. B. (2015). Seeing the whole picture: A comprehensive imaging approach to functional mapping of circuits in behaving zebrafish. *Neuroscience*, *296*, 26–38. https://doi.org/10.1016/j.neuroscience.2014.11.046

Firouzabadi, N., Navabzadeh, N., Moghimi-Sarani, E., & Haghnegahdar, M. (2020). Orexin/hypocretin type 2 receptor (HCRTR2) gene as a candidate gene in sertraline-associated insomnia in depressed patients. *Neuropsychiatric Disease and Treatment*, *16*, 1121–1128. https://doi.org/10.2147/NDT.S250141

Fukuzawa, T. (2015). Ferritin H subunit gene is specifically expressed in melanophore precursor-derived white pigment cells in which reflecting platelets are formed from stage II melanosomes in the periodic albino mutant of Xenopus laevis. *Cell and Tissue Research*, *361*(3), 733–744. https://doi.org/10.1007/s00441-015-2133-8

Gahtan, E., Tanger, P., & Baier, H. (2005). Visual prey capture in larval zebrafish is controlled by identified reticulospinal neurons downstream of the tectum. *Journal of Neuroscience*, *25*(40), 9294–9303. https://doi.org/10.1523/JNEUROSCI.2678-05.2005

Gore, A. V., Pillay, L. M., Venero Galanternik, M., & Weinstein, B. M. (2018). The zebrafish: A fintastic model for hematopoietic development and disease. *Wiley Interdisciplinary Reviews: Developmental Biology*, *7*(3), 1–27. https://doi.org/10.1002/wdev.312

Halpern, M. E., Rhee, J., Goll, M. G., Akitake, C. M., Parsons, M., & Leach, S. D. (2008). *Gal4/UAS Transgenic Tools and Their Application to Zebrafish*. *5*(2).

Higdon, C. W., Mitra, R. D., & Johnson, S. L. (2013). Gene Expression Analysis of Zebrafish Melanocytes, Iridophores, and Retinal Pigmented Epithelium Reveals Indicators of Biological Function and Developmental Origin. *PLoS ONE*, *8*(7).

https://doi.org/10.1371/journal.pone.0067801
Hoff, F. (2015). How to Prepare Your Specimen for Immunofluorescence Microscopy. *Leica Microsystems*, *Immunofluo*, 1–10. http://www.leica-microsystems.com/science-lab/how-to-prepare-your-specimen-for-immunofluorescence-microscopy/
Huang, C. J., Tu, C. T., Hsiao, C. Der, Hsieh, F. J., & Tsai, H. J. (2003). Germ-line transmission of a myocardium-specific GFP transgene reveals critical regulatory elements in the cardiac myosin light chain 2 promoter of zebrafish. *Developmental Dynamics*, *228*(1), 30–40. https://doi.org/10.1002/dvdy.10356
Ihaka, R., & Gentleman, R. (1996). R: A Language for Data Analysis and Graphics. *Journal of Computational and Graphical Statistics*, *5*(3), 299–314. https://doi.org/10.2307/1390807
Jacobson, C., Schnapp, B., & Banker, G. A. (2006). A change in the selective translocation of the kinesin-1 motor domain marks the initial specification of the axon. *Neuron*, *49*(6), 797–804. https://doi.org/10.1016/j.neuron.2006.02.005
Jonkman, J., Brown, C. M., Wright, G. D., Anderson, K. I., & North, A. J. (2020). Tutorial: guidance for quantitative confocal microscopy. *Nature Protocols*, *15*(5), 1585–1611. https://doi.org/10.1038/s41596-020-0313-9
Karlsson, J., Von Hofsten, J., & Olsson, P. E. (2001). Generating transparent zebrafish: A refined method to improve detection of gene expression during embryonic development. *Marine Biotechnology*, *3*(6), 522–527. https://doi.org/10.1007/s1012601-0053-4
Kawakami, K. (2007). Tol2: A versatile gene transfer vector in vertebrates. *Genome Biology*, *8*(SUPPL. 1), 1–10. https://doi.org/10.1186/gb-2007-8-s1-s7
Kikuta, H., & Kawakami, K. (2009). *Chapter 5 - Transient and Stable Transgenesis Using Tol2 Transposon Vectors*. *February*. https://doi.org/10.1007/978-1-60327-977-2
Kim, H., Kim, M., Im, S.-K., & Fang, S. (2018). Mouse Cre-LoxP system: general principles to determine tissue-specific roles of target genes. *Laboratory Animal Research*, *34*(4), 147. https://doi.org/10.5625/lar.2018.34.4.147
Kim, S. Y., Kim, K. W., Kwon, Y. M., & Kim, J. Y. H. (2020). mCherry Protein as an In Vivo Quantitative Reporter of Gene Expression in the Chloroplast of Chlamydomonas reinhardtii. *Molecular Biotechnology*, *62*(5), 297–305. https://doi.org/10.1007/s12033-020-00249-9
Kimura, T., Takehana, Y., & Naruse, K. (2017). Pnp4a Is the causal gene of the medaka iridophore Mutant guanineless. *G3: Genes, Genomes, Genetics*, *7*(4), 1357–1363. https://doi.org/10.1534/g3.117.040675
Kleinhans, D. S., & Lecaudey, V. (2019). Standardized mounting method of (zebrafish) embryos using a 3D-printed stamp for high-content, semi-automated confocal imaging. *BMC Biotechnology*, *19*(1), 1–10. https://doi.org/10.1186/s12896-019-0558-y
Kong, J., Wang, Y., Qi, W., Huang, M., Su, R., & He, Z. (2020). Green fluorescent protein inspired fluorophores. *Advances in Colloid and Interface Science*, *285*, 102286. https://doi.org/10.1016/j.cis.2020.102286
Kunst, M., Laurell, E., Mokayes, N., Kramer, A., Kubo, F., Fernandes, A. M., Förster, D., Dal Maschio, M., & Baier, H. (2019). A Cellular-Resolution Atlas of the Larval Zebrafish Brain. *Neuron*, *103*(1), 21-38.e5. https://doi.org/10.1016/j.neuron.2019.04.034
Lacoste, A. M. B., Schoppik, D., Robson, D. N., Haesemeyer, M., Portugues, R., Li, J. M., Randlett, O., Wee, C. L., Engert, F., & Schier, A. F. (2015). A Convergent and essential interneuron pathway for mauthner-cell-mediated escapes. *Current Biology*, *25*(11), 1526–1534. https://doi.org/10.1016/j.cub.2015.04.025
Li, Y., Jia, Z., Zhang, S., & He, X. (2021). Progress in gene-editing technology of Zebrafish.

Biomolecules, *11*(9). https://doi.org/10.3390/biom11091300

Lin, Y. C., Hsu, C. C. H., Wang, P. N., Lin, C. P., & Chang, L. H. (2020). The Relationship Between Zebrin Expression and Cerebellar Functions: Insights From Neuroimaging Studies. *Frontiers in Neurology*, *11*(April), 1–12. https://doi.org/10.3389/fneur.2020.00315

Lister, J. A., Robertson, C. P., Lepage, T., Johnson, S. L., & Raible, D. W. (1999). Nacre Encodes a Zebrafish Microphthalmia-Related Protein That Regulates Neural-Crest-Derived Pigment Cell Fate. *Development*, *126*(17), 3757–3767. https://doi.org/10.1242/dev.126.17.3757

Lopes, S. S., Yang, X., Müller, J., Carney, T. J., McAdow, A. R., Rauch, G. J., Jacoby, A. S., Hurst, L. D., Delfino-Machín, M., Haffter, P., Geisler, R., Johnson, S. L., Ward, A., & Kelsh, R. N. (2008). Leukocyte tyrosine kinase functions in pigment cell development. *PLoS Genetics*, *4*(3). https://doi.org/10.1371/journal.pgen.1000026

Marquart, G. D., Tabor, K. M., Brown, M., Strykowski, J. L., Varshney, G. K., LaFave, M. C., Mueller, T., Burgess, S. M., Higashijima, S. I., & Burgess, H. A. (2015). A 3D searchable database of transgenic zebrafish gal4 and cre lines for functional neuroanatomy studies. *Frontiers in Neural Circuits*, *9*(November), 1–17. https://doi.org/10.3389/fncir.2015.00078

Marquart, G. D., Tabor, K. M., Horstick, E. J., Brown, M., Geoca, A. K., Polys, N. F., Nogare, D. D., & Burgess, H. A. (2017). High-precision registration between zebrafish brain atlases using symmetric diffeomorphic normalization. *GigaScience*, *6*(8). https://doi.org/10.1093/gigascience/gix056

Martins, S., Monteiro, J. F., Vito, M., Weintraub, D., Almeida, J., & Certal, A. C. (2016). Toward an Integrated Zebrafish Health Management Program Supporting Cancer and Neuroscience Research. *Zebrafish*, *13*(00), S47–S55. https://doi.org/10.1089/zeb.2015.1198

McLellan, M. A., Rosenthal, N. A., & Pinto, A. R. (2017). Cre-loxP-Mediated Recombination: General Principles and Experimental Considerations. *Current Protocols in Mouse Biology*, *7*(1), 1–12. https://doi.org/10.1002/cpmo.22

Monteiro, J. F., Martins, S., Farias, M., Costa, T., & Certal, A. C. (2018). The impact of two different cold-extruded feeds and feeding regimens on zebrafish survival, growth and reproductive performance. *Journal of Developmental Biology*, *6*(3). https://doi.org/10.3390/jdb6030015

Mukherjee, K., & Liao, E. C. (2018). Generation and characterization of a zebrafish muscle specific inducible Cre line. *Transgenic Research*, *27*(6), 559–569. https://doi.org/10.1007/s11248-018-0098-6

Nagai, T., Ibata, K., Park, E. S., Kubota, M., Mikoshiba, K., & Miyawaki, A. (2002). A variant of yellow fluorescent protein with fast and efficient maturation for cell-biological applications. *Nature Biotechnology*, *20*(1), 87–90. https://doi.org/10.1038/nbt0102-87

NHI, N. L. of M. (2022). *mapk1: mitogen-activated protein kinase 1 [Danio rerio (zebrafish)]*. 24th April. https://www.ncbi.nlm.nih.gov/gene/360144/#summary

Pei, W., & Burgess, S. (2019). Chapter 26 - Microinjection in Zebrafish for Genome Editing and Functional Studies. *Springer Nature*, *1874*, 174–178. https://doi.org/https://doi.org/10.1007/978-1-4939-8831-0_26

Preibisch, S., Saalfeld, S., & Tomancak, P. (2009). Globally optimal stitching of tiled 3D microscopic image acquisitions. *Bioinformatics*, *25*(11), 1463–1465. https://doi.org/10.1093/bioinformatics/btp184

Randlett, O., Poggi, L., Zolessi, F. R., & Harris, W. A. (2011). The Oriented Emergence of Axons from Retinal Ganglion Cells Is Directed by Laminin Contact In Vivo. *Neuron*, *70*(2), 266–280. https://doi.org/10.1016/j.neuron.2011.03.013

Randlett, O., Wee, C. L., Naumann, E. A., Nnaemeka, O., Schoppik, D., Fitzgerald, J. E., Portugues,

R., Lacoste, A. M. B., Riegler, C., Engert, F., & Schier, A. F. (2015). Whole-brain activity mapping onto a zebrafish brain atlas. *Nature Methods*, *12*(11), 1039–1046. https://doi.org/10.1038/nmeth.3581

Renaud, O., Herbomel, P., & Kissa, K. (2011). Studying cell behavior in whole zebrafish embryos by confocal live imaging: Application to hematopoietic stem cells. *Nature Protocols*, *6*(12), 1897–1904. https://doi.org/10.1038/nprot.2011.408

Ronneberger, O., Liu, K., Rath, M., Rueβ, D., Mueller, T., Skibbe, H., Drayer, B., Schmidt, T., Filippi, A., Nitschke, R., Brox, T., Burkhardt, H., & Driever, W. (2012). ViBE-Z: a framework for 3D virtual colocalization analysis in zebrafish larval brains. *Nature Methods*, *9*(7), 735–742. https://doi.org/10.1038/nmeth.2076

Rosskothen-Kuhl, N., & Illing, R. B. (2014). G ap43 transcription modulation in the adult brain depends on sensory activity and synaptic cooperation. *PLoS ONE*, *9*(3), 1–16. https://doi.org/10.1371/journal.pone.0092624

Sadowski, I., Ma, J., Triezenberg, S., & Ptashne, M. (1988). GAL4-VP16 is an unusually potent transcriptional activator. *Nature*, *335*(6190), 563–564. https://doi.org/10.1038/335563a0

Sanderson, M. J., Smith, I., Parker, I., & Bootman, M. D. (2016). Fluorescence Microscopy. *Physiology & Behavior*, *2014*(10), 1–36. https://doi.org/10.1101/pdb.top071795.Fluorescence

Santos, D., Monteiro, S. M., & Luzio, A. (2018). General whole-mount immunohistochemistry of zebrafish (Danio rerio) embryos and larvae protocol. *Methods in Molecular Biology*, *1797*, 365–371. https://doi.org/10.1007/978-1-4939-7883-0_19

Schelski, M., & Bradke, F. (2017). Neuronal polarization: From spatiotemporal signaling to cytoskeletal dynamics. *Molecular and Cellular Neuroscience*, *84*, 11–28. https://doi.org/10.1016/j.mcn.2017.03.008

Schindelin, J., Arganda-Carreras, I., Frise, E., Kaynig, V., Longair, M., Pietzsch, T., Preibisch, S., Rueden, C., Saalfeld, S., Schmid, B., Tinevez, J.-Y., White, D. J., Hartenstein, V., Eliceiri, K., Tomancak, P., & Cardona, A. (2012). Fiji: an open-source platform for biological-image analysis. *Nature Methods*, *9*(7), 676–682. https://doi.org/10.1038/nmeth.2019

Scott, E. K. (2009). The Gal4/UAS toolbox in zebrafish: New approaches for defining behavioral circuits. *Journal of Neurochemistry*, *110*(2), 441–456. https://doi.org/10.1111/j.1471-4159.2009.06161.x

Sertori, R., Trengove, M., Basheer, F., Ward, A. C., & Liongue, C. (2016). Genome editing in zebrafish: A practical overview. *Briefings in Functional Genomics*, *15*(4), 322–330. https://doi.org/10.1093/bfgp/elv051

Severi, K. E., Böhm, U. L., & Wyart, C. (2018). Investigation of hindbrain activity during active locomotion reveals inhibitory neurons involved in sensorimotor processing. *Scientific Reports*, *8*(1), 1–11. https://doi.org/10.1038/s41598-018-31968-4

Smith, C. L. (2008). Basic confocal microscopy. *Current Protocols in Molecular Biology*, *SUPPL. 81*, 1–18. https://doi.org/10.1002/0471142727.mb1411s81

Spence, R., Gerlach, G., Lawrence, C., & Smith, C. (2008). The behaviour and ecology of the zebrafish, Danio rerio. *Biological Reviews*, *83*(1), 13–34. https://doi.org/10.1111/j.1469-185X.2007.00030.x

Suster, M. L., Kikuta, H., Urasaki, A., Asakawa, K., & Kawakami, K. (2009). Transgenesis in Zebrafish with the Tol2 transposon system. *Methods in Molecular Biology*, *561*, 41–63. https://doi.org/10.1007/978-1-60327-019-9_3

Takeuchi, M., Matsuda, K., Yamaguchi, S., Asakawa, K., Miyasaka, N., Lal, P., Yoshihara, Y., Koga, A., Kawakami, K., Shimizu, T., & Hibi, M. (2015). Establishment of Gal4 transgenic zebrafish

lines for analysis of development of cerebellar neural circuitry. *Developmental Biology*, *397*(1), 1–17. https://doi.org/10.1016/j.ydbio.2014.09.030

Tallafuss, A., Kelly, M., Gay, L., Gibson, D., Batzel, P., Karfilis, K. V., Eisen, J., Stankunas, K., Postlethwait, J. H., & Washbourne, P. (2015). Transcriptomes of post-mitotic neurons identify the usage of alternative pathways during adult and embryonic neuronal differentiation. *BMC Genomics*, *16*(1), 1–14. https://doi.org/10.1186/s12864-015-2215-8

Tanabe, K., Kani, S., Shimizu, T., Bae, Y. K., Abe, T., & Hibi, M. (2010). Atypical protein kinase C regulates primary dendrite specification of cerebellar Purkinje cells by localizing golgi apparatus. *Journal of Neuroscience*, *30*(50), 16983–16992. https://doi.org/10.1523/JNEUROSCI.3352-10.2010

Tümer, Z., & Bach-Holm, D. (2009). Axenfeld-Rieger syndrome and spectrum of PITX2 and FOXC1 mutations. *European Journal of Human Genetics*, *17*(12), 1527–1539. https://doi.org/10.1038/ejhg.2009.93

Urasaki, A., Morvan, G., & Kawakami, K. (2006). Functional dissection of the Tol2 transposable element identified the minimal cis-sequence and a highly repetitive sequence in the subterminal region essential for transposition. *Genetics*, *174*(2), 639–649. https://doi.org/10.1534/genetics.106.060244

Vaz, R., Hofmeister, W., & Lindstrand, A. (2019). Zebrafish models of neurodevelopmental disorders: Limitations and benefits of current tools and techniques. *International Journal of Molecular Sciences*, *20*(6), 1–26. https://doi.org/10.3390/ijms20061296

Wang, H. Y., Li, Y., Xue, T., Cheng, N., & Du, H. N. (2016). Construction of a series of pCS2+ backbone-based Gateway vectors for overexpressing various tagged proteins in vertebrates. *Acta Biochimica et Biophysica Sinica*, *48*(12), 1128–1134. https://doi.org/10.1093/abbs/gmw107

Witzel, H. R., Cheedipudi, S., Gao, R., Stainier, D. Y. R., & Dobreva, G. D. (2017). Isl2b regulates anterior second heart field development in zebrafish. *Scientific Reports*, *7*, 1–9. https://doi.org/10.1038/srep41043

Wolman, M. A., Sittaramane, V. K., Essner, J. J., Yost, H. J., Chandrasekhar, A., & Halloran, M. C. (2008). Transient axonal glycoprotein-1 (TAG-1) and laminin-α1 regulate dynamic growth cone behaviors and initial axon direction in vivo. *Neural Development*, *3*(1). https://doi.org/10.1186/1749-8104-3-6

Xu, Q. (1999). Microinjection into zebrafish embryos. *Methods in Molecular Biology (Clifton, N.J.)*, *127*, 125–132. https://doi.org/10.1385/1-59259-678-9:125

A

SUPPLEMENTARY INFORMATION

Appendix 1 - Zebrafish embryo mortality and morbidity rates at 24 hpf, after microinjection round 1. The embryos were obtained from a cross of the 2785(1) Tg(elavl3:GFF)ccu5, Tg(UAS:mCherry) line with the 2180(1) wildtype (*wt*) TU line and injected with a mix comprising 25, 30 or 50 ng/µL (concentration in nanograms per microlitre) of the 10xUAS:Kif5c^{560}-EYFP DNA construct and 100 ng/µL of tol2 mRNA.

Microinjection Round 1								
Clutch	ID	Concentration (ng/µL)	Number of dead embryos	Number of living embryos	Number of abnormal embryos	Total	Mortality rate (%) [a]	Morbidity rate (%) [b]
A	Control	-	90	99	-	189	47.6	-
	Injected A	25	84	13	3	97	86.6	23.1
B	Control	-	87	52	-	139	62.6	-
	Injected B1	25	37	5	3	42	88.1	60.0
	Injected B2	30	23	1	0	24	95.8	0
C	Control	-	66	16	-	82	80.5	-
	Injected C	30	57	15	1	62	91.9	20.0
D	Control	-	15	107	-	122	12.3	-
	Injected D1	30	34	9	1	43	79.1	11.1
	Injected D2	25	22	2	1	24	91.7	50.0

[a] - (Number of dead embryos / Total) x 100 | [b] - (Number of abnormal embryos / Number of living embryos) x 100

Appendix 2 - Zebrafish embryo mortality and morbidity rates at 24 hpf, after microinjection round 2. The embryos were obtained from a cross of the 2802(1) Tg(elavl3:GFF)ccu5, Tg(UAS:mCherry) line with the 3057(2) nacre$^{-/-}$ line and injected with a mix comprising 25, 30 or 50 ng/µL (concentration in nanograms per microlitre) of the 10xUAS:Kif5c^{560}-EYFP DNA construct and 100 ng/µL of tol2 mRNA.

Microinjection Round 2								
Clutch	ID	Concentration (ng/µL)	Number of dead embryos	Number of living embryos	Number of abnormal embryos	Total	Mortality rate (%) [a]	Morbidity rate (%) [b]
A	Control	-	28	120	-	148	18.9	-
	Injected A	25	71	27	6	98	72.4	22.2
B	Control	-	62	77	-	139	44.6	-
	Injected B	25	27	15	2	42	64.3	13.3
C	Control	-	54	96	-	150	36.0	-
	Injected C	30	70	37	9	107	65.4	24.3
D	Control	-	26	95	-	121	21.5	-
	Injected D1	30	40	8	5	48	83.3	62.5
	Injected D2	25	35	40	5	75	46.7	12.5

[a] - (Number of dead embryos / Total) x 100 | [b] - (Number of abnormal embryos / Number of living embryos) x 100

Appendix 3 - Zebrafish embryo mortality and morbidity rates at 24 hpf, after microinjection round 3. The embryos were obtained from a cross of the 2785(1) Tg(elavl3:GFF)ccu5, Tg(UAS:mCherry) line with the 2180(1) wildtype (*wt*) TU line and injected with a mix comprising 25, 30 or 50 ng/µL (concentration in nanograms per microlitre) of the 10xUAS:Kif5c^{560}-EYFP DNA construct and 100 ng/µL of tol2 mRNA.

Microinjection Round 3								
Clutch	ID	Concentration (ng/µL)	Number of dead embryos	Number of living embryos	Number of abnormal embryos	Total	Mortality rate (%) [a]	Morbidity rate (%) [b]
A	Control	-	49	75	-	124	39.5	-
	Injected A	25	63	9	7	72	87.5	77.8
B	Control	-	29	74	-	103	28.2	-
	Injected B	25	15	16	1	31	48.4	6.3
C	Control	-	78	59	-	137	56.9	-
	Injected C	30	69	33	2	102	67.6	6.1
D	Control	-	20	76	-	96	20.8	-
	Injected D	30	13	33	0	46	28.3	0

[a] - (Number of dead embryos / Total) x 100 | [b] - (Number of abnormal embryos / Number of living embryos) x 100

Appendix 4 - Zebrafish embryo mortality and morbidity rates at 24 hpf, after microinjection round 4. The embryos were obtained from a cross of the 2802(1) Tg(elavl3:GFF)ccu5, Tg(UAS:mCherry) line with the 3057(2) nacre$^{-/-}$ line and injected with a mix comprising 25, 30 or 50 ng/µL (concentration in nanograms per microlitre) of the 10xUAS:Kif5c^{560}-EYFP DNA construct and 100 ng/µL of tol2 mRNA.

Microinjection Round 4								
Clutch	ID	Concentration (ng/µL)	Number of dead embryos	Number of living embryos	Number of abnormal embryos	Total	Mortality rate (%) [a]	Morbidity rate (%) [b]
A	Control	-	15	122	-	137	10.9	-
	Injected A	25	28	60	22	88	31.8	36.7
B	Control	-	52	95	-	147	35.4	-
	Injected B	25	19	25	1	44	43.2	4.0
C	Control	-	33	106	-	139	23.7	-
	Injected C	30	36	53	4	89	40.4	7.5
D	Control	-	34	63	-	97	35.1	-
	Injected D	30	18	18	2	36	50.0	11.1

[a] - (Number of dead embryos / Total) x 100 | [b] - (Number of abnormal embryos / Number of living embryos) x 100

Appendix 5 - Zebrafish embryo mortality and morbidity rates at 24 hpf, after microinjection round 5. The embryos were obtained from a cross of the 2785(1) Tg(elavl3:GFF)ccu5, Tg(UAS:mCherry) line with the 3186(1) wildtype (*wt*) TU line and injected with a mix comprising 25, 30 or 50 ng/μL (concentration in nanograms per microlitre) of the 10xUAS:Kif5c^{560}-EYFP DNA construct and 100 ng/μL of tol2 mRNA.

Microinjection Round 5								
Clutch	ID	Concentration (ng/μL)	Number of dead embryos	Number of living embryos	Number of abnormal embryos	Total	Mortality rate (%) [(a)]	Morbidity rate (%) [(b)]
A	Control	-	51	101	-	152	33.6	-
	Injected A1	25	122	87	9	209	58.4	10.3
	Injected A2	50	45	28	3	73	61.6	10.7
B	Control	-	58	86	-	144	40.3	-
	Injected B1	50	18	18	1	36	50.0	5.6
	Injected B2	25	42	42	6	84	50.0	14.3
C	Control	-	24	144	-	168	14.3	-
	Injected C1	25	174	120	20	294	59.2	16.7
	Injected C2	50	12	72	3	84	14.3	4.2
D	Control	-	16	86	-	102	15.7	-
	Injected D	50	63	78	9	141	44.7	11.5

[(a)] - (Number of dead embryos / Total) x 100 | [(b)] - (Number of abnormal embryos / Number of living embryos) x 100

Appendix 6 - Zebrafish embryo mortality and morbidity rates at 24 hpf, after microinjection round 6. The embryos were obtained from a cross of the 2802(1) Tg(elavl3:GFF)ccu5, Tg(UAS:mCherry) line with the 3057(2) nacre$^{-/-}$ line and injected with a mix comprising 25, 30 or 50 ng/µL (concentration in nanograms per microlitre) of the 10xUAS:Kif5c^{560}-EYFP DNA construct and 100 ng/µL of tol2 mRNA.

Microinjection Round 6								
Clutch	ID	Concentration (ng/µL)	Number of dead embryos	Number of living embryos	Number of abnormal embryos	Total	Mortality rate (%) [a]	Morbidity rate (%) [b]
A	Control	-	50	106	-	156	32.1	-
	Injected A	50	75	39	3	114	65.8	7.7
B	Control	-	49	46	-	95	51.6	-
	Injected B	50	20	9	2	29	69.0	22.2
C	Control	-	27	128	-	155	17.4	-
	Injected C	50	83	96	7	179	46.4	7.3
D	Control	-	26	137	-	163	16.0	-
	Injected D	50	40	42	2	82	48.8	4.8

[a] - (Number of dead embryos / Total) x 100 | [b] - (Number of abnormal embryos / Number of living embryos) x 100

Appendix 7 - R 3.5.1 code, used to create Figures 3.1 and 3.2.

```
## LIBRARY LOADING: ##
library(gplots)
library(car)
library(multcompView)

## IMPORT OF DATA FROM EXCEL: ##
getwd()
dataZebra <- read.csv("Zebra1.csv", header=TRUE, sep=";")
dataZebra

## DEFINING DATA AS FACTORS OR NUMBERS: ##
dataZebra<-as.data.frame(dataZebra)
dataZebra$Replicate<-as.factor(dataZebra$Replicate)
dataZebra$Concentration<-as.factor(dataZebra$Concentration)
dataZebra$Mortality<-as.numeric(dataZebra$Mortality)
```

```
## DATA ORGANIZATION - ADDING "CONDITION": ##
Condition<-as.factor(paste(sep="_", dataZebra$Replicate, dataZebra$Concentration))
dataZebra<-cbind(Condition, dataZebra)
summary(dataZebra)
View(dataZebra)

## DEFINING "CONDITION" LEVELS: ##
zebraLevels<-levels(dataZebra$Condition)
zebraLevels

## TESTING DATA NORMALITY - MICROINJECTION 1: ##
for(i in 1:nlevels(dataZebra$Condition)){
 zebraSet1<-subset(dataZebra, Condition==zebraLevels[i])
 print(zebraSet1)
 print(zebraLevels[i])
 print(shapiro.test(zebraSet1$Mortality))
 print(shapiro.test(zebraSet1$Morbidity))
}

## TESTING DATA NORMALITY - MICROINJECTION 2: ##
for(i in 5:nlevels(dataZebra$Condition)){
 zebraSet2<-subset(dataZebra, Condition==zebraLevels[i])
 print(zebraSet2)
 print(zebraLevels[i])
 print(shapiro.test(zebraSet2$Mortality))
 print(shapiro.test(zebraSet2$Morbidity))
}

## TESTING DATA NORMALITY - MICROINJECTION 3: ##
for(i in 9:nlevels(dataZebra$Condition)){
 zebraSet3<-subset(dataZebra, Condition==zebraLevels[i])
 print(zebraSet3)
 print(zebraLevels[i])
 print(shapiro.test(zebraSet3$Mortality))
 print(shapiro.test(zebraSet3$Morbidity))
```

```
}

## TESTING DATA NORMALITY - MICROINJECTION 4: ##
for(i in 13:nlevels(dataZebra$Condition)){
 zebraSet4<-subset(dataZebra, Condition==zebraLevels[i])
 print(zebraSet4)
 print(zebraLevels[i])
 print(shapiro.test(zebraSet4$Mortality))
 print(shapiro.test(zebraSet4$Morbidity))
}

## TESTING DATA NORMALITY - MICROINJECTION 5: ##
for(i in 17:nlevels(dataZebra$Condition)){
 zebraSet5<-subset(dataZebra, Condition==zebraLevels[i])
 print(zebraSet5)
 print(zebraLevels[i])
 print(shapiro.test(zebraSet5$Mortality))
 print(shapiro.test(zebraSet5$Morbidity))
}

## TESTING DATA NORMALITY - MICROINJECTION 6: ##
for(i in 21:nlevels(dataZebra$Condition)){
 zebraSet6<-subset(dataZebra, Condition==zebraLevels[i])
 print(zebraSet6)
 print(zebraLevels[i])
 print(shapiro.test(zebraSet6$Mortality))
 print(shapiro.test(zebraSet6$Morbidity))
}

## TESTING DATA HOMOCEDASTICITY (homogeneity of variance): ##
leveneTest(data=dataZebra, Morbidity~Condition)
leveneTest(data=dataZebra, Mortality~Condition)

## MEANS: ##
ZebraMeans_Mortality<-aggregate(data=dataZebra, Mortality~Replicate+Concentration, mean,
na.rm=TRUE)
ZebraMeans_Mortality
```

```
ZebraMeans_Morbidity<-aggregate(data=dataZebra, Morbidity~Replicate+Concentration, mean, na.rm=TRUE)
ZebraMeans_Morbidity

# STANDARD DEVIATIONS: ##
ZebraSD_Mortality <- aggregate(data=dataZebra, Mortality~Replicate+Concentration, sd, na.rm=TRUE)
ZebraSD_Mortality

ZebraSD_Morbidity <- aggregate(data=dataZebra, Morbidity~Replicate+Concentration, sd, na.rm=TRUE)
ZebraSD_Morbidity

## ANOVA (one-way analysis of variance): ##
anovaZebra<-aov(data=dataZebra, cbind(Mortality, Morbidity)~ Replicate*Concentration)
summary(anovaZebra)

## NEW TABLE WITH MORTALITY MEANS AND STANDARD DEVIATIONS: ##
dataMortality<-as.data.frame(
 cbind(
  ZebraMeans_Mortality,
  ZebraSD_Mortality[,3]
 )
)
colnames(dataMortality)<-c("Replicate", "Concentration", "Mean mortality (%)", "SD")
View(dataMortality)

## NEW TABLE WITH MORBIDITY MEANS AND STANDARD DEVIATIONS: ##
dataMorbidity<-as.data.frame(
 cbind(
  ZebraMeans_Morbidity,
  ZebraSD_Morbidity[,3]
 )
)
colnames(dataMorbidity)<-c("Replicate", "Concentration", "Mean malformations (%)", "SD")
View(dataMorbidity)

## ---------- PLOT MICROINJECTION 1: ---------- ##
```

```
## SUBSETS OF DATA FOR PLOT 1: ##
zebraSet_I1_1<-subset(dataMortality, Replicate=="I1")
zebraSet_I1_2<-subset(dataMorbidity, Replicate=="I1")
zebraSet_I1_2<-rbind(zebraSet_I1_2,c("I1", "Control", NA, NA))
zebraSet<-cbind(zebraSet_I1_1, zebraSet_I1_2)
zebraSet<-zebraSet[c(3,1,2),]

## MEANS FOR PLOT 1: ##
plotData<-as.matrix(
 rbind(as.numeric(zebraSet[,3]), as.numeric(zebraSet[,7])),
)
colnames(plotData)<-c("Control", "25", "30")
rownames(plotData)<-c("Mortality", "Malformations")
summary(plotData)

## ERROR BARS (SD) FOR PLOT 1: ##
plotSD<-as.matrix(
 rbind(as.numeric(zebraSet[,4]), as.numeric(zebraSet[,8])),
)
colnames(plotSD)<-c("Control", "25", "30")
rownames(plotSD)<-c("Mortality", "Malformations")
summary(plotSD)

## PLOT 1: ##
windowsFonts(Calibri = windowsFont("Calibri"))
windows(8,6)
par(lwd=2, mar=c(5,5,1,1), family = "Calibri")
ploI1<-barplot2(
 plotData,
 beside=TRUE,
 plot.ci=TRUE,
 ci.u=plotData+plotSD,
 ci.l=plotData-plotSD,
 ylim=c(0, 100),
 col=c("cadetblue","lightsalmon"),
 xlab="Concentration (ng/uL)",
 ylab="Rate (%)",
```

```
 legend=FALSE
)
abline(h=0)


## SAVING PLOT 1 AS A TIFF FILE: ##
 dev.print(tiff,
 "plot_I1.tif",
 width = 16,
 height = 12,
 units = 'cm',
 type="windows",
 res=600
)

## ---------------------------------------- PLOT MICROINJECTION 2: ---------------------------------- ##
## SUBSETS OF DATA FOR PLOT 2: ##
zebraSet_I2_1<-subset(dataMortality, Replicate=="I2")
zebraSet_I2_2<-subset(dataMorbidity, Replicate=="I2")
zebraSet_I2_2<-rbind(zebraSet_I2_2,c("I2", "Control", NA, NA))
zebraSet<-cbind(zebraSet_I2_1, zebraSet_I2_2)
zebraSet<-zebraSet[c(3,1,2),]

## MEANS FOR PLOT 2: ##
plotData<-as.matrix(
 rbind(as.numeric(zebraSet[,3]), as.numeric(zebraSet[,7])),
)
colnames(plotData)<-c("Control", "25", "30")
rownames(plotData)<-c("Mortality", "Malformations")
summary(plotData)

## ERROR BARS (SD) FOR PLOT 2: ##
plotSD<-as.matrix(
 rbind(as.numeric(zebraSet[,4]), as.numeric(zebraSet[,8])),
)
colnames(plotSD)<-c("Control", "25", "30")
rownames(plotSD)<-c("Mortality", "Malformations")
```

```
summary(plotSD)

## PLOT 2: ##
windowsFonts(Calibri = windowsFont("Calibri"))
windows(8,6)
par(lwd=2, mar=c(5,5,1,1), family = "Calibri")
ploI1<-barplot2(
 plotData,
 beside=TRUE,
 plot.ci=TRUE,
 ci.u=plotData+plotSD,
 ci.l=plotData-plotSD,
 ylim=c(0, 100),
 col=c("cadetblue","lightsalmon"),
 xlab="Concentration (ng/uL)",
 ylab="Rate (%)",
 legend=FALSE
)
abline(h=0)

## SAVING PLOT 2 AS A TIFF FILE: ##
 dev.print(tiff,
 "plot_I2.tif",
 width = 16,
 height = 12,
 units = 'cm',
 type="windows",
 res=600
)

## ---------------------------------- PLOT MICROINJECTION 3:  ---------------------------------- ##
## SUBSETS OF DATA FOR PLOT 3: ##
zebraSet_I3_1<-subset(dataMortality, Replicate=="I3")
zebraSet_I3_2<-subset(dataMorbidity, Replicate=="I3")
zebraSet_I3_2<-rbind(zebraSet_I3_2,c("I3", "Control", NA, NA))
zebraSet<-cbind(zebraSet_I3_1, zebraSet_I3_2)
zebraSet<-zebraSet[c(3,1,2),]
```

```
## MEANS FOR PLOT 3: ##
plotData<-as.matrix(
 rbind(as.numeric(zebraSet[,3]), as.numeric(zebraSet[,7])),
)
colnames(plotData)<-c("Control", "25", "30")
rownames(plotData)<-c("Mortality", "Malformations")
summary(plotData)

## ERROR BARS (SD) FOR PLOT 3: ##
plotSD<-as.matrix(
 rbind(as.numeric(zebraSet[,4]), as.numeric(zebraSet[,8])),
)
colnames(plotSD)<-c("Control", "25", "30")
rownames(plotSD)<-c("Mortality", "Malformations")
summary(plotSD)

## PLOT 3: ##
windowsFonts(Calibri = windowsFont("Calibri"))
windows(8,6)
par(lwd=2, mar=c(5,5,1,1), family = "Calibri")
plot1<-barplot2(
 plotData,
 beside=TRUE,
 plot.ci=TRUE,
 ci.u=plotData+plotSD,
 ci.l=plotData-plotSD,
 ylim=c(0, 100),
 col=c("cadetblue","lightsalmon"),
 xlab="Concentration (ng/uL)",
 ylab="Rate (%)",
 legend=FALSE
)
abline(h=0)

## SAVING PLOT 3 AS A TIFF FILE: ##
 dev.print(tiff,
```

```
 "plot_I3.tif",
 width = 16,
 height = 12,
 units = 'cm',
 type="windows",
 res=600
)

## ---------------------------------- PLOT MICROINJECTION 4:  ---------------------------------- ##
## SUBSETS OF DATA FOR PLOT 4: ##
zebraSet_I4_1<-subset(dataMortality, Replicate=="I4")
zebraSet_I4_2<-subset(dataMorbidity, Replicate=="I4")
zebraSet_I4_2<-rbind(zebraSet_I4_2,c("I4", "Control", NA, NA))
zebraSet<-cbind(zebraSet_I4_1, zebraSet_I4_2)
zebraSet<-zebraSet[c(3,1,2),]

## MEANS FOR PLOT 4: ##
plotData<-as.matrix(
 rbind(as.numeric(zebraSet[,3]), as.numeric(zebraSet[,7])),
)
colnames(plotData)<-c("Control", "25", "30")
rownames(plotData)<-c("Mortality", "Malformations")
summary(plotData)

## ERROR BARS (SD) FOR PLOT 4: ##
plotSD<-as.matrix(
 rbind(as.numeric(zebraSet[,4]), as.numeric(zebraSet[,8])),
)
colnames(plotSD)<-c("Control", "25", "30")
rownames(plotSD)<-c("Mortality", "Malformations")
summary(plotSD)

## PLOT 4: ##
windowsFonts(Calibri = windowsFont("Calibri"))
windows(8,6)
par(lwd=2, mar=c(5,5,1,1), family = "Calibri")
plot1<-barplot2(
```

```
 plotData,
 beside=TRUE,
 plot.ci=TRUE,
 ci.u=plotData+plotSD,
 ci.l=plotData-plotSD,
 ylim=c(0, 100),
 col=c("cadetblue","lightsalmon"),
 xlab="Concentration (ng/uL)",
 ylab="Rate (%)",
 legend=FALSE
)
abline(h=0)

## SAVING PLOT 4 AS A TIFF FILE:  ##
 dev.print(tiff,
 "plot_I4.tif",
 width = 16,
 height = 12,
 units = 'cm',
 type="windows",
 res=600
)

## ------------------------------------ PLOT MICROINJECTION 5: ---------------------------------- ##
## SUBSETS OF DATA FOR PLOT 5: ##
zebraSet_I5_1<-subset(dataMortality, Replicate=="I5")
zebraSet_I5_2<-subset(dataMorbidity, Replicate=="I5")
zebraSet_I5_2<-rbind(zebraSet_I5_2,c("I5", "Control", NA, NA))
zebraSet<-cbind(zebraSet_I5_1, zebraSet_I5_2)
zebraSet<-zebraSet[c(3,1,2),]

## MEANS FOR PLOT 5: ##
plotData<-as.matrix(
 rbind(as.numeric(zebraSet[,3]), as.numeric(zebraSet[,7])),
)
colnames(plotData)<-c("Control", "25", "50")
rownames(plotData)<-c("Mortality", "Malformations")
```

```
summary(plotData)

## ERROR BARS (SD) FOR PLOT 5: ##
plotSD<-as.matrix(
 rbind(as.numeric(zebraSet[,4]), as.numeric(zebraSet[,8])),
)
colnames(plotSD)<-c("Control", "25", "50")
rownames(plotSD)<-c("Mortality", "Malformations")
summary(plotSD)

## PLOT 5: ##
windowsFonts(Calibri = windowsFont("Calibri"))
windows(8,6)
par(lwd=2, mar=c(5,5,1,1), family = "Calibri")
plol1<-barplot2(
 plotData,
 beside=TRUE,
 plot.ci=TRUE,
 ci.u=plotData+plotSD,
 ci.l=plotData-plotSD,
 ylim=c(0, 100),
 col=c("cadetblue","lightsalmon"),
 xlab="Concentration (ng/uL)",
 ylab="Rate (%)",
 legend=FALSE
)
abline(h=0)

## SAVING PLOT 5 AS A TIFF FILE:  ##
 dev.print(tiff,
 "plot_l5.tif",
 width = 16,
 height = 12,
 units = 'cm',
 type="windows",
 res=600
)
```

```
## ---------------------------------------- PLOT MICROINJECTION 6: ---------------------------------- ##
## SUBSETS OF DATA FOR PLOT 6: ##
zebraSet_I6_1<-subset(dataMortality, Replicate=="I6")
zebraSet_I6_2<-subset(dataMorbidity, Replicate=="I6")
zebraSet_I6_2<-rbind(zebraSet_I6_2,c("I6", "Control", NA, NA))
zebraSet<-cbind(zebraSet_I6_1, zebraSet_I6_2)
zebraSet<-zebraSet[c(2,1),]

## MEANS FOR PLOT 6: ##
plotData<-as.matrix(
 rbind(as.numeric(zebraSet[,3]), as.numeric(zebraSet[,7])),
)
colnames(plotData)<-c("Control", "50")
rownames(plotData)<-c("Mortality", "Malformations")
summary(plotData)

## ERROR BARS (SD) FOR PLOT 6: ##
plotSD<-as.matrix(
 rbind(as.numeric(zebraSet[,4]), as.numeric(zebraSet[,8])),
)
colnames(plotSD)<-c("Control", "50")
rownames(plotSD)<-c("Mortality", "Malformations")
summary(plotSD)

## PLOT 6: ##
windowsFonts(Calibri = windowsFont("Calibri"))
windows(8,6)
par(lwd=2, mar=c(5,5,1,1), family = "Calibri")
ploI1<-barplot2(
 plotData,
 beside=TRUE,
 plot.ci=TRUE,
 ci.u=plotData+plotSD,
 ci.l=plotData-plotSD,
 ylim=c(0, 100),
 col=c("cadetblue","lightsalmon"),
```

```
 xlab="Concentration (ng/uL)",
 ylab="Rate (%)",
 legend=FALSE
)
abline(h=0)
## SAVING PLOT 6 AS A TIFF FILE: ##
 dev.print(tiff,
 "plot_I6.tif",
 width = 16,
 height = 12,
 units = 'cm',
 type="windows",
 res=600
)
## ------------------------------------ MICROINJECTION AVERAGE: ---------------------------------- ##

## MEANS FOR PLOT AVERAGE: ##
MortalityMeans <- aggregate(data=dataZebra, Mortality~Dose, mean, na.rm=TRUE)
MortalityMeans<-MortalityMeans[c(4, 1, 2, 3),]
DeficiencyMeans <- aggregate(data=dataZebra, Deficiency~Dose, mean, na.rm=TRUE)
DeficiencyMeans<-rbind(c("Control", NA), DeficiencyMeans)

## ERROR BARS (SD) FOR PLOT AVERAGE: ##
MortalitySDs <- aggregate(data=dataZebra, Mortality~Dose, sd, na.rm=TRUE)
MortalitySDs<-MortalitySDs[c(4, 1, 2, 3),]
DeficiencySDs <- aggregate(data=dataZebra, Deficiency~Dose, sd, na.rm=TRUE)
DeficiencySDs<-rbind(c("Control", NA), DeficiencySDs)

## REORGANIZATION OF DATA ##
plotTable2<-as.matrix(
 rbind(
  as.numeric(MortalityMeans[,2]),
  as.numeric(DeficiencyMeans[,2])
 )
)
colnames(plotTable2)<-MortalityMeans[,1]
rownames(plotTable2)<-c("Mortality", "Morbidity")
```

```
summary(plotTable2)
View(plotTable2)

plotTableSD2<-as.matrix(
 rbind(
  as.numeric(MortalitySDs[,2]),
  as.numeric(DeficiencySDs[,2])
 )
)
colnames(plotTableSD2)<-MortalitySDs[,1]
rownames(plotTableSD2)<-c("Mortality", "Morbidity")
summary(plotTableSD2)
View(plotTableSD2)

## ANOVA ANALYSIS ##
anovaZebra1<-aov(data=dataZebra, cbind(Mortality, Deficiency)~ Replicate*Dose)
summary(anovaZebra1)
anovaZebraMortality2<-aov(data=dataZebra, Mortality~ Dose)
anovaZebraMorbidity2<-aov(data=dataZebra, Deficiency~ Dose)
summary(anovaZebraMortality2)
summary(anovaZebraMorbidity2)
TukeyMortality2<-TukeyHSD(anovaZebraMortality2)
TukeyMordidity2<-TukeyHSD(anovaZebraMorbidity2)

## LETTERS FOR THE PLOT: ##
LettersMortality<-multcompLetters(TukeyMortality2$Dose[,4])

## PLOT AVERAGE: ##
windows()
plot2<-barplot2(
 plotTable2,
 beside=TRUE,
 plot.ci=TRUE,
 ci.u=plotTable2+plotTableSD2,
 ci.l=plotTable2-plotTableSD2,
 ylim=c(0, 100),
 col=c("cadetblue","lightsalmon"),
```

```
 xlab="Concentration (ng/uL)",
 ylab="Rate (%)",
 legend=FALSE
)
abline(h=0)
text(
 plot2[1,],
 (plotTable2[1,]+plotTableSD2[1,])*1.05,
 LettersMortality$Letters,
 cex=1
)

## FOR SAVING PLOT AVERAGE: ##
 dev.print(tiff,
 "plot_Average.tif",
 width = 16,
 height = 12,
 units = 'cm',
 type="windows",
 res=600
)
```

2022 INÊS GONÇALVES GENERATION AND CHARACTERIZATION OF TRANSGENIC ZEBRSFISH LINES FOR THE STUDY OF VERTEBRATE BRAIN STRUCTURE AND FUNCTION

NOVA SCHOOL OF SCIENCE & TECHNOLOGY